INVESTIGATION OF THE INCOMMENSURATE (INC) PHASE BETWEEN α AND β PHASES IN QUARTZ AND RELATED MATERIALS

A THESIS SUBMITTED TO
THE GRADUATE SCHOOL OF NATURAL AND APPLIED SCIENCES
OF
MIDDLE EAST TECHNICAL UNIVERSITY

BY

SIMGE ATEŞ

IN PARTIAL FULFILLMENT OF THE REQUIREMENTS
FOR
THE DEGREE OF DOCTOR OF PHILOSOPHY
IN
PHYSICS

FEBRUARY 2021

Approval of the thesis:

INVESTIGATION OF THE INCOMMENSURATE (INC) PHASE BETWEEN α AND β PHASES IN QUARTZ AND RELATED MATERIALS

I hereby declare that all information in this document has been obtained and presented in accordance with academic rules and ethical conduct. I also declare that, as required by these rules and conduct, I have fully cited and referenced all material and results that are not original to this work.

Name, Surname: Simge Ateş

Signature :

ABSTRACT

INVESTIGATION OF THE INCOMMENSURATE (INC) PHASE BETWEEN α AND β PHASES IN QUARTZ AND RELATED MATERIALS

Ateş, Simge
Ph.D., Department of Physics
Supervisor:

February 2021, 114 pages

Incommensurate (INC) phase as an intermediate sinusoidal phase which exists in a narrow temperature range ($\sim 1.3°C$) between the low-temperature α and the high-temperature β phases in quartz, is investigated extensively. The phase transitions of the α -INC and INC- β occurring as first order and second order type, respectively, are studied using the experimental data from the literature. Order-disorder transition between the α and β quartz through the incommensurate phase is described by temperature and pressure dependence of the experimentally measurable macroscopic parameters in relation to the microscopic order parameter according to various models, mainly the Landau phenomenological model.

Our methods in this study form a guide to investigate crystals with similar phase diagram with quartz as tridymite and cristobalite, and incommensurate phases in some other materials with similar crystal structure to quartz such as $NaNO_2$, K_2SeO_4 and $AlPO_4$.

Keywords: Landau Model, Phase Transitions, Incommensurate phase, Quartz

ÖZ

QUARTZ VE İLGİLİ MALZEMELERDE α VE β FAZLARI ARASINDAKİ INCOMMENSURATE FAZIN İNCELENMESİ

Ateş, Simge
Doktora, Fizik Bölümü
Tez Yöneticisi:

Şubat 2021 , 114 sayfa

Kuartzda düşük-sıcaklık α ve yüksek-sıcaklık β fazları arasındaki dar bir sıcaklık aralığında ($\sim\ 1.3°C$) var olan, bir ara (orta) sinüssel faz olarak incommensurate (INC) fazı kapsamlı olarak incelenmektedir. Sırasıyla birinci ve ikinci derece tip olarak görülen α -INC ve INC- β faz geçişleri, literatürdeki deneysel veriler kullanılarak çalışılmıştır. α ve β quartz arasındaki incommensurate fazı üzerinden düzenlilik-düzensizlik geçişi deneysel olarak ölçülebilen makroskopik parametrelerin sıcaklık ve basınç bağımlılıklarını mikroskobik düzen parametresiyle ilişkilendirerek çeşitli modellere, esasen Landau fenomenolojik modeline, göre tanımlanmaktadır.

Bu çalışmadaki yöntemlerimiz quartza benzer faz diyagramı olan tridymite ve cristobalite gibi kristalleri ve $NaNO_2$, K_2SeO_4 ve $AlPO_4$ gibi quartza benzer kristal yapısı olan bazı diğer malzemelerdeki incommensurate fazları incelemek için bir rehber oluşturmaktadır.

Anahtar Kelimeler: Landau Modeli, Faz Geçişi, Incommensurate faz, Kuartz

To my family

ACKNOWLEDGMENTS

I would like to express my deepest gratitude to my academic advisor Prof. Dr. Hamit Yurtseven for his guidance, support and encouragement during this study.
I would also like to present my gratitude to Prof.Dr. Bekir Sıtkı Kandemir and Prof. Dr. Hakan Altan for their judgments and critics as the Ph.D Thesis committee.
I am indebted to my parents for their endless love, support and patience. I also would like to thank my sister Sezgi Ateş for seeing me as capable of anything.
I would like to thank Özge Akay for her invaluable friendship from the very first week of freshman year.

TABLE OF CONTENTS

ABSTRACT v

ÖZ vi

ACKNOWLEDGMENTS viii

TABLE OF CONTENTS ix

LIST OF TABLES xi

LIST OF FIGURES xv

LIST OF ABBREVIATIONS xxii

CHAPTERS

1 INTRODUCTION 1

1.1 Phase transitions 3

1.2 Silica Polymorphes and Phases of Quartz 4

2 THEORY 7

2.1 Thermodynamic Base of the Phase Transition 7

2.2 Structural Phase Transitions 11

2.3 Landau Phenomenological Model 12

2.4 Critical Exponents 20

2.5 Soft Mode Concept 23

2.6 Pippard Relations 23

2.7 Grüneisen Parameter 24

2.8 25

2.9 Structure and Phases of Quartz 27

3 CALCULATIONS AND RESULTS 31

3.1 Calculations of the tilt angle (ϕ^4) and the tilt angle susceptibility (χ_ϕ^{-1}) 31

3.2 Calculations of the thermodynamic properties via Landau model with the cubic term 36

3.3 Calculation of the Grüneisen parameter with the second Pippard relation by the piezoelectric resonant frequency shifts in relation to the elastic constants 52

3.4 Variation of the piezoelectric resonance frequency (υ) with the temperature associated with the anomalous strain (ΔL) close to the incommensurate phase of quartz 57

3.5 Calculation of the damping constant (Γ_{sp}) and the relaxation time (τ_{LA}^{-1}) of the LA mode in the incommensurate phase of quartz 64

3.6 Heat capacity (C_p) renormalization analysis with the renormalized critical exponents 79

3.7 Landau mean field model with the coupling terms in the presence of the electric field 87

4 CONCLUSIONS 101

REFERENCES 105

LIST OF TABLES

TABLES

Table 1.1 Transition tempratrures for the α-β transition of the low pressure phases of silica 5

Table 2.1 List of the critical exponents 22

Table 2.2 Enantimorphic space groups of α and β phases of quartz 28

Table 2.3 Symmetry modes of quartz [64] 29

Table 3.1 Coefficients a_0, a_1 and a_2 (Eq. 3.4) and c_0 and c_1 (Eq. 3.10) which were determined by using the experimental data [24] for the α-β transition in quartz ($T_c = 846K$). 33

Table 3.2 Values of the ratio of the parameters given in the free energy (Eq.2.19) for the α-β transition in quartz ($T_c = 846K$). [2] 34

Table 3.3 $a^{'}$ and $b^{'}$(Eq.3.14), a_0 and a_1 (Eq.3.21) for the α-β transition in quartz with the observed values [18] of the transition (T_{tr}) and critical (T_c) temperatures. 38

Table 3.4 Values of the parameters a, u and b (Eq.3.11), u^* and b^* (Eq.3.16) and, the values of the order parameter Q_0 (at $T = T_{tr}$) (Eq.2.35), latent heat L (Eq.2.41) and the observed entropy S_β (in the β phase) [76] for the α- β transition in quartz. Observed values of the transition temperature (T_{tr}) and the critical temperature (T_c) are also given [5, 18] 39

Table 3.5 Values of the observed spontaneous strain V_0 and $V_{s,0}$ (at $T = T_{tr}$) [18], coefficients c_0 and c_1 (Eq.3.25) with the observed critical temperature (T_c), and the values of the coefficients $c_0^{'}$ and $c_1^{'}$ (Eq.3.26) for the α- β transition in quartz [5]. 45

Table 3.6 "Values of the coefficients b_0 and b_1 (Eq.3.29), $b_0^{'}$ and $b_1^{'}$ (Eq.3.30), within the temperature intervals indicated with the observed transition temperature T_0 for the elastic stain ΔL [70] close to the incommensurate (INC)- β transition in quartz." [5] 46

Table 3.7 The coefficients A and B (Eq.3.32) within the temperature interval indicated for the α-β transition in quartz with the observed values [18] of the transition (T_{tr}) and critical (T_c) temperatures. 50

Table 3.8 Values of the isobaric mode Grüneisen parameter (γ_p) of the $A_g - 2$ mode and the volume variation with the temperature due to the linear incompressibilities $(1/K_1$ and $1/K_3)$ and the isothermal compressibility (κ_T) according to Eq.3.33 within the temperature range indicated for the α-quartz. The α-β transition temperature and the observed $\frac{dP}{dT}$ [18] values are given here [5]. 55

Table 3.9 Power law parameters according to Eq. 3.40 using the experimental data of the piezoelectric resonance frequency [34] close to the INC-β transition in quartz. 59

Table 3.10 Values of the parameters of a_0 and a_1 (Eq. 3.44), b_0 and b_1 (Eq.3.45) within the temperature intervals indicated by using the experimental data for the piezoelectric resonance frequency [34] and the anomalous strain [70] for the INC-β phase transition in quartz [3]. 60

Table 3.11 Fitting parameters of the normalized piezoelectric resonance frequency (υ^2) in relation to the square root of the normalized anomalous strain $(\Delta L^{1/2})$ according to Eq.3.46 for the INC-β transition in quartz. . . 61

Table 3.12 Values of the transition temperatures (T_c and $T_i = T_c + 1.43\,K$), background damping constants (Γ_0 and $\Gamma_0^{'}$) and the amplitudes (A and $A^{'}$) of the LA mode in the temperature intervals ($T_0 = 846.93\,K$) indicated according to the PS and EF models for the incommensurate phase of quartz ($P = 0$) 67

Table 3.13 Values of the transition temperatures T_c, $T_{i1} = T_c + 6.18\,K$ and $T_{i3} = T_c + 4.36\,K$, background damping constants (Γ_0 and $\Gamma_0^{'}$) and the amplitudes (A and $A^{'}$) of the LA mode in the temperature intervals ($T_0 = 848.82\,K$) indicated according to the PS and EF models for the incommensurate phase of quartz ($P = 80.5MPa$) 67

Table 3.14 Values of the transition temperatures T_c, T_i ($P = 0$), T_{i1} ($P = 80.5MPa$), and T_{i3} ($P = 80.5MPa$) and the temperature T_{max} at the maximum value of the linewidth Γ_{LA} of the observed LA mode [81]. Also, values of the critical exponent η and the amplitude $\Gamma^{'}(0)$ are given within the temperature intervals indicated ($P = 0$ and $P = 80.5MPa$) according to Eq.3.49 for the incommensurate phase of quartz. 70

Table 3.15 Values of the transition temperatures T_c, T_i ($P = 0$), T_{i1} ($P = 80.5MPa$), and T_{i3} ($P = 80.5MPa$) for the frequency shifts $\Delta\upsilon$ of the observed LA mode [81]. Also, values of the critical exponent β for the order parameter, amplitude A, the frequency shift $\Delta\upsilon_0$ at the transition temperature and the coefficient a within the temperature intervals indicated ($P = 0$ and $P = 80.5MPa$) according to Eqs.3.50 and 3.50, are given for the incommensurate phase of quartz. 70

Table 3.16 Values of the activation energy E_a (Eq.3.53) and the coefficients a and b (Eqs.3.55 and 3.56) of the LA mode with the values of $T_c(K)$, $T_i(K)$, $T_{i1}(K)$, $T_{i3}(K)$ and $T_0(K)$ for the pressures within the temperature intervals indicated in the incommensurate phase of quartz. 74

Table 3.17 Values of the critical exponent α and α_R (renormalized) (Eq.3.60) for the heat capacity C_p with the parameters A, B and D according to Eq.3.58 for the transitions within the temperature intervals indicated for quartz. Transition temperatures (T_c, T_c' and T_i) are also given from the observed C_p data [1, 32]. Quality of fits is also given for the transitions studied. 80

Table 3.18 Values of the critical exponent α and α_R (renormalized) (Eq.3.60) for the heat capacity C_p with the parameters A, B and D according to Eq.3.58 for the transitions within the temperature intervals indicated for the cooling run in quartz. Transition temperatures (T_c and T_i) are also given from the observed C_p data [33]. Quality of fits is also given for the transition studied. 80

Table 3.19 Values of the critical exponents α and α_R (renormalized) (Eq.3.60) for the heat capacity C_p with the parameters A, B, and D according to Eq.3.58 for the transitions within the temperature intervals indicated for the heating run in quartz. Transition temperatures (T_c and T_i) are also given from the observed C_p data [33]. Quality of fits is given for the transition studied. 81

Table 3.20 Coefficients determined by using the experimental data for the α-β transition [6] according to Eq.(3.70) within the temperature interval indicated in quartz. 88

Table 3.21 Observed electric (E) field values with the transition temperatures T_c (α-INC transition) and T_i (INC-β transition) from the $E-T$ phase diagram [90]. 89

Table 3.22 Coefficients determined by using the experimental data for the INC-β transition [90] according to equations within the temperature interval indicated in quartz. 94

Table 3.23 Coefficients determined by using the experimental data for the α-INC transition [90] according to Eq.(3.91) with the values of a, b and c (Table 3.20) within the temperature interval indicated in quartz. 98

LIST OF FIGURES

FIGURES

Figure 1.1 Schematic phase diagram for water. 3

Figure 1.2 Phase diagram of silica schematically obtained from the observed data in the literature [11]. 5

Figure 2.1 1^{st} order phase transition representations for the thermodynamic potential (G), external state function S (Eq.2.4) and thermal response function C_p (Eq.2.5) in the vicinity of the transition temperature (T_m) [38]. 10

Figure 2.2 2^{nd} order phase transition representations for thermodynamic potential (G), external state function S (Eq.2.4) and thermal response function C_p (Eq.2.5) in the vicinity of the transition temperature (T_m) [38]. 10

Figure 2.3 Reconstructive transition from graphite to diamond [39]. 11

Figure 2.4 Unitcell of perovskite structures with ABO_3 general formula (a) and structural change due to rotation of ϕ (b) [37]. 12

Figure 2.5 Order parameter dependence of Landau free energy (a) and temperature dependence of order parameter (b) for a second order transition 16

Figure 2.6 Order parameter dependence of the Landau free energy (a) and temperature dependence of order parameter (b) for a first order transition. 17

Figure 2.7 Schematic representation of SiO_4 tetrahedra. 27

Figure 2.8 Structural representation of the 2D projections of α and β configurations [59]. Pink dots refer Oxygen atoms and small black dots are Silicon atoms. 28

Figure 3.1 Temperature dependence of the tilt angle (ϕ) for the α-β transition in quartz with the fit of Eq.3.4 to the experimental data [24] ($T_c = 846K$). 32

Figure 3.2 Variation of the function $\psi = \phi^4 + \frac{b}{c}\phi^2$ (Eq. 3.7) with temperature, which was obtained for the α-β transition in quartz ($T_c = 846K$). . 33

Figure 3.3 Inverse tilt angle susceptibility χ_ϕ^{-1} as a function of $T_c - T$, which was calculated for the α-β transition in quartz ($T_c = 846K$). . . . 34

Figure 3.4 Temperature dependence of normalized order parameter calculated for the α-β transition in quartz by using Eq.3.12 according to the Landau phenomenological model with the cubic term (Eq.3.11) and compared to observed data (η/η_0) [6, 74] and (ϕ/ϕ_0) [75] 37

Figure 3.5 "Variation of normalized order parameter with the observed Raman soft-mode frequency ω (squared)($\sim 100cm^{-1}$ at $500°C$) in the α phase ($T < T_c$) with the uncertainties [75] according to Eq.3.12 through Eq.3.14 close to the α-β transition in quartz. 38

Figure 3.6 $(\chi/\chi_{max})^{-1}$ calculated as a function of temperature according to Eq.3.15 through Eq.3.12 for the α-β transition in quartz (black dots). Calculated values with different methods [18, 71] are also shown. 40

Figure 3.7 Variation of the inverse susceptibility (χ^{-1}) calculated (Eq.3.16) with the square of the observed Raman frequency ω (squared) of the silent soft phonon in the β phase [67] for the α-β transition in quartz [5]. 41

Figure 3.8 Temperature dependence of entropy S calculated according to Eq.3.17 in the α phase of quartz. Observed data [76] are also shown. . . 42

Figure 3.9 Temperature dependence of the heat capacity C_p calculated in the form of $(T/C_P)^2$ according to Eq. 3.18 for the α phase of quartz with the observed data [18]. 43

Figure 3.10 Temperature dependence of the spontaneous strain V_s calculated according to Eq.3.24 for the α -β transition in quartz as shown with the calculated V_s values [18] from the neutron and X-ray diffraction data . 44

Figure 3.11 (a)Variation of the normalized order parameter Q (Eq.3.12) with the spontaneous strain (Eq.3.24) through Eq.3.26 for the α-β transition in quartz. V_s values calculated from the neutron and X-ray data [18] are also shown here. (b)Variation of the normalized order parameter Q (Eq.3.12) with the observed [70] elastic strain ΔL (normalized) (Eqs.3.29 and 3.30) for the α-β transition in quartz [5]. 47

Figure 3.12 Variation of the tilt angle ϕ with the macroscopic order parameter Q according to Eq. 3.32 in the α phase close to the α-β transition in quartz. 51

Figure 3.13 The resonance frequency shifts $(1/\nu)\,(\partial\nu/\partial T)_P$ of the $A_g - 2$ mode as a function of temperature using the observed data [19] in the α phase ($T < T_c = 573^{\circ}C$) of quartz. 53

Figure 3.14 Temperature dependence of the linear incompressibilities (K_1 and K_3) according to Eqs. 3.34 and 3.35 with the observed data [19] for the α-β transition in quartz. 54

Figure 3.15 Variation of the resonance frequency shifts of the $A_g - 2$ mode with the inverse incompressibilities (K_1 and K_3) as a function of the isothermal compressibility (κ_T) according to Eq.3.33 by using the observed data [19] for α-quartz ($T < T_c = 573^{\circ}C$). 54

Figure 3.16 Temperature dependence of the piezoelectric resonance frequency (υ) in the log-log scale according to Eq. 3.40 using the experimental data of cooling run [34] close to the INC-β transition in quartz. 59

Figure 3.17 The normalized piezoelectric resonance frequency [34] in relation to the normalized anomalous strain [70] close to the INC-β transition in quartz in accordance with the Eq.3.44. 60

Figure 3.18 Piezoelectric resonance frequency (normalized) (υ^2) fitted to the anomalous strain (normalized) ($\Delta L^{1/2}$) as a function of temperature using Eq.3.44 through Eq.3.46 in the vicinity of the INC-β transition in quartz. 61

Figure 3.19 Variation of the linewidth of the LA mode (Eq.3.47) according to the PS model with the temperature at $P = 0$. The observed Γ_{LA} data [81] are also shown in the INC phase of quartz. 66

Figure 3.20 Variation of the linewidth of the LA mode (Eq.3.47) according to the PS model with the temperature at $P = 80.5\,MPa$. The observed Γ_{LA} data [81] are also shown in the INC phase of quartz. 66

Figure 3.21 Variations of the linewidth of the LA mode (Eq.3.48) by the EF model at $P = 0$ with the temperature. The observed Γ_{LA} data are also shown [81] in the INC phase of quartz. 68

Figure 3.22 Variations of the linewidth of the LA mode (Eq.3.48) by the EF model at $P = 80.5\,MPa$ with the temperature. The observed Γ_{LA} data are also shown [81] in the INC phase of quartz. 68

Figure 3.23 Analysis of the temperature dependence of the damping constant Γ_{LA} at $P = 0$ (a) and $80.5\,MPa$ (b) according to the power law formula (Eq.3.49) for the LA mode using the observed data [81]. Solid lines represent the best fits to the experimental data [81]. 71

Figure 3.24 Frequency shifts ($\Delta\upsilon_{LA}$) squared as a function of temperature according to Eqs.3.50 and 3.51 below and above the transition temperature T_i at $P = 0$ and T_{i1} at $P = 80.5MPa$ respectively, which were fitted to the experimental $\Delta\upsilon_{LA}$ of the LA mode [81] in the commensurate phase of quartz. Solid lines represent the best fits to the experimental data [81]. 72

Figure 3.25 Inverse relaxation time (τ_{LA}^{-1}) calculated as a function of temperature for the LA mode according to Eq.3.52 where the observed data for the frequency shifts ($\Delta\upsilon$) and the linewidth (Γ_{LA}) of this mode [26] were used at the pressures of $\mathrm{P} = 0$ (a) and $80.5\mathrm{MPa}$ (b) in the incommensurate phase of quartz. Straight lines above T_i $(\mathrm{P} = 0)$ and $T_c(80.5\ \mathrm{MPa})$ denote the best fits to the τ^{-1} values. 75

Figure 3.26 Relaxation time (τ_{LA}) in the logarithmic form of the LA mode as a function of the inverse temperature to determine the values of the activation energy (E_a) according to Eq.3.54 for $\mathrm{P} = 0$ (a) and $80.5\mathrm{MPa}$ (b) in the incommensurate phase of quartz. Solid lines represent best fits to the predicted values (τ_{LA}). 76

Figure 3.27 Variation of the heat capacity C_p with the reduced temperature t (Eq.3.59) according to Eq.3.58 for the transitions of α-INC for $T < T_c^{'}$ (a) and INC-α for $T > T_c$ (b) using the observed data [1, 32] in quartz with the critical temperatures $T_c^{'}$ and T_c (Table 3.17). 83

Figure 3.28 Variation of the heat capacity C_p with the reduced temperature t (Eq.3.59) according to Eq.3.58 for the transitions of INC-β for $T < T_i$ (a) and β-INC for $T > T_i$ (b) using the observed data [1, 32] in quartz. T_i is the critical temperature (Table 3.17). 84

Figure 3.29 Variation of the heat capacity C_p with the reduced temperature t (Eq.3.59) according to Eq.3.58 for the transitions of α-INC for $T < T_c$ (a) and INC-α for $T > T_c$ (b) for heating and cooling runs, respectively, using the observed data [33] in quartz with the critical temperature T_c (Tables 3.18 and 3.19). 85

Figure 3.30 Variation of the heat capacity C_p with the reduced temperature t (Eq.3.59) according to Eq.3.58 for the transitions of INC-β for $T < T_i$ (a) and β-INC for $T > T_i$ (b) for heating and cooling runs, respectively, using the observed data [33] in quartz with the critical temperature T_i (Tables 3.18 and 3.19). 86

Figure 3.31 Temperature dependence of the order parameter η (Eq.3.70) and the observed data [6] for the α-β transition in quartz within the temperature interval $319 < T(K) < 847$. 89

Figure 3.32 The order parameter calculated as a function of temperature for various electric fields (E) for the α-INC phase transitions in quartz. Observed η at $E = 0$ [6] are also shown within the temperature interval of $825 < T(K) < 850$. 90

Figure 3.33 Temperature dependence of the order parameter ξ of the INC phase in the normalized form, which was calculated according to the Eq.3.66 within the temperature interval of $832.5 < T(K) < 850$ with the $E - T$ values [90] (Table 3.21). 91

Figure 3.34 Temperature dependence of the inverse susceptibility χ_η^{-1} calculated from Eqs.3.69 and 3.74 in the presence of E-field. 91

Figure 3.35 The inverse susceptibility χ_ξ^{-1} of the order parameter ξ in the incommensurate (INC) phase ($T_c < T < T_i$) as a function of temperature at constant electric fields for the α-INC transition in quartz. T_i denotes the transition temperature above which the β phase occurs in quartz. . . 92

Figure 3.36 Temperature dependence of the order parameter ξ for the incommensurate (INC) phase according to Eq.(3.84) at constant electric fields in quartz. T_i indicates the temperature for the INC-β transition (Table 3.21) 94

Figure 3.37 Order parameter η of the α phase as a function of the temperature in the incommensurate (INC) phase for the INC-β transition at constant electric fields according to Eq. (3.66). 95

Figure 3.38 Inverse susceptibility susceptibility calculated from Eq.(3.87) in the incommensurate (INC) phase for the INC-β transition at constant electric fields in quartz. 96

Figure 3.39 Inverse susceptibility χ_η^{-1} calculated as a function of the temperature at constant electric fields according to Eq.(3.89) for the INC-β transition in quartz. T_i denotes the temperature for the INC-β transition (Table 3.21). 96

Figure 3.40 The $E-T$ phase diagram according to the phase line equations, Eqs. (3.91) and (3.94) for the transitions of α-INC (α-I) and the INC-β (I-β), respectively, which were fitted (solid lines) to the experimental data [90] in quartz. 98

LIST OF ABBREVIATIONS

ABBREVIATIONS	
INC	Incommensurate
PS	Pseudo-spin
EF	Energy fluctuation
2D	2 Dimensional
3D	3 Dimensional
TA	Transverse Acoustic
LA	Longitudinal Acoustic

CHAPTER 1

INTRODUCTION

Phase transitions have a pivotal place in structural condensed matter physics. Therefore, it is important to understand the concept of phase and phase transition from classical to the catastrophic point of view. Although, there have been quite amount of studies about the structural phase transitions both theoretically and experimentally, there are still some unexplained processes especially in the vicinity of the transition temperature.

Quartz is one of the most abundant crystalline on the earth and it is used in various applications and technological device developments as in crystal oscillators, ultrasound devices, satellites and so on. Change in the thermodynamic parameters such as pressure, temperature, volume and chemical replacement results in a change in the crystal structure. Quartz exhibits a structural phase transition from α-phase to β-phase through the incommensurate (INC) phase at around $T_c = 573°C$. Therefore, investigating quartz gives a lot information about crystal structure, nature of the structural phase transitions, thermodynamic properties of the transition and the other mechanisms occurring during the transition. In particular, INC phase needs more investigation. Since it is the intermediate phase, both α and β phases can coexist and it shows properties of both phases [1].

On the basis of statistical mechanics and thermodynamics, there are many models as Ising model and mean field theory that can explain the critical behavior of phase transition around the critical point. For example, by the Landau phenomenological model the changes in thermodynamic quantities during the transition can be investigated, and the macroscopic observations of a system can be related to the microscopic theories by defining an order parameter. With this method, it can be seen that very

different structures seem to be similar around the critical point in terms of the order parameter and the Landau energy which leads to explain their critical behavior. In other words, investigating quartz with the Landau model can be a guide to understand materials $NaNO_2$, K_2SeO_4 $AlPO_4$ and the like.

In this dissertation, the $\alpha - \beta$ phase transition through the incommensurate (INC) phase of quartz is studied theoretically by mainly using the Landau phenomenological model with the help of experimental data from the literature. Fourth power of the tilt angle (ϕ^4) is used as an order parameter in the calculation of the temperature dependence of the order parameter and susceptibility by means of the Landau phenomenological model for the $\alpha - \beta$ transition in quartz [2]. The piezoelectric resonance frequency (ν) is also used as an order parameter in the analysis of the temperature dependence of the order parameter according to the power law formula for the INC phase of quartz. In addition, anomalous strain is correlated to the piezoelectric resonance frequency as an order parameter [3]. Resonance frequency shifts ($\Delta\nu$) are correlated to the elastic constants via spectroscopically modified Pippard relations for the $\alpha - \beta$ transition in quartz [4]. Due to asymmetry, expansion of the Landau model in terms of the order parameter with the cubic term is used to calculate the thermodynamic quantities at various temperatures [5]. Pseudo-spin (PS) coupling and the energy fluctuation (EF) models are used to calculate the temperature dependence of the damping constant (Γ_{LA}) of the LA mode for the INC phase of quartz. By using the power law analysis of the damping constant and frequency shifts ($\Delta\nu_{LA}$), inverse relaxation time (τ^{-1}) and the activation energy (E_a) are predicted in the vicinity of the INC phase of quartz. Close to the α-INC-β transition in quartz, heat capacity C_P is calculated as a function of temperature by renormalization-group expression with the first order correction to the scaling term. Finally, the temperature dependence of the order parameter (η) of the α-phase and the inverse susceptibility (χ^{-1}) of the α-INC-β transition in quartz are calculated by using free energy expansion of the Landau phenomenological model in the absence and presence of the electric field. The temperature dependence of the order parameter (ξ) and the inverse susceptibility (χ^{-1}) of the incommensurate (INC) phase of quartz are predicted.

Theoretical background of these calculations are given in the Chapter 2 and detailed calculations by use of the experimental data from the literature are given in the Chap-

ter 3. In Chapter 4, discussions for the results of Chapter 3 results and some future applications are expressed. Before passing to Theory chapter some introductory information about phase transitions and quartz material are given in this chapter.

1.1 Phase transitions

α-β transition in quartz is a structural-first order transition. But, with the introduction of INC phase [1], classification of the α-INC-β transition in quartz includes a second order transition between INC-β phases [6]. Before jumping into structural phase transitions, some basic definitions should be made like phase and phase transitions. Materials can show different mechanical, optical, electrical, etc. properties under different thermodynamic conditions despite having fixed chemical composition. These different states of the matter which is uniform by means of thermodynamic parameters like heat capacity, entropy and density in a macroscopic sense are the phases of the material of interest. The equilibrium relationships between these phases are often shown by graphical representations called phase diagrams which are mostly functions of pressure, temperature and structural composition.

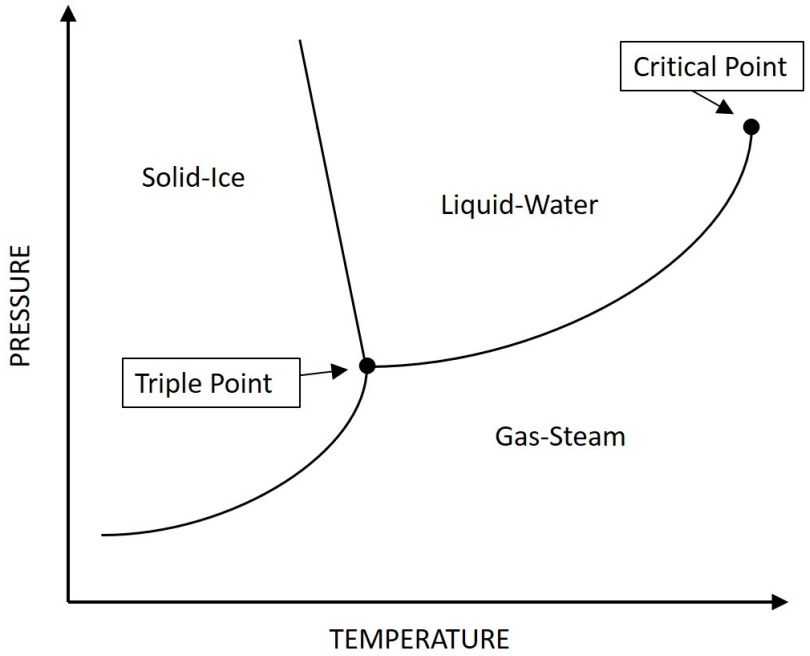

Figure 1.1: Schematic phase diagram for water.

Water is an every day example which shows three natural phases of the matter, that

are solid, liquid and gaseous under specific conditions. For higher temperature and pressure conditions there is also the fourth phase known as plasma. Schematic phase diagram for water can be seen Fig1.1 at various pressures and temperatures. While solid, liquid and gas phases of the pure substance can be found in areas separated by the solid lines, both neighboring phases can coexists on these phase boundaries. Critical point is the top of the liquid-steam equilibrium which means over a certain temperature there is no any possibility of condensation via pressure. All three phases can exists together on the triple point. Simply by changing temperature and pressure conditions, change in the phase can be observed in the phase diagram which is called the phase transition but this is not the only way of transitioning. To be stable, some solids exhibit phase transition without turning into liquid or gas instead slightly changing the orientation of atoms like quartz crystal. Besides liquid-gas transitions, this could happen between the paramagnetic and ferromagnetic, ordered and disordered, and conducting and superconducting phases. Phase transitions have been classified based on thermodynamics (Ehrenfest [7], 1933), mechanism (Buerger [8], 1951) and kinetics (le Chatelier-Roy [9], 1973) over the time. The binary classification, first order (discontinuous) and second order (continuous) phase transition, which is the evolved version of Ehrenfest's classification is used in this work. With in this context, Landau phenomenological model can be used to investigate and explain both type of the phase transition in the vicinity of the critical point, although it is mainly suggested for the continuous phase transitions at first [10].

1.2 Silica Polymorphes and Phases of Quartz

The compound silica, SiO_2, has 11 crystalline and 2 non-crystalline polymorphs. Quartz is the only stable form of them at ambient conditions. If enough time is given all other silica polymorphs will eventually be transformed into quartz. Other forms of silica have special conditions like high pressure and temperature in order to be stable. Pure silica phases under certain temperature and pressure conditions are given in Fig 1.2. At very high temperature and low pressure, silica takes liquid form as a stable phase (yellow region on the diagram), and all the other parts are the solid phases. Metastable states (e.g. moganite) and gaseous form which is above $2477°C$ at normal

pressure are not shown in this diagram [11].

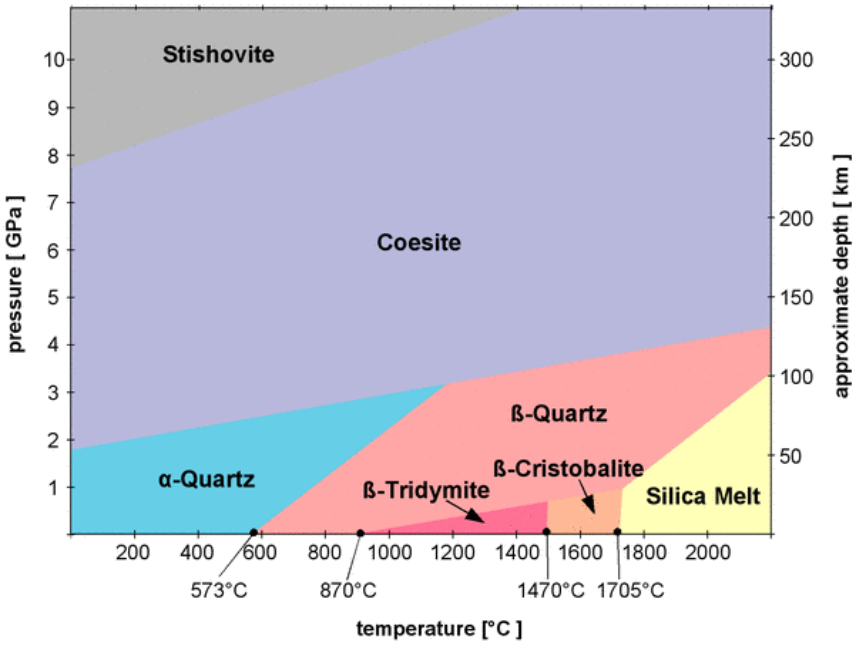

Figure 1.2: Phase diagram of silica schematically obtained from the observed data in the literature [11].

Stishovite and Coesite are the high pressure phases of quartz and they are stable in the earth's mantle and crust respectively [12]. Low pressure phases Quartz, Tridymite and Cristobalite have two forms as the low temperature-α phase and the high temperature-β phase in terms of the stability whose transition temperatures are given in Table 1.1. For tridymite and Cristobalite transition temperatures are outside of the stablity range of the phases but this does not prevent the transition it still occurs [13]. α-quartz

Table 1.1: Transition tempratrures for the α-β transition of the low pressure phases of silica

α-β transition	Quartz	Tridymite	Cristobalite
Transition Temperature ($^{\circ}C$)	573	110-180	218 ± 2

is the most abundant form in ambient conditions and its transition to β-quartz has been the focus of many studies since the discovery of α-β transition in quartz by Le Chatelier (1889) [14]. Transition between α and β phases of quartz has been investigated thermodynamically by measuring the heat capacity [1, 15], thermal diffusivity [16], elastic constants and thermal expansion [17–20], dielectric constant and

thermal dilatation [21]. Additionally, the spectroscopic studies have also been conducted by using Raman spectroscopy [22, 23], neutron [1, 24, 25], Brillouin [26, 27] and light [28] scattering, experimentally. During these studies, the existence of an intermediate region has been suggested as an heterogeneous structure where both phases (α and β) can coexist [29, 30]. Afterwards, this intermediate region called INC (incommensurate) phase due to the coupling of the order parameter to the elastic strains [31] was proven experimentally [1]. Although INC phase occurs in a narrow temperature interval ($\sim$ 1.2 K), the critical behavior of the heat capacity was shown during measurements of INC-β transition [32, 33]. Behavior of the acoustic phonons in the INC phase of quartz was also studied experimentally [34].Then, piezoelectric properties of α, INC and β phases of quartz were obtained [35]. INC phase of quartz occurs in a relatively large and experimentable temperature interval with respect to other crystallines with the INC phases, which makes the investigation of the INC phase of quartz essential as well as interesting.

CHAPTER 2

THEORY

In order to form a complete picture of α-INC-β transition in quartz, thermodynamic motivations and types of phase transition are discussed and Landau phenomenological model in relation to thermodynamic properties for the first and second order transition is established in this chapter. The concepts of the soft mode and the critical exponents are stated to support the Landau theory. Rippard relations, Grüneisen paramater and damping constant are described to obtain relations between structural changes and thermodynamic properties. Structure of α and β phases in quartz and its relation to INC phase during transition are explained.

2.1 Thermodynamic Base of the Phase Transition

Stability of a Phase

Unstable materials undergo phase transition to achieve stability. Specific thermodynamic conditions can refer specific states of the matter and stability of these states can be explained by the entropy (S) change. Thermodynamic conditions of a state are represented by a thermodynamic potential which is composed of the thermodynamic variables of as pressure (p), temperature (T), volume (V) and amount of substance (N). The internal energy (U), the Helmholtz free energy (F), the Gibbs free energy (G), the enthalpy (H), and the grand potential (Ω) are five of the most common thermodynamic potentials that give the equation of the state by Legendre transforma-

tions [36]:

$$\begin{aligned} Internal\,Energy &: dU = TdS - pdV + \mu dN \\ Helmholtz\,Free\,Energy &: dF = -SdT - pdV + \mu dN \\ Gibbs\,Free\,Energy &: dG = -SdT + Vdp + \mu dN \\ Enthalpy &: dH = TdS + Vdp + \mu dN \\ Grand\,Potential &: d\Omega = -SdT - pdV - Nd\mu \end{aligned} \tag{2.1}$$

Each equation (Eq.2.1) gives information about the thermodynamic state and its stability under different constraints. Stability of the phase is directly related to the minimum of these thermodynamic potentials. For a hypothetical transition without particle fluctuation ($dN = 0$), Gibbs Duhem stability condition of internal energy can be written as,

$$\Delta U + p\Delta V - T\Delta S \geq 0 \tag{2.2}$$

where Δ is the divergence of thermodynamic quantities from the equilibrium. Stability characterization of each thermodynamic potential with constant corresponding thermodynamic variable (Eq.2.1) can be derived as in Eq.2.2. Stability also requires maximum value of entropy ($\delta S = 0$ and $\delta^2 S < 0$) with constant internal energy and volume. By expanding ΔS close to the equilibrium as,

$$\Delta S = \delta S + (1/2)\delta^2 S + (1/3!)\delta^3 S + (1/4!)\delta^4 S + ... \tag{2.3}$$

where δ^n ($n = 1, 2, 3...$) n^{th} order differentials, stability conditions can be defined due to entropy. For maximum entropy conditions ($\delta S = 0$ and $\delta^2 S < 0$), an equilibrium is called **stable**, if $\Delta S < 0$ (Eq.2.3). If $\delta^2 S > 0$, it is a violation of maximum entropy conditions and the state is **unstable**. Despite satisfying the maximum entropy conditions, some states violate stability condition and have $\Delta S > 0$ which is a **metastable** equilibrium. Metastability is kind of an intermadiate phase that shows the thermodaynamic possibility of incommensurate phase [37]. Unstable and metastable materials eventually undergo a phase transition to be more stable and this transition can show different effects on thermodynamic quantities according to its order.

Classification of Phase Transitions

Discontinuities of thermodynamic state quantities are one of many evidences of phase transitions and Paul Ehrenfest classified phase transition due to these discontinuities as first and second order [7].First order derivative of the state functions in terms of state variables (Eq.2.1) gives the observables as volume, pressure or temperature, nonobservable entropy or relation to the other type of energy as enthaply. Crystals are like a closed box,therefore there is no particle fluctuations ($dN = 0$). By defining the state variables as temperature and pressure, governing thermodynamic potential becomes Gibbs free energy whose first order derivatives are given in Eq.2.4.

$$S = -\left(\frac{\partial G}{\partial\, T}\right)_p, \qquad V = \left(\frac{\partial\, G}{\partial p}\right)_T, \qquad H = -T\left(\frac{\partial G}{\partial T}\right) \tag{2.4}$$

Second order derivative of the state functions (Eq.2.1) gives thermal response function, heat capacity (C_p), and mechanical response functions isothermal susceptibility (χ_T), isothermal compressibility (κ_T) and thermal expansivity (α_P) by means of Maxwell relations.

$$\begin{aligned} C_p &= T\left(\frac{\partial^2 G}{\partial T^2}\right)_p = T\left(\frac{\partial S}{\partial\, T}\right)_p \\ \kappa_T &= -\frac{1}{V}\left(\frac{\partial^2 G}{\partial p^2}\right)_T = -\frac{1}{V}\left(\frac{\partial V}{\partial p}\right)_T \\ \alpha_p &= \frac{1}{V}\left(\frac{\partial^2 G}{\partial T \partial p}\right) = \frac{1}{V}\left(\frac{\partial V}{\partial T}\right)_p \end{aligned} \tag{2.5}$$

Thermodynamic classification of phase transition is defined by the order of discontinuous derivative of the state functions of the phase (Eq.2.1) in terms of the state variables. If the discontinuity is on the first order derivative, it is called **first order (discontinuous) phase transition** (Eq.2.4). If the discontinuity is on the second order derivative, it is called **second order (continuous) phase transition** (Eq.2.5) which means that the lowest order discontinuous derivative of the thermodynamic potential determines the type of transition. A latent heat is also involved in first order phase transitions. Latent heat is the change in the enthalpy (Eq.2.1) and under constant pressure latent heat of a first order transition can be written as,

$$L = \Delta S T_{tr} \tag{2.6}$$

where T_{tr} is the transition temperature. Possible higher order transitions are called multicritical transitions according to Ehrenfest or λ-transitions due to the λ shaped temperature dependence of the heat capacity which includes the second order (continuous) phase transition later on. Thermodynamic quantities for the first and second order transitions are given in Figures 2.1 and 2.2, respectively. The step ΔS in the entropy graph is corresponding to the latent heat (Eq.2.6) of the first order transition.

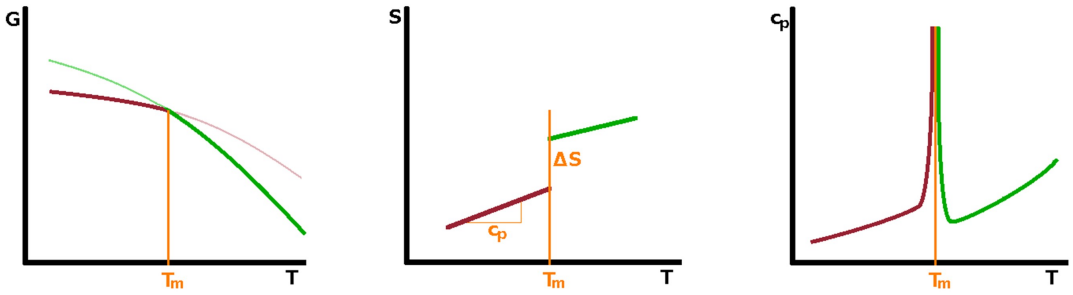

Figure 2.1: 1^{st} order phase transition representations for the thermodynamic potential (G), external state function S (Eq.2.4) and thermal response function C_p (Eq.2.5) in the vicinity of the transition temperature (T_m) [38].

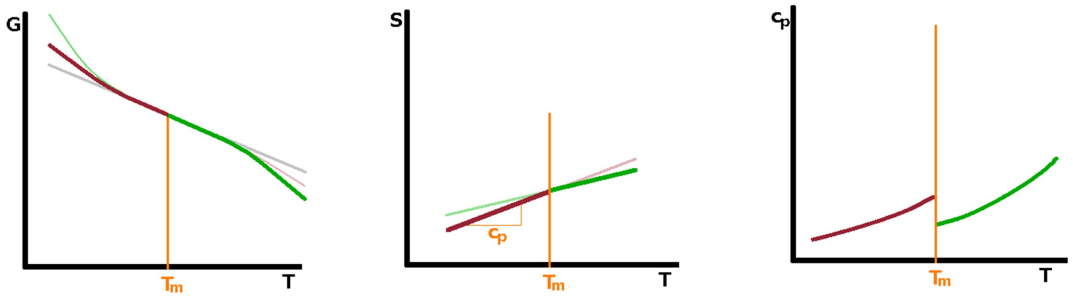

Figure 2.2: 2^{nd} order phase transition representations for thermodynamic potential (G), external state function S (Eq.2.4) and thermal response function C_p (Eq.2.5) in the vicinity of the transition temperature (T_m) [38].

Thermodynamic classification of the phase transition is important to understand the transition behavior without dispute, but it is only one aspect and sometimes it is insufficient to describe all the transitions in that matter. Transitions can result with a new physical property as ferroelectricity, ferromagnetism or superconductivity due to the change of symmetry, structure or order. These type of transitions can be classified as structural phase transitions.

2.2 Structural Phase Transitions

During phase transitions, besides the change in the thermodynamic quantities, solid state materials exhibit some structural change as distortion in the crystal structure, breaking of the symmetry , and change in the interatomic distance etc. Hence, it is called structural phase transition and classified as reconstructive and displacive transitions by Buerger due to the transition mechanism [8].

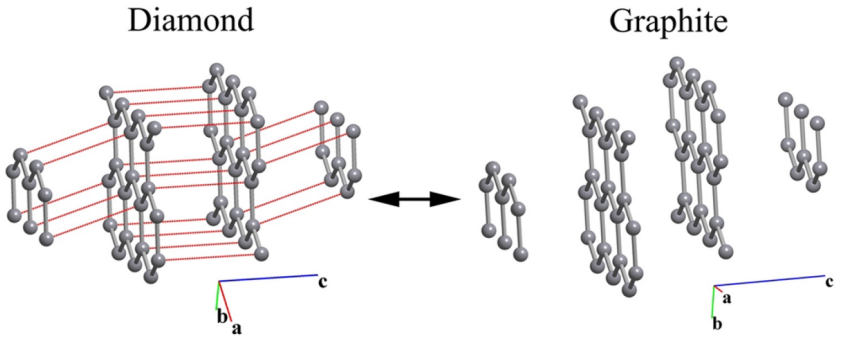

Figure 2.3: Reconstructive transition from graphite to diamond [39].

Reconstructive transition is a result of major rebuilding of chemical, crystallographic or both structures by diffusion. Therefore, it is also known as diffusional transition [40]. Characteristically, it involves the breaking of interatomic primary or secondary bonds and there is no group-subgroup relationship between parent and product phases. Transition of graphite to diamond by forming new bonds (Fig.2.3) is an example of reconstructive transition which requires significant amount of energy and time, so also referred as sluggish transition. Quartz-cristobalite transition is also a reconstructive transition example.

Displacive transition is a result of lattice distortion by dilatation or rotation due to the collective movements of atoms without changing the chemical composition and net symmetry of material. Unlike reconstructive transition, parent and product phases have a group-subgroup relationship, and it is a rapid transition due to the lack of diffusion. Ferroelectric- paraelectric and low(α phase)-high (β phase) quartz transitions are the examples of the displacive transitions. Rotational changes of perovskite structures as an example of displacive transition are given in Figure 2.4. If the given

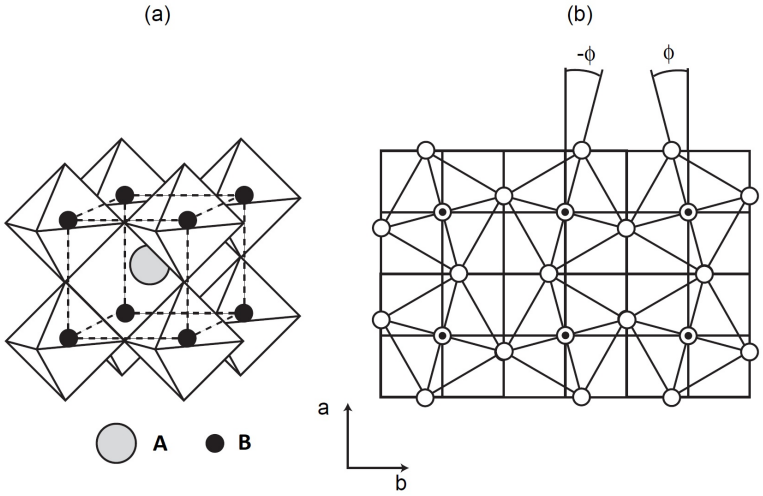

Figure 2.4: Unitcell of perovskite structures with ABO_3 general formula (a) and structural change due to rotation of ϕ (b) [37].

perovskite structure is $BaTiO_3$, cubic symmetry of high temperature paraelectric phase reduces into tetragonal symmetry with decreasing temperature which results with the ferroelectricity due to the distortion of polyhedra and displacement of ionic elements. If the given perovskite structure is $SiTiO_3$, it experiences the same symmetry change without ferroelectric properties. These type of transitions are also called *order-disorder transitions*.

There are also transitions without structural change like superfluid transition of liquid helium below 2.17K and superconductor transitions of some metallic and organic compounds below certain temperatures [37]. Covering the generalization and categorization of all types of phase transition in all types of materials is a quite extensive topic and it is hard to express all of them in this study. Due to the displacive character of α-INC-β transition of quartz, structural transition requires further attention. Properties of structural phase transitions can be investigated by using the Landau theory in addition to the soft mode concept.

2.3 Landau Phenomenological Model

Landau phenomenological theory was first suggested for the second order (continuous) phase transitions [41] to describe the transition mechanism in the vicinity of crit-

ical transition region. Along with the indication of feasibility for the first order [10] and the other types of transitions as reconstructive [42], superfluid [43] transitions and so on, it becomes the modern theory of phase transition. By means of statistical mechanics, investigation of a phase transition and behavior of a system during the transition requires to study microscopic interactions like exchange and dipole interactions of a magnetic system, pairing interactions of a superconductor or Coulomb and Van der Waals interaction of a structural transition. These atomic level calculations of the partition function eventually give information about the macroscopic system by relating to the thermodynamic variables. Without any need to these microscopic calculations, Landau phenomenological model gives a general understanding of phase transitions by defining an *order parameter* that is related to the change in the system. The change is the symmetry change for structural transitions which is the foundation of *universality* concept. Since, chemically and physically different systems with similar symmetries show quite similar characteristics within the Landau theory.

Starting point of the Landau theory is the order parameter and Landau potential relation in the vicinity of transition. Therefore, it is important to define a proper order parameter for the transition. Order parameter is an extensive physical quantity which occurs in the ordered (low symmetry) phase and vanishes in the disordered (high symmetry) phase. Different types of transitions have different order parameters. In paramagnetism-ferromagnetism transition it can be the magnetization m, in paraelectricity-ferroelectricity transition it can be the polarization p and in displacive transitions, it can be the tilt angle ϕ or distance between atoms η or ξ [37]. In this study, generalized macroscopic order parameter Q will be used for integrity of the study and to show multiple possible relation to different properties.

Order parameters of some structural transitions like α-INC-β transition in quartz, are defined by active irreducible representations (*irreps*) of parent phase due to the group-subgroup relation to the product phase. Stability of low symmetry phase is driven by a single active irrep of the high symmetry phase which turns into the order parameter of low symmetry phase by becoming nonzero in this phase. To define this type of order parameters (active irreps), space groups of at least one of the low and high symmetry phases should be known and the other should be confined to a small number of possible space groups [44]. As parent β phase has $P6_421$ space group representa-

tion, α phase has $P3_222$ space group representation as product during cooling from β phase, which satisfies the group-subgroup relation.

After definition of the proper order parameter (Q), Landau free energy and order parameter relation can be constructed. Landau free energy is a continuous function of the order parameter and transition drivers, temperature or pressure, through the transition like thermodynamic potentials Gibbs (G) and Helmholtz (F) free energies. Hence both notation F and G can appear as the Landau free energy during calculations. Since it is continuous, excess free energy due to transitions is infinitesimal in the vicinity of transition.The order parameter is also quite small and approaches zero close to the transition. Therefore, Taylor series expansion of the Landau free energy in terms of order parameter can be written as,

$$G(Q,T,P) = \alpha Q + \frac{1}{2}\beta Q^2 + \frac{1}{3}uQ^3 + \frac{1}{4}bQ^4 + \frac{1}{5}\gamma Q^5 + \frac{1}{6}cQ^6 + ... \tag{2.7}$$

where $\alpha, \beta, u, b, \gamma$ and c are the Landau coefficients which could depend on pressure and temperature. Under constant pressure condition, transition is driven by temperature change and symmetry changes are observed around the critical temperature T_c. The linear term (αQ) generally refers to the coupling of order parameter to an external field and it is zero ($\alpha = 0$) in the absence of that external field. Equilibrium conditions due to minimization of Landau free energy are expressed as,

$$\left(\frac{\partial G}{\partial Q}\right) = 0, \qquad \left(\frac{\partial^2 G}{\partial Q^2}\right) > 0 \tag{2.8}$$

With the vanishing of the order parameter ($Q = 0$) in the high symmetry (disorder) phase, equilibrium conditions of the transition (Eq.2.8) suggest positive and temperature dependent β which changes sign at the transition temperature ($T = T_c$).

$$\beta = a(T - T_c) \tag{2.9}$$

where a is a positive constant. Sign of β determines whether the phase is low temperature phase ($\beta < 0$) or high temperature ($\beta > 0$) phase. As a result Landau free energy takes the form of

$$G(Q,T) = \frac{1}{2}a(T - T_c)Q^2 + \frac{1}{3}uQ^3 + \frac{1}{4}bQ^4 + \frac{1}{5}\gamma Q^5 + \frac{1}{6}cQ^6 + ... \tag{2.10}$$

Classification of phase transition by Landau model is divided into two as symmetric and asymmetric cases. In symmetric case, Landau free energy remains unchanged

under inversion and reflection as shown in,

$$G(Q) = G(-Q) \tag{2.11}$$

Therefore, symmetry considerations of transition (Eq.2.11) does not allow the odd order terms which leads to free energy to its classic form

$$G = \frac{1}{2}a(T - T_c)Q^2 + \frac{1}{4}bQ^4 + \frac{1}{6}cQ^6 + ... \tag{2.12}$$

Minimizing symmetric free energy at the transition temperature gives the information about the order of the transition. In the symmetric case, quadratic term (with respect to Q^2) is dominant and sign of this term is deterministic. Under appropriate conditions, positive quadratic term ($b > 0$) induces second order transition, negative quadratic term ($b < 0$) induces fist order transition in the sense of Ehrenfest classification. However, presence of odd order terms bring asymmetry and discontinuity. In the asymmetric case, cubic term becomes dominant and transition is first order with a latent heat due to discontinuity.

Symmetric case with positive quadratic term $(b > 0)$

In the presence of positive quadratic term $(b > 0)$, sixth order term can be neglected $(c = 0)$ which leads to the second order transition with a continuous order parameter.

$$G(Q, T) = \frac{1}{2}a(T - T_c)Q^2 + \frac{1}{4}bQ^4 \tag{2.13}$$

Minimization of the reduced Landau free energy of Eq.2.13 $(\partial G/\partial Q = 0)$ gives, the root of $Q = 0$ and nonzero roots of order parameter (Q) as

$$Q = \pm \left[\frac{a}{b}(T_c - T)\right]^{1/2} \tag{2.14}$$

Combining Eqs. 2.13 and 2.14, Landau free energy of second order transition becomes,

$$G = -\frac{1}{4}\frac{a^2}{b}(T - T_c)^2 \tag{2.15}$$

Continuous behavior of the order parameter (Fig.2.5) implies the transition is of second order. Two deeps in the low temperature (ordered) phase $(T < T_c)$ in Fig.2.5 which are represented by the two identical free energy, can be related to the twinning

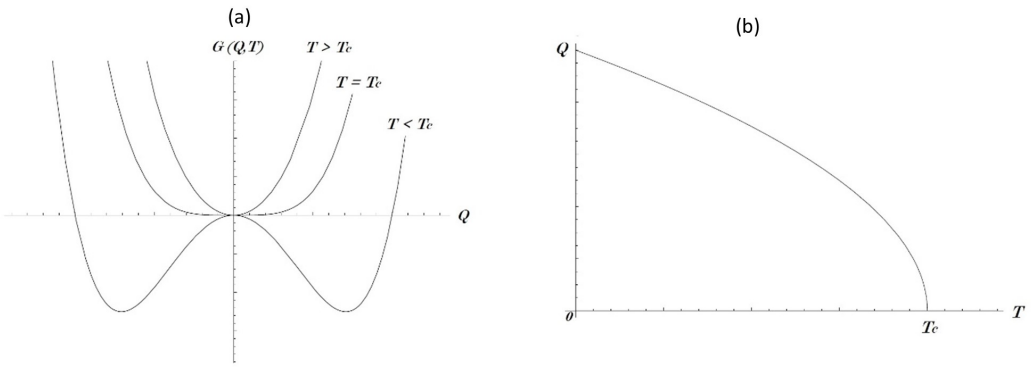

Figure 2.5: Order parameter dependence of Landau free energy (a) and temperature dependence of order parameter (b) for a second order transition

structures of the low temperature α-phase of quartz. Since temperature dependence of the free energy is obtained (Eq.2.15) in relation to Eq.2.14, thermodynamic quantities can be deduced by taking first and second order derivatives of the free energy as in Eqs. 2.4 and 2.5. The enthalpy H of the transition is deduced as

$$H = -\frac{1}{2}aT_cQ^2 + \frac{1}{4}bQ^4 \tag{2.16}$$

as a function of order parameter for a second order transition. Excess entropy S of the transition can be subtracted as

$$S = -\frac{1}{2}aQ^2 \tag{2.17}$$

which is a continuous function of order parameter for given conditions of the second order transition. Heat capacity is a characteristic parameter for the second order transition where the discontinuity occurs. The excess heat capacity C_p can be derived as

$$C_p = T\left(\frac{\partial S}{\partial T}\right)_p = \frac{1}{2}\frac{a^2}{b}T \tag{2.18}$$

at constant pressure. Since there is no order paramter ($Q = 0$) in the disordered phase, it also refers the jump in the heat capacity (ΔC_p) as discontinuity. However, in most experimental examples it is not like a step discontinuity but a divergent λ shape discontinuity. As a result, Landau model should be supported by fluctuations around the critical point.

Symmetric case with negative quadratic term $(b < 0)$

In the presence of negative quadratic term $(b < 0)$, positive sixth order term $(c > 0)$ become necessary due to symmetry and transition is called the fist order transition with a latent heat. By minimizing Landau free energy

$$G = \frac{1}{2}a(T - T_c)Q^2 + \frac{1}{4}bQ^4 + \frac{1}{6}cQ^6 \tag{2.19}$$

for the first order transition, temperature dependence of the order parameter can be obtained as

$$Q^2 = \frac{-b \pm \sqrt{b^2 - 4ac(T - T_c)}}{2c} \tag{2.20}$$

with the zero root $Q = 0$ describing the disordered phase. For the first order transition, transition temperature T_{tr} is higher than the critical temperature T_c. At the transition temperature, Q can be equal to zero and Q_0 (change from zero during transition)

$${Q_0}^2 = \frac{-b \pm \sqrt{b^2 - 4ac(T_{tr} - T_c)}}{2c} \tag{2.21}$$

to form an equilibrium between the ordered and disordered phases which is also shown in Fig.2.6. Discontinuity of the order parameter can easly be seen in Fig.2.6 at T_{tr} as an indication of the first order transition.

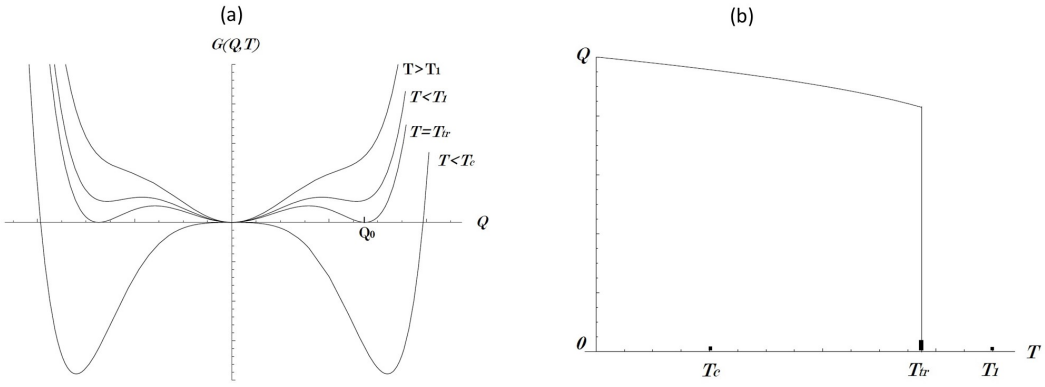

Figure 2.6: Order parameter dependence of the Landau free energy (a) and temperature dependence of order parameter (b) for a first order transition.

At the transition temperature where $Q = \pm Q_0$, both $G = (\pm Q_0)$

$$0 = \frac{1}{2}a(T_{tr} - T_c) + \frac{1}{4}b{Q_0}^2 + \frac{1}{6}c{Q_0}^4 \tag{2.22}$$

and the first order derivative of G with respect to the order parameter

$$0 = a(T_{tr} - T_c) + b{Q_0}^2 + c{Q_0}^4 \tag{2.23}$$

become zero by using Eq.2.19. Solving Eqs. 2.22 and 2.23 gives the expressions for ${Q_0}^2$ and ${Q_0}^4$ as

$${Q_0}^2 = \frac{-4a}{b}(T_{tr} - T_c), \;\; and \;\; {Q_0}^4 = \frac{3a}{c}(T_{tr} - T_c) \tag{2.24}$$

where T_{tr} takes the form of

$$T_{tr} = T_c + \frac{3b^2}{16ac} \tag{2.25}$$

Eq.2.24 shows that strength of the first order transition is directly related to the coefficent of qaudratic term. Since $b < 0$, decreasing b increases the gap between critical and transition temperatures as well as discontinuity. By combining Eqs. 2.24 and 2.25 the change of the order parameter can be expressed as

$${Q_0}^2 = -\frac{3b}{4c} \tag{2.26}$$

which is a constant at the transition temperature. As a result, thermodynamic quantities enthalpy and excess entropy of the first order transition can be expressed as

$$H = -\frac{1}{2}aT_cQ^2 + \frac{1}{4}bQ^4 + \frac{1}{6}cQ^6 \tag{2.27}$$

and

$$S = -\frac{1}{2}aQ^2 \tag{2.28}$$

respectively, in the same way as the second order. Latent heat of a first order transition is defined as the change in the enthalpy at the transition temperature and constant pressure, which can be written as

$$L = -\frac{1}{2}aT_{tr}{Q_0}^2 \tag{2.29}$$

That is also defined over entropy as $L = \Delta S T_{tr}$ due to the jump in the entropy of first order transition.

Asymmetric case with the cubic term $(u > 0)$

Asymmetric case involves the odd order terms to the classic form of free energy. Adding only the cubic term is effective enough to show the characteristics of transition and positive quadratic term (with respect to Q^2) is necessary to maintain the

continuity of the free energy during transition.

$$G(Q,T) = \frac{1}{2}a(T-T_c)Q^2 + \frac{1}{3}u|Q|^3 + \frac{1}{4}bQ^4 \tag{2.30}$$

Applying equilibrium condition of the first order transition $(G(Q) = G(0))$ to the Eq.2.30 gives

$$0 = 6a\,(T-T_c) + 4u\,|Q| + 3bQ^2 \tag{2.31}$$

with the roots of

$$Q_{1,2} = -\frac{2u}{3b}\left\{1 \pm \left[1 - \frac{9ab}{2u^2}\,(T-T_c)\right]^{1/2}\right\} \tag{2.32}$$

Due to the nonzero order parameter at the transition temperature, the difference between T_{tr} and T_c can be deduced from 2.32 as

$$T_{tr} - T_c = \frac{2u^2}{9ab} \tag{2.33}$$

Combining Eqs. 2.32 and 2.33 results with

$$Q = -\frac{3a}{u}(T_{tr}-T_c)\left\{1 \pm \left[1 - \frac{(T-T_c)}{(T_{tr}-T_c)}\right]^{1/2}\right\} \tag{2.34}$$

and at the transition temperature $T = T_{tr}$, this gives a constant order parameter Q_0 as

$$Q\,(T=T_{tr}) = Q_0 = -\frac{3a}{u}(T_{tr}-T_c) \tag{2.35}$$

and $Q\,(T=T_c) = 2Q_0$ at the critical temperature $T = T_c$, where the first order transition starts. Minimizing free energy (2.30) with respect to the order parameter as in the previous part, gives

$$0 = a\,(T-T_c) + u\,|Q| + bQ^2 \tag{2.36}$$

with the root of

$$Q_{1,2} = -\frac{u}{2b}\left\{1 \pm \left[1 - \frac{4ab}{u^2}\,(T-T_c)\right]^{1/2}\right\} \tag{2.37}$$

By inserting Eqs. 2.33 and 2.35 into the Eq.2.37, the temperature dependence of the order parameter can be rewritten as

$$Q = \frac{3}{4}Q_0\left\{1 + \left[1 - \frac{8}{9}\frac{(T-T_c)}{(T_{tr}-T_c)}\right]^{1/2}\right\} \tag{2.38}$$

In order to deduce the thermodynamic quantities in the asymmetric case for the first order transition, free energy with the qubic term (Eq.2.30) and the temperature dependence of the order parameter (Eq.2.38) can be combined. Enthalpy and excess entropy of the transition can be obtained as

$$H = \frac{1}{2}aT_cQ^2 + \frac{1}{3}u|Q|^3 + \frac{1}{4}bQ^4 \tag{2.39}$$

and

$$S = -\frac{1}{2}aQ^2 \tag{2.40}$$

respectively. Since this is a first order transition, accompanying latent heat due to entropy change is

$$L = -\frac{1}{2}aT_{tr}{Q_0}^2 \tag{2.41}$$

The order parameter dependence of the excess entropy has the same formulation for all transitions (Eqs.2.17, 2.28 and 2.40), that shows the ciritcal behavior of the transition is governed by the order parameter. In addition, the inverse susceptibility of the phases can be defined as

$$\chi_Q^{-1} = \frac{\partial^2 G}{\partial Q^2} \tag{2.42}$$

which gives information about the types of transitions close to the transition temperature as a response function.

Although Landau model gives the general picture about the phase transitions and their thermodynamic interpretations as shown up to this point, close to the critical region it needs to be supplemented by considering displacive nature of the transition as microscopic fluctuations with the soft mode concept and critical exponents.

2.4 Critical Exponents

Power laws are suggested to simplify problems which include a great number of degrees of freedom within a correlation length ξ as in the critical phenomena and quantum field theory. During phase transition, correlation length ξ gets larger close to the critical point (transition temperature) and becomes infinite at the critical point. So, the system parameters and functions such as the order parameter, specific heat, susceptibiliy etc. show some rapid changes or jumps close to the critical point. By

the definition of the proper order parameter (Section2.3), critical behavior of a system close to the transition temperature due to discontinuities or singularities, can be expressed by the power laws

$$jump \sim constant(-t)^{critical\,exponents} \tag{2.43}$$

where t is the dimensionless reduced temperature as

$$t = \frac{T - T_c}{T_c} \tag{2.44}$$

which shows divergence from the critical temperature T_c [45]. From this point on, temperature dependence of the order parameter can be written as

$$Q \sim (T - T_c)^{\beta} \tag{2.45}$$

in the vicinity of the transition and β is the critical exponent of the order parameter. In Section 2.3 for the symmetric second order transition, temperature dependence of the order parameter was obtained as $Q = \pm \left[\frac{a}{b}(T_c - T)\right]^{1/2}$ (Eq. 2.14). By setting $Q = 1$ at $T = 0$, it becomes

$$Q = \left(\frac{T_c - T}{T_c}\right)^{1/2} \tag{2.46}$$

with $\frac{b}{a} = T_c$ and critical exponent $\beta = 1/2$ below the transition temperature for the Landau model. Under these conditions, Eq.2.15 takes the form of

$$G = -\frac{b}{4}\left(\frac{T_c - T}{T_c}\right)^2 \tag{2.47}$$

By using the above equation, the inverse isothermal susceptibility (mechanic response function) derived from Eq.2.42 ig given by

$$\chi^{-1} = \frac{\partial^2 G}{\partial Q^2} = -\frac{b}{2}\left(\frac{T_c - T}{T_c}\right) \tag{2.48}$$

with the critical exponent $\gamma = 1$ from the Landau model. Other critical exponents can be derived in the same way or by using different models such as Ising model or spherical model. This is a simple example of scaling and renormalization for classical theories. Critical exponents for different parameters are given in Table 2.1 [45].

Very different systems can have the same critical exponents close to the transition, which is called the universal critical behavior. Systems with the same critical exponents and scaling can be assigned to the same universality class. Scaling is set

Table 2.1: List of the critical exponents

Critical exponent	Property	Classical Theories	Ising model $(d = 2)$	Ising model $(d = 3)$
α	Specific heat	0	0	0.110
β	Order parameter	1/2	1/8	0.325
γ	Response function	1	7/4	1.24
ν	Correlation term	1/2	1	0.64
δ	Critical isotherm	3	15	4.82

of rules to relate the critical exponents and was presented by different scientists as Stanley, Kadanoff and Fisher independently [46]. When the experimental results for critical exponents showed dissimilarities from the calculated ones, necessity for the more precise theory occurred. To solve this problem, Wilson suggested *renormalization group theory* which includes the transformation of the system Hamiltonian by mapping the critical point onto a fixed point [47]. Introduction of the renormalization group theory brings an update the scaling laws. Scaling rules of Rushbrooke, Widom and Griffiths can be constructed by using correlation function and dimensional analysis with the renormalization group theory. Rusbrooke's scaling law is given as [37,45]

$$\alpha + 2\beta + \gamma = 2 \tag{2.49}$$

by relating critical exponents. Fisher also renormalized the critical exponents as

$$\alpha_R = -\frac{\alpha}{1-\alpha} \text{ and } \gamma_R = \frac{\gamma}{1-\alpha} \tag{2.50}$$

where α_R and γ_R are renormalized critical exponents of real systems due to hidden variables [48, 49]. Thermodynamic properties can be expressed over renormalization group theory by means of the approximated free energy. The renormalization group expression for the specific heat can be written as

$$C_p = A^{\pm}|t|^{-\alpha}\left(1 + D^{\pm}|t|^{\Delta}\right) + B \tag{2.51}$$

where α is the critical exponent and $\Delta = 0.5$ with the constants $A^{\pm}$, $D^{\pm}$ for above and below T_c and the constant B. First order corrections are implemented to scaling term [47, 50]. Soft mode related fluctuations of the α-INC-β transition can be investigated with the above expressions of renormalization group.

2.5 Soft Mode Concept

In displacive transitions, atoms or ions change their positions or orientations which distorts lattice dynamics with specific vibrational phonon modes. These phonon modes can be optical modes of the zone center or acoustic modes of the zone boundary. Phonon frequency of these modes decreases as getting closer to the transition region, that is called softening of the phonon mode, and it becomes zero (frozen) at some point which induces the transition. After the transition, for stabilization soft optic modes come to a new dynamic equilibrium, *zone center transition*, while soft acoustic modes become a new zone center by folding, *zone boundary transition*. Relation of soft modes to the Landau model is given by [51]

$$\omega^2 \propto \chi^{-1} \tag{2.52}$$

where ω is the soft mode frequency and χ^{-1} is the susceptibility with the formula

$$\chi^{-1} = \frac{\partial^2 G}{\partial Q^2} = \frac{\partial H}{\partial Q} \tag{2.53}$$

over the free energy and enthalpy.

Besides the explanation of structural phase transition, soft mode concept is important to explain the existence of the incommensurate phase of quartz between α and β phases. During the α-β transition in quartz, a heterogeneous structure was observed due to the coexistence of phases and it was defined by the coupling of the transverse acoustic (TA) modes with the soft modes [32].

In relation to the soft mode frequencies, Pippard relations and Grüneisen parameter give another way to relate lattice dynamics to the thermodynamic properties to see the compatibility of the used models.

2.6 Pippard Relations

Pippard relations can be suggested to relate the thermodynamic and elastic properties in the vicinity of a transition temperature T_λ (λ point) by assuming the entropy surface as a cylindrical surface [52]. By means of this cylindrical approximation, entropy can

be expressed in terms of pressure p and temperature T close to T_λ

$$S(p,T) = S_0 + aT + f\left[T\left(\frac{dp}{dT}\right)_\lambda - p\right] \tag{2.54}$$

where S_0 and a are constants and λ notation is due to the λ like shape of specific heat (C_p) close to the transition. By using Eq.2.54, the relation between specific heat (C_p) and thermal expansion (α_p) the first Pippard relation can be derived in the form of

$$\frac{C_p}{T} = V\alpha_p\left(\frac{dp}{dT}\right) + \left(\frac{dS}{dT}\right)_V \tag{2.55}$$

where V is the volume. By using Eq.2.54, the relation between thermal expansion, $\alpha_p \equiv \left(\frac{1}{V}\frac{dV}{dT}\right)_p$ and the isothermal compressibility $\kappa_T \equiv -\left(\frac{1}{V}\frac{dV}{dp}\right)_T$ as the second Pippard relation can be derived in the form of

$$\alpha_p = \left(\frac{dp}{dT}\right)\kappa_T + \frac{1}{V}\left(\frac{dV}{dT}\right) \tag{2.56}$$

This Pippard relation will be used to form the relationship between the vibrational modes and elastic constants of the α-INC-β transition in quartz with the Grünesien parameter.

2.7 Grüneisen Parameter

Güneisen parameter (γ) can be defined both macroscopically in terms of termodynamic properties with the quasiharmonic approximation and microscopically by the vibrational frequencies and atomic motion. For the same material, both definitions should refer to the same dimensionless value which gives the way to correlate structural dynamics to the thermodynamic properties. The mode Grüneisen parameter can be defined as

$$\gamma = -\frac{V}{\nu}\left(\frac{d\nu}{dV}\right) \tag{2.57}$$

in terms of vibrational frequency (ν) and specific volume (V) [53]. At a constant pressure, the isobaric mode Grüneisen parameter (γ_p) can be generated from Eq.2.57 by its temperature dependence as

$$\gamma_p = -\frac{V\left(\partial\nu/\partial T\right)_p}{\nu\left(\partial V/\partial T\right)_p} = -\frac{\left(1/\nu\right)\left(\partial\nu/\partial T\right)_p}{\alpha_p} \tag{2.58}$$

where $\alpha_T \equiv \frac{1}{V}\left(\frac{\partial V}{\partial T}\right)_p$ is the isothermal expansion. Similarly, at a constant temperature, the isothermal mode Grüneisen parameter (γ_T) can be generated from Eq.2.57 by its pressure dependence as

$$\gamma_T = -\frac{V\left(\partial\nu/\partial p\right)_T}{\nu\left(\partial V/\partial p\right)_T} = \frac{\left(1/\nu\right)\left(\partial\nu/\partial p\right)_T}{\kappa_T} \tag{2.59}$$

where $\kappa_T \equiv -\frac{1}{V}\left(\frac{\partial V}{\partial p}\right)_T$ is the isothermal compressibility. For both forms of the mode Grüneisen parameter, ν can be related to the piezoelectric resonance and soft mode frequencies can be predicted for the α-INC-β transition in quartz which is the next part of our study.

2.8

a. Damping Constant

The soft mode relation to the structural transition was mentioned in the Section 2.5. Coupling of the soft optical mode to the transverse acoustic mode and its relation to the order parameter was shown for the α-INC-β transition in quartz by neutron scattering measurements [6, 54]. Evidently, temperature dependence of the damping constant (linewidth) of these phonon modes can be investigated by coupled models. Foundation of this pseudospin- phonon interaction was first described over the damping constant $\Gamma(\mathbf{k}\nu, \omega_\nu)$ as a function of the wave vector (k) and the peak frequency (ω) of ν^{th} phonon by Matsushita [55].The Lorentzian shaped dynamic scattering function $S(\mathbf{q}, \omega)$,with the pseudospin wave vector q, can be used to find the FWHM (full width at half maximum) which was related to the damping constant over an integration of all q in the Brillouin zone (BZ) as

$$\Gamma(\mathbf{k}\nu, \omega_\nu) \approx A \int_{BZ} S(q, 0) dq \tag{2.60}$$

where A is a proportionality constant with the slight temperature dependence and $\omega \approx 0$ due to the Debye type behaviour of $S(\mathbf{q}, \omega \approx 0)$ below the critical temperature [56]. Calculation of the integral in Eq.2.60 for KDP (K_2PO_4 is a crystalline which undergoes structural phase transition with the vibrational behavior) type of crystals, leads to the temperature dependence of the damping constant close to the transition

temperature T_c as

$$\Gamma_{sp} \approx A(1-Q^2)ln\left(\frac{T_c}{T-T_c(1-Q^2)}\right) \tag{2.61}$$

where Q is the order parameter [57]. This approximate relation can be expressed as

$$\Gamma_{sp} = \Gamma_0{}' + A'(1-Q^2)ln\left(\frac{T_c}{T-T_c(1-Q^2)}\right) \tag{2.62}$$

where Γ_0' and A' are background damping constant and the magnitude, respectively, and Eq.2.62 can be called as the pseudospin-phonon coupled (PS) model.
Another model for the calculation of the temprature dependence of the damping constant (Γ_{sp}) was suggested for the pseudospin-phonon coupled systems, by taking into account the energy fluctuations due to the phonon frequency shifts [58]. The mode frequency shifts of the phonon modes result in the broadening of the linewidths [56], which leads to the simplified damping constant as

$$\Gamma_{sp} \approx \left(\frac{T(1-Q^2)}{T-T_c(1-Q^2)}\right)^{1/2} \tag{2.63}$$

As in the previous model, this approximate relation for the linewidth of the pseudospin-phonon coupled system close to T_c can also be expressed as

$$\Gamma_{sp} = \Gamma_0 + A\left(\frac{T(1-Q^2)}{T-T_c(1-Q^2)}\right)^{1/2} \tag{2.64}$$

where Γ_0 and A are background damping constant and the magnitude, respectively,as before and Eq.2.64 can also be called as the energy fluctiation (EF) model.

b. Relaxation time

The inverse relaxation time of a pseudospin-phonon coupled system for the relaxation of the soft modes can be expressed as

$$\tau^{-1} = \frac{\omega^2}{\Gamma} \tag{2.65}$$

and, both PS and EF models can be used to describe the damping constant (Γ). Temperature dependence of the relaxation time according to the Arrhenius law can be written as

$$\tau = \tau_0 exp\left(-\frac{E_a}{k_B T}\right) \tag{2.66}$$

where τ_0, E_a and k_B are the attempt relaxation time, activation energy and the Boltzmann constant, respectively. Eq.2.66 can be rewritten in the logarithmic form

$$ln\tau = ln\tau_0 - \frac{E_a}{k_B T} \tag{2.67}$$

By combining Eqs. 2.65 and 2.67, activation energy of the crystalline system can be obtained.

2.9 Structure and Phases of Quartz

Quartz structure is a SiO_4 tetrahedra whose neighboring silica atoms share each oxygen atoms (Fig.2.7) and it is reduced to a SiO_2 . Orientation of Si-O-Si angle changes with temperature and pressure to maintain the stability and forms the different phase of quartz as high-temperature (β phase) and low-temperature quartz (α phase). Si-O-Si angle is $144°C$ for the α phase and $153°C$ for the β phase. Structural representation of the 2D projections of the α and β phase configurations due to the Si-O-Si link angle is given in Fig.2.8. SiO_4 piles in helical order and projected onto **c** plane.

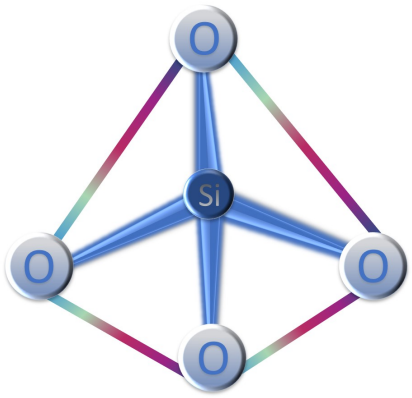

Figure 2.7: Schematic representation of SiO_4 tetrahedra.

α **phase** is stable at low pressure and temperature to be exact below $573°C$. It has three fold-trigonal symmetry with space group D_3^4. Adjacent tetrahedral structures SiO_4 in quartz piled in a hellical order (Fig.2.8), crystal has trigonal symmetry as a result. β **phase** is the high temperature phase of quartz at low pressure and stable between 573 and $870°C$. β phase has six fold-hexagonal symmetry with space group D_6^4. **Incommensurate phase** is a metastable phase which occurs between two com-

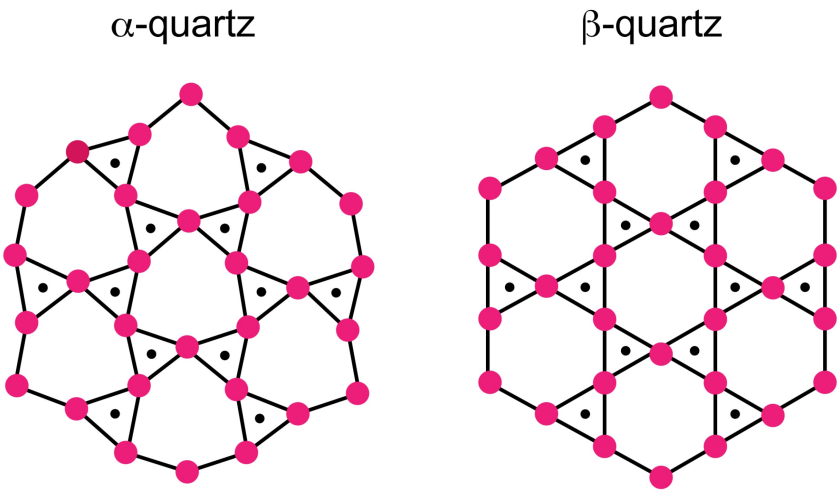

Figure 2.8: Structural representation of the 2D projections of α and β configurations [59]. Pink dots refer Oxygen atoms and small black dots are Silicon atoms.

mensurate phases during structural phase transition, in this case it is INC phase of quartz between α-β phases. While the coupling of TA modes with soft modes anisotopically is the reason of the occurrence of INC phase of quartz [31], damping of the LA modes can be related to the order parameter [60]. As an intermediate phase, INC phase does not show translational periodicity but 3D long range order.

Table 2.2: Enantimorphic space groups of α and β phases of quartz

Quartz	Right handed	Left handed
α phase	$P3_222$	$P3_121$
β phase	$P6_221$	$P6_422$

Due to the discontinuity of order parameter, α-INC-β phase transition in quartz is a first order transition with an accompanying latent heat. It is also a displacive transition according to the rotation of hexagonal structure to the trigonal lattice structure without changing the net hexagon while transforming from β to α phase of quartz through the INC phase or vice versa with inverse symmetries [18]. Both α and β phases have mirror symmetry enantimorphs with space groups given in Table 2.2. During transition, rotation can be right or left handed which results in the twinning structures mainly Dauphine and Brazil twins. Dauphine (electrical) twin structure consists of only either right or left handed symmetry. Along the **a** axis of this twin structure,

Table 2.3: Symmetry modes of quartz [64]

Crystal	Spatial Symmetry	Optic vibrations	Acoustic vibrations
α quartz	D_3^4	$4A_1 + 4A_2 + 8E$	$A_2 + E$
β quartz	D_6^4	$A_1 + 3B_1 + 2A_2 + 2B_2 + 4E_1 + 4E_2$	$A_2 + E$

mechanic pressure does not induce polarization. Brazil (optical) twin structure is formed of both right and left handed structure. While passing through the **c** axis, incident light changes its orientation in the direction of handedness in this twinning. Combination of these two twin structures is called Japan twin but it is not as common [11]. Although Brazil twin structure cannot be observed by diffraction experiments as a result of optic effect, Dauphine twin structure occurs around the critical point in the INC phase of quartz during transition. Observed structures have mirror symmetry over optical axis [61–63].

There is also a symmetry argument over group theoretical analysis. Quartz's unit cell consists of three SiO_2 tetrahedra in other words, nine atoms, so that the α and β phases have 27 vibrational normal modes ($3n$, $n = 9$) which can be expressed in terms of symmetry modes or irreducible representations (Table 2.3). A (rotationally symmetric), B (rotationally antisymmetric) and E (doubly degenerate) are Mulliken symbols for irreducible representations with subscripts 1 and 2 which represent symmetry and anti-symmetry with respect to a mirror plane (σ_v) that is perpendicular to the principle axis, respectively, as shown in Table 2.3. There are also subscripts g for the inversion symmetry and u for anti-symmetry [65, 66]. These vibrational modes can be Raman and infrared active or inactive due to the symmetries they have and one of them can become soft mode during transition. For the α-β transition in quartz, B_1 silent and A_1 Raman active modes are the soft modes in the β and α phases of quartz, respectively, [67]. These soft modes can be used to describe elastic properties of quartz [24] as we used in Sections 3.3 and 3.4. During α-β transition in quartz, elastic constants (C_{ij}) alter with respect to each other [19]. Such change effects intensely the direction related the physical properties due to the quite anisotropic characteristics of quartz. Therefore, complete set of elastic constants (C_{ij}) and their linear combinations as shear moduli (C_{44} and C_{66}) and linear incompressibilities (K_1 and K_3) were obtained experimentally [19, 68] and theoretically [69] for the α phase of quartz.

For the α-β transition in quartz, the elastic constants in connection with the transformation strain should decrease while approaching the 2^{nd} order transition point and vanish at that point. For small lattice strain, transition changes its character to a 1^{st} order transition close to the 2^{nd} order due to the coexistence of α and β phases which corresponds to the INC phase [25]. Elastic [34] and piezoelectric [35] properties of INC phase and thermal strain [70] close the transition have been measured for the α-β transition in quartz.

CHAPTER 3

CALCULATIONS AND RESULTS

3.1 Calculations of the tilt angle (ϕ^4) and the tilt angle susceptibility (χ_ϕ^{-1})

Temperature dependence of the order parameter and susceptibility is calculated by using Landau phenomenological model for the $\alpha - \beta$ transition in quartz.The fourth power of the tilt angle (ϕ^4) is defined as an order parameter which was fitted to the experimental data [24] according to the Landau model.

For the symmetric first order transition, using the temperature dependence of the order parameter (Eq.2.20), we can obtain

$$Q^4 = \frac{b^2}{2c^2} - \frac{a}{c}(T - T_c) \pm \frac{b^2}{2c^2}\left[1 - \frac{4ac}{b^2}(T - T_c)\right]^{1/2} \tag{3.1}$$

by taking the square of both side of the equation. Square root in the Eq.3.1 can be expanded up to x^2 in the power series as

$$(1 - x)^{1/2} = 1 - \frac{1}{2}x + \frac{1}{8}x^2 - ..... \tag{3.2}$$

by neglecting all the higher order terms and with the condition that $x \ll 0$, we find

$$x = \frac{4ac}{b^2}(T - T_c) \tag{3.3}$$

The above approximation reduces Eq.3.1 to a quadratic equation in the form of

$$Q^4 = a_0 + a_1 T + a_2 T^2 \tag{3.4}$$

with the constants a_0, a_1 and a_2. This quadratic equation of the order parameter was fitted to the experimental data for the tilt angle [24] as an order parameter $(Q = \phi)$ for the α phase of quartz. As pointed out in Section 2.3, order parameter can take different forms, which is the tilt angle (ϕ) in this study. The constants a_0, a_1 and a_2

were obtained from the fit as given in Table 3.1. Fig. 3.1 shows that the tilt angle (ϕ) fitted to the Eq.3.4 withe the observed data [24].

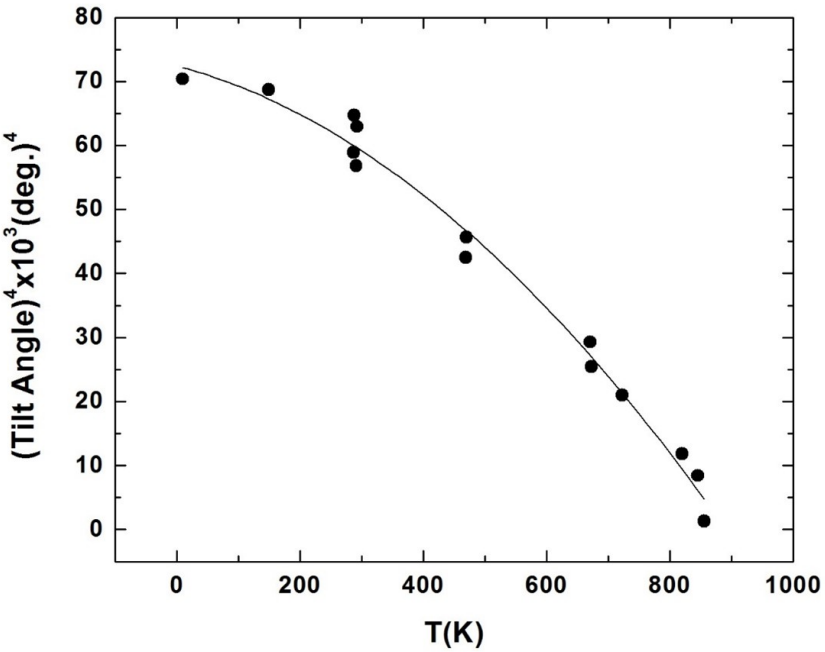

Figure 3.1: Temperature dependence of the tilt angle (ϕ) for the α-β transition in quartz with the fit of Eq.3.4 to the experimental data [24] ($T_c = 846K$).

Eq.2.20 can also be written in the form of

$$Q^2 + \frac{b}{2c} = \pm\sqrt{\frac{b^2}{4c^2} - \frac{a}{c}(T - T_c)} \tag{3.5}$$

By taking square of both sides, one can obtain

$$Q^4 + \frac{b^2}{4c^2} + \frac{b}{c}Q^2 = \frac{b^2}{4c^2} - \frac{a}{c}(T - T_c) \tag{3.6}$$

which simplifies to

$$\psi = Q^4 + \frac{b}{c}Q^2 = -\frac{a}{c}(T - T_c) \tag{3.7}$$

The above equation is approximately equivalent to the inverse susceptibility (Eq.2.42) of order parameter above T_c which can be found from the definition

$$\chi_Q^{-1} = \frac{\partial^2 G}{\partial Q^2} = a(T - T_c) + 3bQ^2 + 5cQ^4 \tag{3.8}$$

in the ordered α phase and

$$\chi_Q^{-1} = a(T - T_c) \tag{3.9}$$

in the disordered β phase since the order parameter is zero in the β phase. By using the experimental data for the tilt angle [24], the function ψ can be calculated as a function of the temperature difference according to Eq.3.7 as shown in Figure 3.2. ψ function was fitted to calculated data in the form of

$$\psi = c_0 + c_1(T_c - T) \tag{3.10}$$

with the constats c_0 and c_1 in the α phase of quartz and placed in Table 3.1

Table 3.1: Coefficients a_0, a_1 and a_2 (Eq. 3.4) and c_0 and c_1 (Eq. 3.10) which were determined by using the experimental data [24] for the α-β transition in quartz ($T_c = 846K$).

a_0x10^4	a_1 (K^{-1})	a_2x10^{-2} (K^{-2})	c_0x10^{-2}	c_1 (K^{-1})
7.24	-24.9	6.33	22.73	66.13

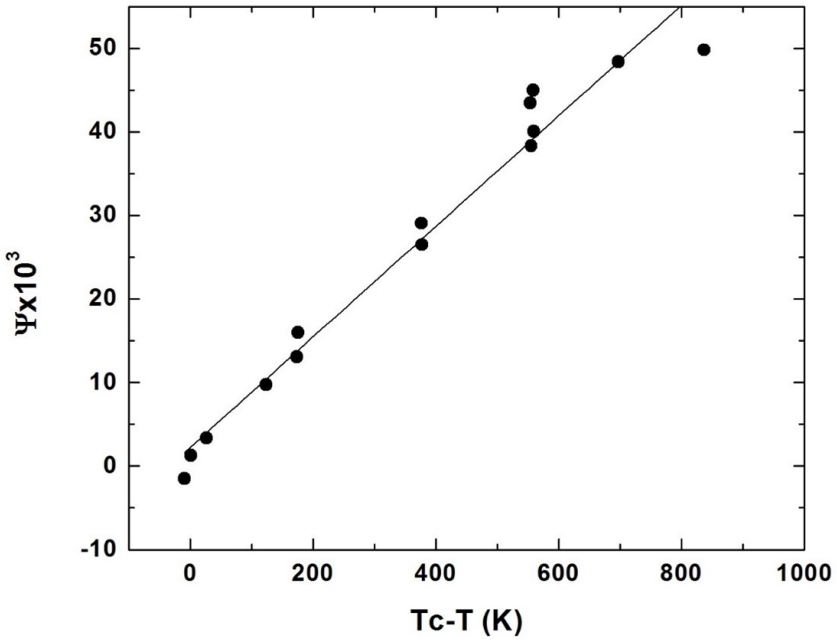

Figure 3.2: Variation of the function $\psi = \phi^4 + \frac{b}{c}\phi^2$ (Eq. 3.7) with temperature, which was obtained for the α-β transition in quartz ($T_c = 846K$).

Inverse susceptibility of the tilt angle χ_ϕ^{-1} ($Q = \phi$) was calculated by using the constants (Table 3.1) according to Eq.3.8 for the low temperature α phase and the high temperature β phase (Eq.3.9) as plotted in Figure 3.3 as a function of temperature difference $(T_c - T)$.

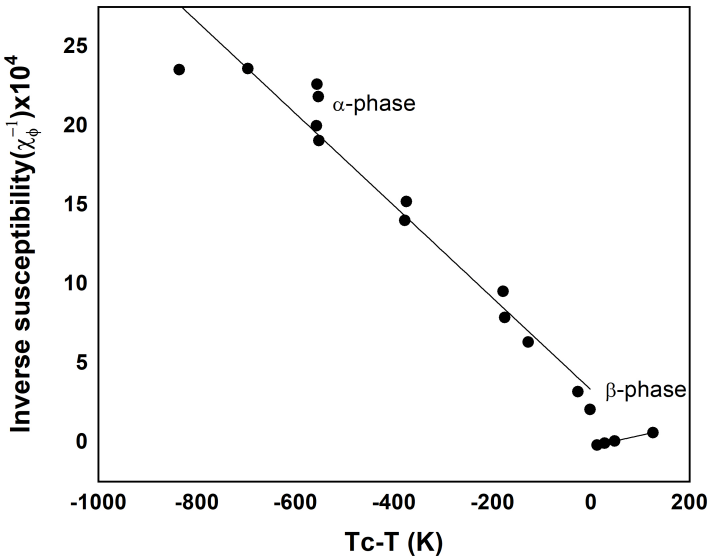

Figure 3.3: Inverse tilt angle susceptibility χ_ϕ^{-1} as a function of $T_c - T$, which was calculated for the α-β transition in quartz ($T_c = 846K$).

In this study, the fourth power of the tilt angle (ϕ) as an order parameter and the inverse susceptibility of the tilt angle (χ_ϕ^{-1}) were analyzed as a function of the temperature for the α-β transition of quartz by using the Landau model (Eq.2.19).

Table 3.2: Values of the ratio of the parameters given in the free energy (Eq.2.19) for the α-β transition in quartz ($T_c = 846K$). [2]

a/c	b/c	a/b	$(4ac/b^2)$ x10^{-2}
66.13	-77.65	-0.85	4.4

For this analysis, the symmetric solution of the Landau phenomenological model for the first order transition (Eq.2.20) was fitted to the experimental data for the tilt angle [24] in the form of the quadratic equation (Eq.3.4) with the help of the approximation (Eq.3.2) close to the critical temperature T_c of quartz. Figure 3.1 shows that the fit is reasonably well with the constants (Table 3.1). Once the tilt angle was set as an order parameter, inverse susceptibility of the tilt angle (χ_ϕ^{-1}) was predicted as a function of temperature according to Eq.3.8 via Eq.3.7 in the form of Eq.3.10. The ratio of constants of the free energy (Eq.2.19) and order parameter (Eq.2.20) were determined from Eq.3.1 through Eq.3.4 and ψ (Eqs.3.7 and 3.10) with the use of experimental

values of tilt angle [24] as listed in Table 3.2. These ratios and the experimental data [24] were also used in the determination of the temperature dependence of the tilt angle inverse susceptibility (χ_{ϕ}^{-1}) by Eq.3.8 (Fig.3.3). Inverse susceptibility of the tilt angle χ_{ϕ}^{-1} decreases linearly with decreasing temperature difference $T_c - T$ in the α phase and increases also linearly above T_c in the β phase as expected from the molecular dynamics calculations [71].

During the phase transition from the β phase to the α phase, SiO_4 tetrahedra rotates through tilt angle (ϕ) [72] which occurs in the α phase and vanishes in the β which has as disordered structure [24]. According to the Landau theory, the order parameter can take two opposite values in the α phase of quartz which leads to Dauphine twin structure through rotations [18] which is directly related to the tilt angle. Therefore, temperature dependence of the most physical properties can be expressed in terms of order parameter in the α phase of quartz as shown in Section 2.3 and given in the previous study [32] for the first order transition of Landau theory.

3.2 Calculations of the thermodynamic properties via Landau model with the cubic term

By using continuity of Gibbs free energy through the phase transition, thermodynamic properties such as entropy S, susceptibility χ and heat capacity C_p can be expressed over the temperature dependence of the order parameter according to the Landau theory. This was studied for the symmetric first order transition of Landau phenomenological model by means of free energy expansion in terms of the order parameter with the even terms up to sixth order [18]. Introduction of the INC phase [1] brings the effects of fluctuations which can be provided by including the cubic term to the free energy expansion in the Landau theory [73]. Thermodynamic properties of interest were derived from the expansion of the Gibbs free energy by including the cubic term as demonstrated in Section 2.3 with the experimental data of the excess heat capacity ΔC_p [18]. Temperature dependence of these quantities were also compared with the experimental counterparts from the literature [6, 18, 74–76]

Order parameter (Q) calculations

Free energy expansion with the cubic term is given (Eq.2.30) as

$$G(Q,T) = \frac{1}{2}a(T-T_c)Q^2 + \frac{1}{3}u|Q|^3 + \frac{1}{4}bQ^4 \tag{3.11}$$

with the solution

$$Q = \frac{3}{4}Q_0\left\{1 + \left[1 - \frac{8}{9}\frac{(T-T_c)}{(T_{tr}-T_c)}\right]^{1/2}\right\} \tag{3.12}$$

under equilibrium conditions and constrictions of the α phase of quartz (Section 2.3). Eq.3.12 was normalized with respect to Q_0 at T_{tr} and the normalized order parameter (Q/Q_0) was calculated as a function of temperature as plotted in Figure 3.4 with the observed data (η/η_0) [6, 74] and (ϕ/ϕ_0) [75].

The relation for the soft mode frequency (ω) and the macroscopic order parameter was given in Section 2.5 and the order parameter was related to the fourth power of the tilt angle (ϕ) in the previous study. Therefore, their relation can be written as

$$\phi^4 \propto Q \propto \omega^2 \tag{3.13}$$

According to the above equation, linear relationship between normalized macroscopic order parameter Q/Q_0 and the square of the soft mode frequency ω^2 was constructed in the form of

$$Q/Q_0 = a^{'} + b^{'}\omega^2 \tag{3.14}$$

where $a^{'}$ and $b^{'}$ are coefficients. At $T < T_c$ in the α phase of quartz, calculated normalized order parameter (Q/Q_0) (Eq.3.12) was plotted as a function of the soft mode frequency (squared) according to Eq.3.14 in Fig.3.5. The soft mode observed Raman data were used with the uncertainties for the α-β transition in quartz [75]. The coefficients $a^{'}$ and $b^{'}$ (Eq.3.14) were obtained from fit to the observed data as given in Table 3.3.

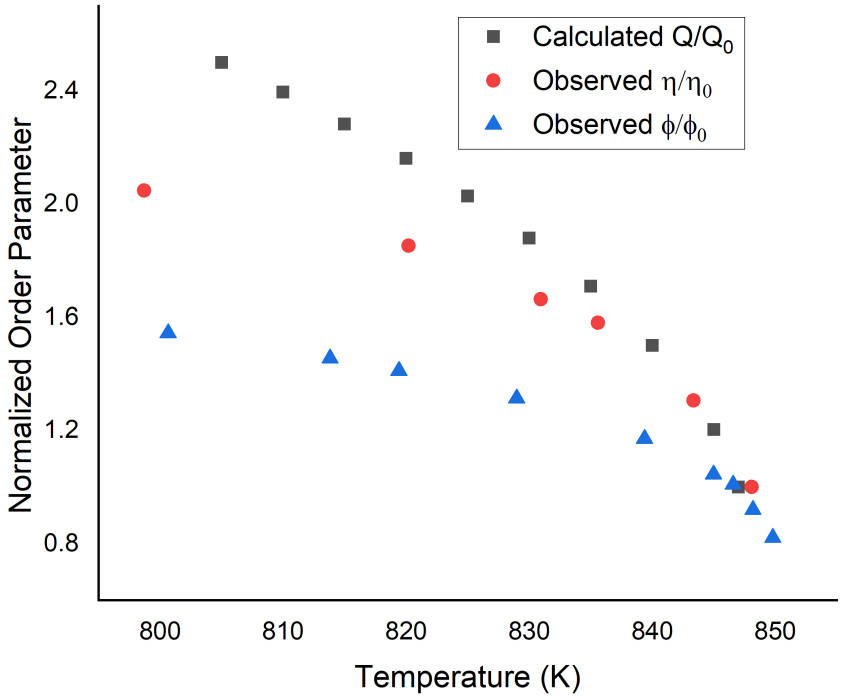

Figure 3.4: Temperature dependence of normalized order parameter calculated for the α-β transition in quartz by using Eq.3.12 according to the Landau phenomenological model with the cubic term (Eq.3.11) and compared to observed data (η/η_0) [6, 74] and (ϕ/ϕ_0) [75]

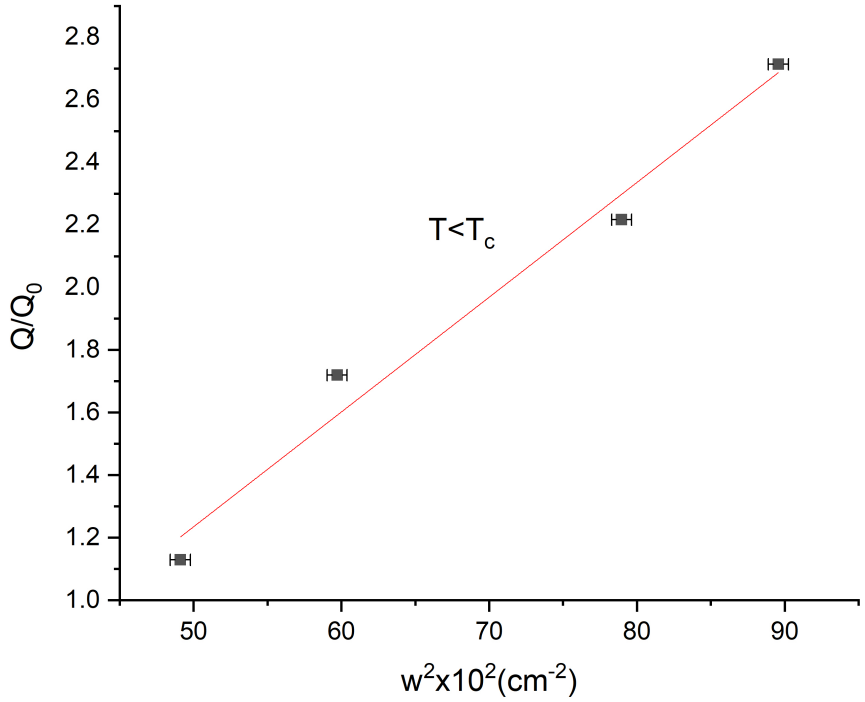

Figure 3.5: "Variation of normalized order parameter with the observed Raman soft-mode frequency ω (squared)($\sim 100cm^{-1}$ at $500°C$) in the α phase ($T < T_c$) with the uncertainties [75] according to Eq.3.12 through Eq.3.14 close to the α-β transition in quartz.

Table 3.3: $a^{'}$ and $b^{'}$(Eq.3.14), a_0 and a_1 (Eq.3.21) for the α-β transition in quartz with the observed values [18] of the transition (T_{tr}) and critical (T_c) temperatures.

Quartz	$T_{tr}(K)$	$T_c(K)$	$-a^{'}$	$b^{'}(cm^2)$	a_0x10^5 $(K^4.J^{-2}.mol^2)$	$-a_1$ $(K^3.J^{-2}.mol^2)$
$\alpha-\beta$ transition	847	840	0.5998	0.0367	1.73	200.3

Inverse susceptibility (χ^{-1}) calculations

Inverse susceptibility of both α and β phases can be obtained from the definition of the inverse susceptibility (Eq.2.42) by the free energy (Eq.3.11) as

$$\chi^{-1} = a\,(T - T_c) + 2u\,|Q| + 3bQ^2 \tag{3.15}$$

which can be related to soft mode frequencies through Eq.3.13 as

$$\chi^{-1} = a\,(T - T_c) + 2\,u^*\omega^2 + 3b^*\omega^4 \tag{3.16}$$

with the renormalized coefficients u^* and b^*.

Table 3.4: Values of the parameters a, u and b (Eq.3.11), u^* and b^* (Eq.3.16) and, the values of the order parameter Q_0 (at $T = T_{tr}$) (Eq.2.35), latent heat L (Eq.2.41) and the observed entropy S_β (in the β phase) [76] for the α- β transition in quartz. Observed values of the transition temperature (T_{tr}) and the critical temperature (T_c) are also given [5, 18]

Quartz	$T_{tr}(K)$	$T_c(K)$	$-ux10^3$ (J/mol)	$bx10^3$ (J/mol)	$-u*$ $(J/mol.cm^{-2})$	$b*$ $(J/mol.cm^{-6})$
$\alpha-\beta$ transition	847	840	18.27	104.1	0.237	0.292
			a $(J/K.mol)$	Q_0	$-L$ (J/mol)	S_β $(J/K.mol)$
			101.8	0.117	590.2	105.079

Temperature dependence of the normalized inverse susceptibility was estimated over Eq.3.15 by means of Eq.3.11 and Eq.3.12 for the low and high temperature phases of quartz with the coefficients a,u and b of Eq.3.11 (Table3.4) which were obtained from the analysis of the order parameter according to the Landau mean field model with a cubic term. Above T_c in β phase, order parameter becomes zero $(Q = 0)$ and the inverse susceptibility equation (Eq.3.15) reduces to $\chi^{-1} = a\,(T - T_c)$ which was plotted in Figure 3.6. In this figure, the inverse susceptibility values calculated from the Landau model with the cubic term are shown (black dots) and with the even powers (Q^4) [18] (triangles) for comparison. Molecular dynamics simulation results [71] for two different number of atoms (N) with the system size $N = 1080$ (black squares) and $N = 2060$ (empty squares) were also shown in Fig.3.6 for the inverse susceptibility per atom.

Inverse susceptibility as a function of the soft-mode frequency (squared) was also calculated by Eq.3.16 using the experimental data for the α-phase ($T < T_c$) [75] and β-phase ($T > T_c$) [67]. Silent soft mode dependence of the inverse susceptibility is given in Figure 3.7 in the β-phase of quartz ($T > T_c$) with the renormalized coefficients u^* and b^* (Eq.3.16) (Table 3.4). They were determined from the fit to the

observed data [67] for the β-phase. For the calculations below T_c , Eq.3.16 was fitted to the observed data [75]. However, this did not work out for the α-phase.

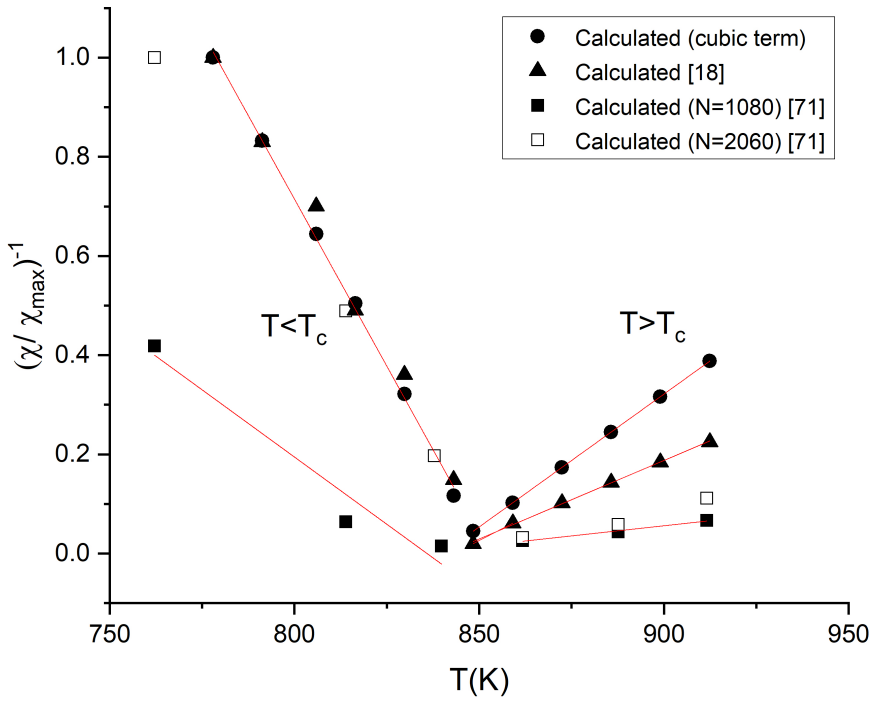

Figure 3.6: $(\chi/\chi_{max})^{-1}$ calculated as a function of temperature according to Eq.3.15 through Eq.3.12 for the α-β transition in quartz (black dots). Calculated values with different methods [18, 71] are also shown.

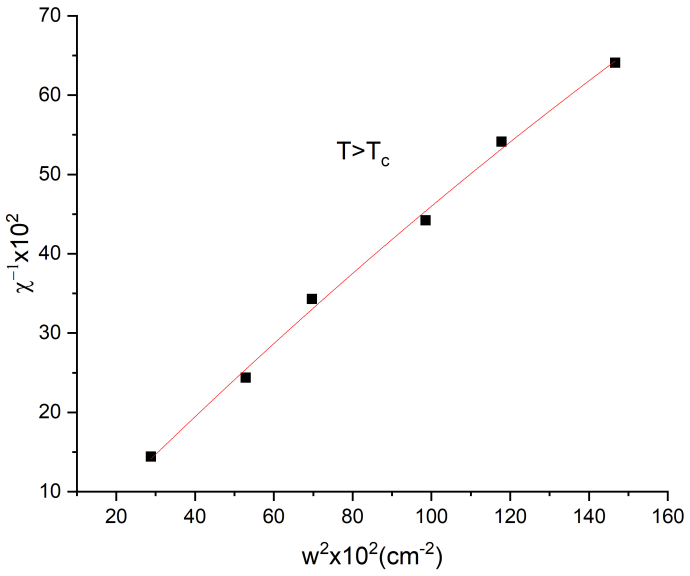

Figure 3.7: Variation of the inverse susceptibility (χ^{-1}) calculated (Eq.3.16) with the square of the observed Raman frequency ω (squared) of the silent soft phonon in the β phase [67] for the α-β transition in quartz [5].

Excess entropy (ΔS) calculations

By using the latent heat definition for the first order transition $L = -\frac{1}{2}aT_{tr}{Q_0}^2$ (Eq.2.41) and temperature dependence of the order parameter (Eq.3.12), excess entropy in relation to the free energy as shown in Section 2.3 with $S = -\frac{1}{2}aQ^2$ (Eq.2.40), can be rewritten in the form of

$$S = \frac{9}{16}\frac{L}{T_{tr}}\left\{1 + \left[1 - \frac{8}{9}\frac{(T - T_c)}{(T_{tr} - T_c)}\right]^{1/2}\right\}^2 \tag{3.17}$$

for α-β transition in quartz. Excess entropy (ΔS) was defined as the entropy difference between α- phase (S_α) and β- phase (S_β) and it was calculated by Eq.3.17 and by fitting to the observed data [76] with the constant entropy at $T = 850K$ in the β phase (Fig.3.8). Calculated latent heat L and constant entropy S_β are given in Table 3.4. Calculated and observed entropy values [76] are given in Figure 3.8.

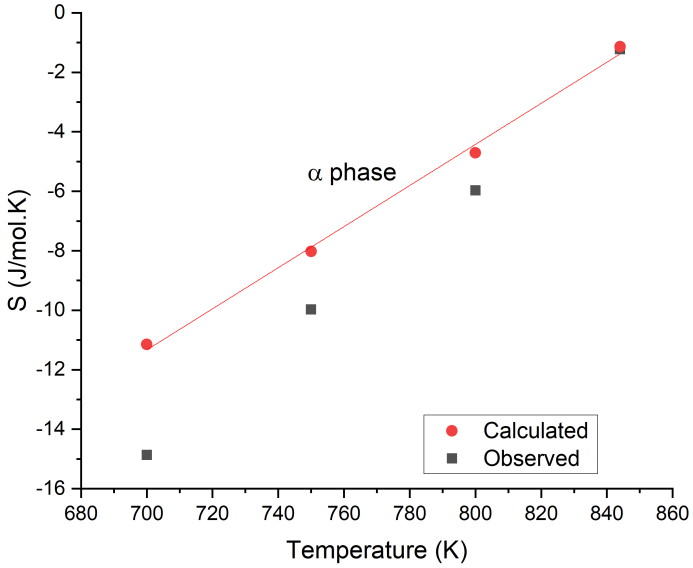

Figure 3.8: Temperature dependence of entropy S calculated according to Eq.3.17 in the α phase of quartz. Observed data [76] are also shown.

Excess heat capacity (ΔC_p) calculations

By using the free energy expansion with the cubic term (Eq.3.11) and its relation to the heat capacity (C_p) (Eq.2.5) with the excess entropy (ΔS) (Eq.3.17), temperature dependence of heat capacity can be obtained in the form of

$$\left(\frac{T}{C_p}\right)^2 = \frac{16\,(T_{tr}-T_c)^2}{a^2 Q_0^4}\left\{1+\left[1-\frac{8}{9}\frac{(T-T_c)}{(T_{tr}-T_c)}\right]^{-1/2}\right\}^{-2} \tag{3.18}$$

By using above equation, excess heat capacities were deduced at the critical temperature

$$\frac{T}{\Delta C_p} = \frac{2\,(T_{tr}-T_c)}{aQ_0^2}\ at\ T=T_c \tag{3.19}$$

and at transition temperature

$$\frac{T}{\Delta C_p} = \frac{(T_{tr}-T_c)}{aQ_0^2}\ at\ T=T_{tr} \tag{3.20}$$

for the α-β transition in quartz. Temperature dependence of the heat capacity is plotted in the form of $(T/C_p)^2$ in Figure 3.9 with the observed data [18] in the α-phase of quartz. Linearity of $(T/C_p)^2$ with the temperature was limited between temperatures 720K and 840K where the critical and the transition temperatures are

840K and 847K. Linear variation of the $(T/C_p)^2$ was fitted to the observed [18] data according to

$$(T/C_p)^2 = a_0 + a_1 T \tag{3.21}$$

with the coefficients a_0 and a_1 as given in Table 3.3.

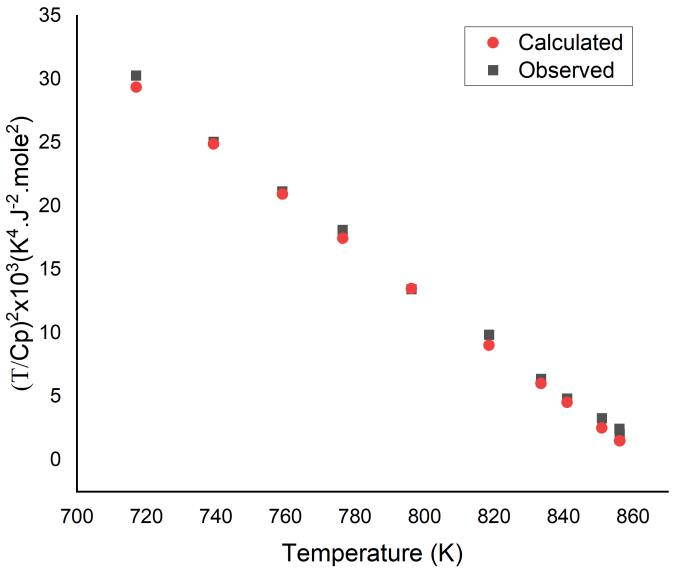

Figure 3.9: Temperature dependence of the heat capacity C_p calculated in the form of $(T/C_P)^2$ according to Eq. 3.18 for the α phase of quartz with the observed data [18].

Spontaneous strain (V_s) calculations

Spontaneous strain (V_s) can be defined by the lattice parameter V (volume) of the α phase as

$$V_s = \frac{V - V_0}{V_0} = \frac{\Delta V}{V_0} \tag{3.22}$$

where V_0 is the reference parameter due to the stability field of high temperature β phase by extrapolating to the same temperature [18]. By using the relation between the order parameter and strain as

$$V_s \propto Q^2 \tag{3.23}$$

for the α-β transition in quartz [18] and the temperature dependence of order parameter (Eq.3.12), spontaneous strain can be written in the form of

$$V_s = \frac{9}{16} V_{s,0} \left\{ 1 + \left[1 - \frac{8}{9} \frac{(T - T_c)}{(T_{tr} - T_c)} \right]^{\frac{1}{2}} \right\}^2 \tag{3.24}$$

with the discontinuity value $V_{s,0}$ [18] at the transition temperature. Proportionality in Eq.3.23 leads to $V_{s,0} \propto Q_0^2$ by the definitions in Eq.3.12 and Eq.3.24.

To calculate the dependence of the spontaneous strain, the temperature dependence of V_0 was first reconstructed according to

$$V_0 = c_0 + c_1 T \tag{3.25}$$

with the constants c_0 and c_1 above the transition temperature T_{tr}. By fitting Eq.3.25 to the observed neutron and X-ray diffraction data [18], constants were determined as shown in Table 3.5 with the reference volume $V_0 = 118.5$Å at the stability field of β-phase ($T_c = 1138K$) [18]. $V_{s,0}$ value was deduced from Eq.3.24 with the help of the observed V value [18] at the transition temperature of $847K$ as also shown in the Table 3.5.

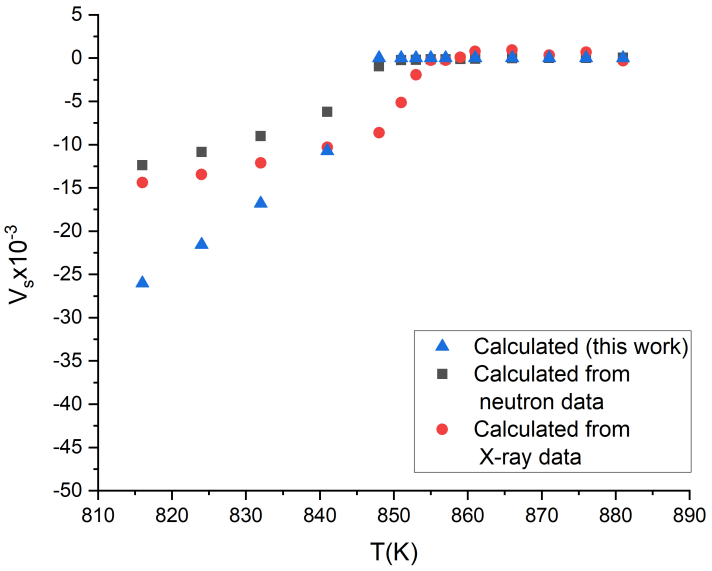

Figure 3.10: Temperature dependence of the spontaneous strain V_s calculated according to Eq.3.24 for the α -β transition in quartz as shown with the calculated V_s values [18] from the neutron and X-ray diffraction data

Spontaneous strain was calculated from Eq.3.24 as a function of temperature for α-β transition in quartz. Calculated values (triangles) from the Landau mean field model with the cubic term are shown in Figure 3.10 with those calculations from the observed data [18]. Neutron (squares) and X-ray (dots) diffraction calculations were obtained from the Landau model with the even order terms up to the fourth power where the critical temperature was found as $T_c = 843.9K$ [18] which was shifted about $\Delta T_c = 3.9K$ to match the critical temperature of our calculations $(T_c = 840K)$.

By using the relation between strain and the order parameter (Eq.3.23), normalized order parameter squared can be obtained as

$$(Q/Q_0)^2 = c_0^{'} + c_1^{'} V_s \tag{3.26}$$

as a linear function of V_s where $c_0^{'}$ and $c_1^{'}$ are constants (Table 3.5). Calculated normalized order parameter $(Q/Q_0)^2$ according to the Landau model with the cubic term (Eq.3.11) plotted as a function of spontaneous strain V_s (Eq.3.24) in Figure 3.11a with the calculated values from the observed neutron and X-ray diffraction data [18] for the α phase of quartz.

Table 3.5: Values of the observed spontaneous strain V_0 and $V_{s,0}$ (at $T = T_{tr}$) [18], coefficients c_0 and c_1 (Eq.3.25) with the observed critical temperature (T_c), and the values of the coefficients $c_0^{'}$ and $c_1^{'}$ (Eq.3.26) for the α- β transition in quartz [5].

Quartz	V_0(Å^3) at 1138 K	c_0 (Å^3)	$-c_1 x 10^{-5}$ (Å$^3/K$)	$T_c(K)$	$-V_{s,0} x 10^3$ (Å^3)	$c_0^{'}$	$c_1^{'} x 10^{-3}$
$\alpha - \beta$ transition	118.15	118.15	3.64	843.9	5.1	0	5.1

Besides spontaneous strain, the relation between order parameter η [70] and anomalous strain ΔL can be stated as

$$\Delta L \propto \langle \eta^2 \rangle \tag{3.27}$$

by the definition

$$\Delta L\,(T) = L\,(T) - L_B(T) \tag{3.28}$$

with the background elastic strain $L_B(T)$ whose temperature dependence is given as

$$L_B\,(T) = b_0 + b_1 T \tag{3.29}$$

with constants b_0 and b_1 [70] (Table 3.6).

Calculated normalized order parameter (squared) $(Q/Q_0)^2$, is plotted as a function of $\Delta L/L_B$ ratio (Fig.3.11b), which was calculated by Eq.3.28 with the observed elastic strain ΔL data [70] and the background elastic strain $L_B(T)$ (Eq.3.29) for the INC-β transition in quartz. This nonlinear relation was also constructed according to

$$(Q/Q_0)^2 = b_0^{'} + b_1^{'}(\Delta L/L_B) \tag{3.30}$$

where constants $b_0^{'}$ and $b_1^{'}$ were obtained due to the two temperature intervals (Fig.3.11b) as given in Table 3.6. Experimentally obtained critical ($T_c = 838.7$K) and transition ($T_0 = T_{tr} = 845.7$K) temperatures [70] with the temperature difference $T_0 - T_c = 7$K were shifted to $T_c = 840$K and $T_{tr} = 847$K for the observed data [18], which were used in our calculations (Fig.3.11b).

Table 3.6: "Values of the coefficients b_0 and b_1 (Eq.3.29), $b_0^{'}$ and $b_1^{'}$ (Eq.3.30), within the temperature intervals indicated with the observed transition temperature T_0 for the elastic stain ΔL [70] close to the incommensurate (INC)- β transition in quartz." [5]

Quartz	$T_0(K)$	$b_0(cm)$	b_1x10-5 (cm/K)	Temperature Interval (K)	$-b_0{'}$	$b_1^{'}$	Temperature Interval (K)
INC-β transition	845.7	1.00834	1.5386	$842.23 < T < 846.7$	6.002	7.185	$801.1 < T < 826.8$
					1.803	4.002	$831.9 < T < 846.2$

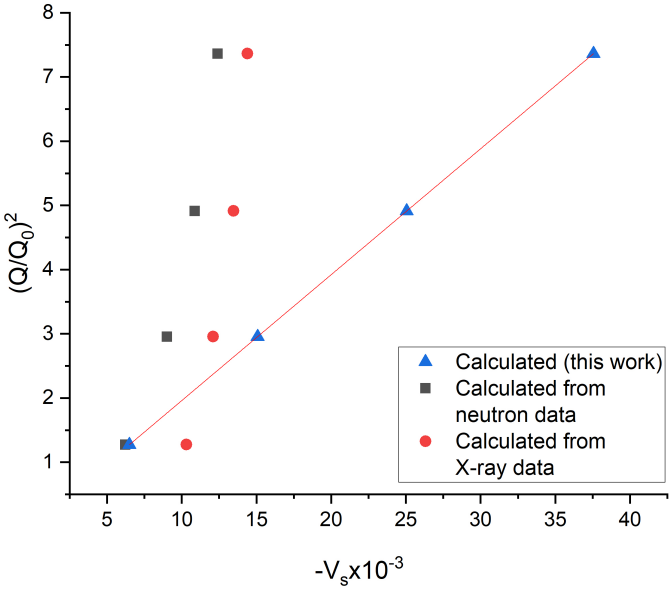

(a)

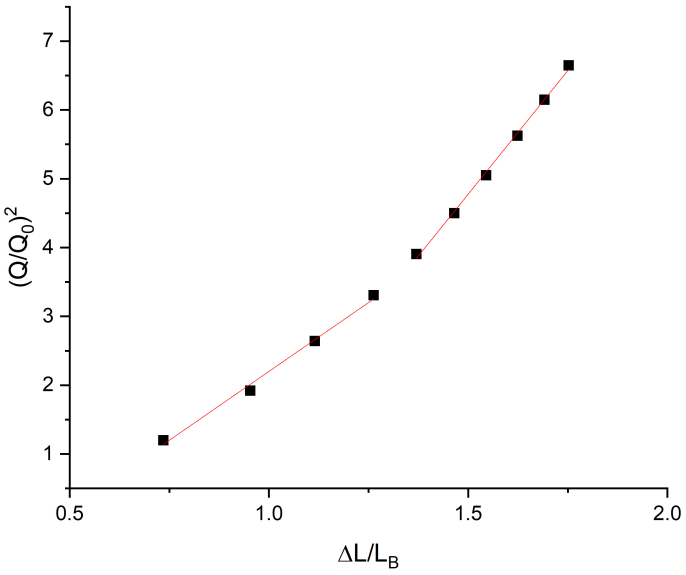

(b)

Figure 3.11: (a)Variation of the normalized order parameter Q (Eq.3.12) with the spontaneous strain (Eq.3.24) through Eq.3.26 for the α-β transition in quartz. V_s values calculated from the neutron and X-ray data [18] are also shown here. (b)Variation of the normalized order parameter Q (Eq.3.12) with the observed [70] elastic strain ΔL (normalized) (Eqs.3.29 and 3.30) for the α-β transition in quartz [5].

Discussions

Temperature dependence of the normalized order parameter (Q/Q_0) was calculated according to Eq.3.12 by the Landau mean field model with the cubic term. Anomalous behavior of the order parameter close to the transition temperature (T_{tr}) was obtained (Figure 3.4) both with our calculations and the observed values of η/η_0 [6, 74] and ϕ/ϕ_0 [75] for the α-β transition in quartz. Compared to the observed ones, our calculated normalized order parameter has an increasing slope with the slightly higher magnitude. A linear variation of the order parameter with the Raman soft mode frequency ω^2 (squared) was obtained according to Eq.3.14 as shown in Figure 3.5 for the low temperature α-phase of quartz. This linear relation suggests that the soft mode frequency (squared) can be correlated to the order parameter for the α-β transition in quartz.

Variation of the inverse susceptibility (normalized) with temperature was derived from Eq.3.15 by the Landau mean field model with the cubic term (Q^3) and it was compared to the other calculated values from the literature by the Landau mean field model with the even order terms up to the fourth power Q^4 [18] and molecular dynamics simulations with the system sizes of $N = 1080$ and 2060 [71] in the vicinity of the α-β transition in quartz. All calculations show the same linear and the critical behavior in the vicinity of transition temperature (Fig.3.6). The inverse susceptibility (χ^{-1}) decreases with the temperature for both approaching from below and above the critical temperature T_c. Our calculated values of χ^{-1} with the cubic term matches with the χ^{-1} values by the even power calculations [18] below T_c while they are relatively higher than the other calculated values [18, 71] above T_c.

The relation between the inverse susceptibility χ^{-1} and the soft mode frequency ω^2 (squared) was also investigated by Eq.3.16 using the Raman soft mode with the frequency $\sim 100cm^{-1}$ at $500°C$ [67] in the β phase $(T > T_c)$. Within the studied temperature interval, the inverse susceptibility (χ^{-1}) varies with the square of the soft mode frequency ω^2 linearly (Fig.3.7) above T_c as expected, in the vicinity of the α-β transition. This linear relation suggests that the soft mode frequency (squared) can be correlated to the order parameter and it can be used in the free energy expansion as an order parameter (Eq.3.16) for the α-β transition in quartz.

Temperature dependence of the excess entropy (S) which was calculated according to Eq.3.17, shows also a linear increase while approaching the critical temperature T_c from below in the α-phase (Fig.3.8) as the experimental data give [76]. This linear increase suggests that the nearest-neighbor coupling constant is large and it is intensely associated with the motions of the SiO_4 tetrahedra with respect ro the nearest-neighbors. Sufficiently enough above T_c, entropy is expected to saturate in the β phase which causes stabilization in quartz.

Excess heat capacity C_p which was calculated as a function of temperature in the form of $(T/C_p)^2$ shows linear variation according to the Landau model with the cubic term in the given temperature interval ($720 < T(K) < 860$) as shown in Figure 3.9 close to the α-β transition in quartz. According to Eq.3.18, the temperature dependence of $(T/C_p)^2$ becomes nonlinear with decreasing temperature in the α phase. Within the studied temperature interval here, linear temperature dependence of $(T/C_p)^2$ deduced from the Landau model with the cubic term Q^3 according to Eq.3.21, agrees with those from the Landau model with the even order terms up to the fourth order (Q^4) which was obtained as

$$(T/C_p)^2 = 1.47x10^5 - 173.0T \tag{3.31}$$

in relation to the constants a_0 and a_1 (Table 3.3). It can be concluded that the temperature dependence of $(T/C_p)^2$ shows similar critical behavior for values derived from both Landau model with the Q^3 term (Eq.3.21 through Eq.3.18) and with the even order terms (Eq.3.31) [18] within the approximately same temperature interval (Fig.3.9).

Variation of the spontaneous strain (V_s) with the temperature was obtained by using the Gibbs free energy expansion including the cubic term Q^3 (Eq.3.24), which shows anomalous behavior in the vicinity of the transition. In the α phase, spontaneous strain increases as approaching the transition temperature (T_{tr}) while it get stabilized above T_{tr} in the β phase (Fig.3.10). Our calculated results with the Q^3 term agree with those calculated from the Landau model with the Q^4 term by using neutron and X-ray diffraction data [18] as shown in Fig.3.10. In addition, almost linear correlation between the spontaneous strain and order parameter in the form of $(Q/Q_0)^2$ was obtained from Eq.3.26 in the α phase of quartz (Fig.3.11a). Linearity is restricted in

a temperature interval of $793.9 < T(K) < 845.9$. However, the correlation between the elastic strain $\Delta L/L_B$ (normalized) and the normalized order parameter (squared), $(Q/Q_0)^2$, is nonlinear (Fig.3.11b) for the α-β transition in quartz. Yet, the linear dependence of $(Q/Q_0)^2$ to $\Delta L/L_B$ was obtained for the two temperature intervals (Table 3.6) with the values of coefficients $b_0^{'}$ and $b_1^{'}$ (Eq.3.30).

The rotations of the SiO_4 tetrahedral can be defined with the tilt angle ϕ during the structural transition, therefore it was associated with the macroscopic order parameter and its anomalous behavior for the α-β transition in quartz [18] as

$$\phi = AQ + BQ^2 \tag{3.32}$$

with the constants A and B. Our calculated values of the macroscopic order parameter (Eq.3.12) were fitted to the experimental data of Young as given previously [6] and the structure refinements [77] according to Eq.3.32 and the constants A and B were determined in the given temperature interval (Table 3.7). The linear variation of tilt angle ϕ with the order parameter (Fig.3.12) suggests that the measured tilt angle of the SiO_4 tetrahedra (ϕ) can be accepted as an order parameter (Q) for the α-β transition in quartz.

Table 3.7: The coefficients A and B (Eq.3.32) within the temperature interval indicated for the α-β transition in quartz with the observed values [18] of the transition (T_{tr}) and critical (T_c) temperatures.

Quartz	$T_{tr}(K)$	$T_c(K)$	$A(^\circ)$	$-B(^\circ)$	Temperature Interval (K)
α-β transition	847	840	22.009	4.058	$273 < T < 823$

In this study, we used the free energy expansion of the Landau phenomenological model with the cubic term (Q^3) (Eq.3.11) to obtain the temperature dependence of the thermodynamic properties such as entropy, heat capacity, inverse susceptibility and the spontaneous strain in relation to the macroscopic order parameter (Eq.3.12) close to the α-β transition in quartz. Below the transition temperature in the α phase, macroscopic order parameter was correlated with the physical properties such as the piezoelectric and elastic constants, which show nonlinear behavior due to the thermal fluctuations close to the transition temperature [74]. Our calculated results agree with the observed ones in a limited temperature interval close to the transition temperature. Calculated (normalized) order parameter also agrees with the experimental data in

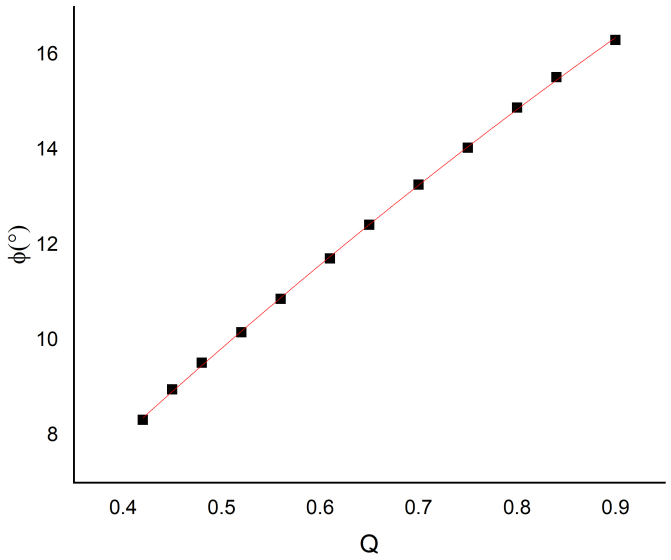

Figure 3.12: Variation of the tilt angle ϕ with the macroscopic order parameter Q according to Eq. 3.32 in the α phase close to the α-β transition in quartz.

the temperature interval of $830 < T(K) < 847$ [6, 74] and $845 < T(K) < 850$ [75] in the vicinity of α-β transition in quartz (Fig.3.4). Regarding the temperature variation of the calculated heat capacity in the form of $(T/C_p)^2$ which agrees with the experimental data [18], the acceptable temperature interval of $720 < T(K) < 850$ is according to the Landau mean field model with the cubic term (Fig.3.9). As shown in Figure 3.8, calculated entropy is highly dependent of temperature and it is in agreement with the observed [76] data in a noticeably short temperature interval. It also deviates quickly from the experimental values [76] as approaching the transition temperature. In a very small temperature interval, order parameter can couple with the acoustic phonons, which leads to the formation of an INC-phase [73,78]. Coupling of the order parameter to the strain was constructed to explain the first order transition in quartz [1]. In this study, we used Landau mean field model including the cubic term without any coupling terms. It is efficient enough to explain the thermodynamic properties in the vicinity of the α-β transition in quartz. For further investigation the coupling terms can be included to the free energy expansion (Eq.3.11) of the Landau model.

3.3 Calculation of the Grüneisen parameter with the second Pippard relation by the piezoelectric resonant frequency shifts in relation to the elastic constants

By using spectroscopically modified Pippard relations, temperature dependence of the piezoelectric resonance frequency shifts (ν) and the inverse incompressibilities ($1/K$) were obtained. This was done by the deducing isobaric mode Grüneisen parameter (γ_p) by using the experimental data [19] close to the α-β transition in quartz.

Quartz has 27 normal modes as given in Section 2.9 and several measurements of mode frequencies have carried out previously [19, 67–69] by using the various techniques. The aim of this study is to show the correlation between the order parameter and frequency shifts by considering the irreducible representations. For this, the frequency measurements of $A_g - 2$ mode was used to calculate the frequency shifts as a function of temperature (Fig.3.13). $A_g - 2$ mode has rotation and inversion symmetry and it is Raman active. Spectroscopically modified second Pipard relation was used for this investigation. By combining second Pippard relation (Eq.2.56) and the isobaric mode Grüneisen parameter (γ_p) (Eq.2.58), second Pippard relation can be written in the form of

$$\left(\frac{1}{\nu}\right)\left(\frac{\partial\nu}{\partial T}\right)_p = -\gamma_p\left(\frac{dp}{dT}\right)\kappa_T + \frac{1}{V}\left(\frac{dV}{dT}\right) \tag{3.33}$$

where $(1/\nu)\left(\partial\nu/\partial T\right)_p$ is the resonant frequency shifts under constant pressure and $\kappa_T \equiv -\left(\frac{1}{V}\frac{dV}{dp}\right)_T$ is the isothermal compressibility. Eq. 3.33 refers to a linear relation between resonant frequency shifts and the isothermal compressibility from which the isobaric mode Grüneisen parameter can be deduced with the $\frac{dp}{dT}$ (it is the slope of p-T phase diagram).

Besides the isothermal compressibility, the linear incompressibilities K_1 and K_3 for the isotropic dilatation can be defined as the linear combinations of the elastic constants (C_{ij}) as

$$K_1 = \left(\frac{C_{11} + C_{12} + C_{13}}{3}\right) \tag{3.34}$$

in the direction perpendicular to the **c**-axis and

$$K_3 = \left(\frac{C_{33} + 2C_{13}}{3}\right) \tag{3.35}$$

which is in the direction also parallel to the **c**-axis. Their temperature dependences were obtained from the observed data [19] above and below the critical temperature $T_c = 573°C$ as plotted in Fig.3.14.

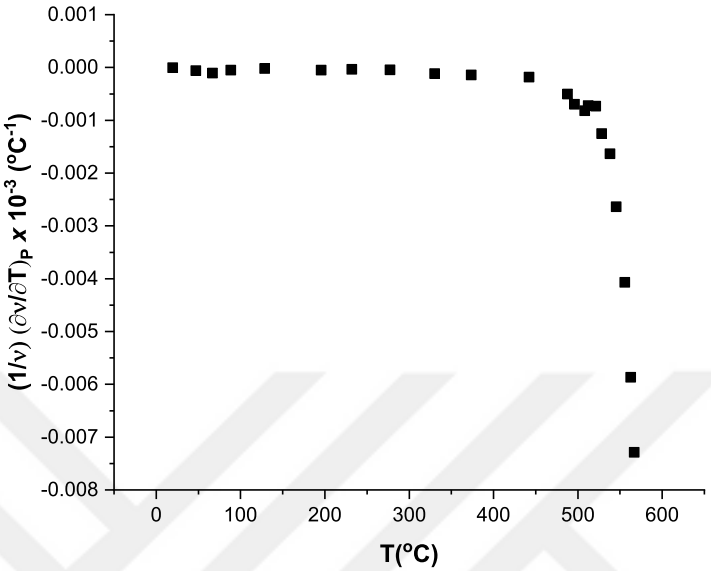

Figure 3.13: The resonance frequency shifts $(1/\nu)\,(\partial\nu/\partial T)_P$ of the $A_g - 2$ mode as a function of temperature using the observed data [19] in the α phase ($T < T_c = 573°C$) of quartz.

Resonant frequency shifts were also related to the inverse linear incompressibilities $1/K_1$ and $1/K_2$ according to Eq.3.33 in the α phase of quartz for $T < T_c = 573°C$ as shown in Fig. 3.15. The isobaric mode Grüneisen paramater can be deduced from Fig. 3.15 by using the experimental value of $\frac{dp}{dT} = 47bar/K$ [18] of the $A_g - 2$ vibrational mode for the α-β transition in quartz. Calculated values of the Grüneisen paramater γ_p using the slope and volume variations $(1/V)\,(\partial V/\partial T)$ from the intercept, are given in Table 3.8.

Resonant frequency shifts $(1/\nu)\,(\partial\nu/\partial T)_P$ in relation to isothermal compressibility κ_T was also investigated with the experimental data of bulk modulus ($K_{VRH} = 1/\kappa_T$) [19] in the α phase of quartz. Grüneisen paramater γ_p and volume variations $(1/V)\,(\partial V/\partial T)$ γ_p of the $A_g - 2$ mode were calculated by using experimental value of $\frac{dp}{dT} = 47Bar/K$ [18] for the α phase as before and given in Table 3.8.

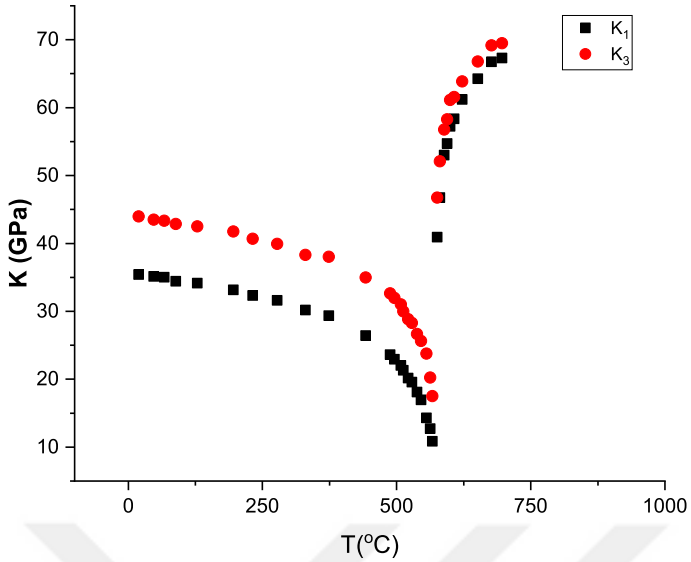

Figure 3.14: Temperature dependence of the linear incompressibilities (K_1 and K_3) according to Eqs. 3.34 and 3.35 with the observed data [19] for the α-β transition in quartz.

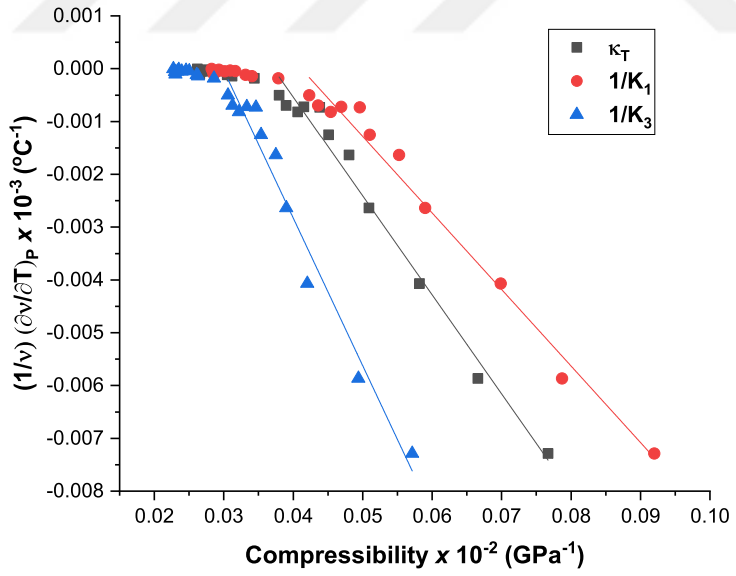

Figure 3.15: Variation of the resonance frequency shifts of the $A_g - 2$ mode with the inverse incompressibilities (K_1 and K_3) as a function of the isothermal compressibility (κ_T) according to Eq.3.33 by using the observed data [19] for α-quartz ($T < T_c = 573°C$).

Table 3.8: Values of the isobaric mode Grüneisen parameter (γ_p) of the $A_g - 2$ mode and the volume variation with the temperature due to the linear incompressibilities ($1/K_1$ and $1/K_3$) and the isothermal compressibility (κ_T) according to Eq.3.33 within the temperature range indicated for the α-quartz. The α-β transition temperature and the observed $\frac{dP}{dT}$ [18] values are given here [5].

$T_c(^\circ C)$	Mode	Compressibility (GPa^{-1})	γ_p	$(1/V)\,(\partial V/\partial T)\,x10^{-3}$ ($^\circ C^{-1}$)	$\frac{dP}{dT}$ (bar/K)	Temperature Interval ($^\circ C$)
573	A_g-2	$1/K_1$	0.032	3.59	47	496.4<T<566.4
		$1/K_3$	0.017	5.31		
		κ_T	0.034	4.15		

Correlation between the resonant frequency shifts, $(1/\nu)\,(\partial\nu/\partial T)_P$, and the elastic constants (C_{ij}) in the form of the linear inverse incompressibility, $1/K$ ($1/K_1$ and $1/K_3$) was obtained by using spectroscopically modified second Pipard relation (Eq.3.33) close to the α-β transition in quartz. Due to the anomalous behavior of the resonance frequency shifts (Fig.3.13) and the elastic parameters (Fig3.14) close to the transition in the α phase, linear variation of the frequency shifts $(1/\nu)\,(\partial\nu/\partial T)_P$ with the inverse incompressibility $(1/K)$ was obtained below T_c (Fig.3.15). Unlike highly symmetric β quartz, anomalous nature of the α quartz was already shown experimentally [19] and it is also valid for our correlation which is satisfactory below T_c.

Deviation of the linearity which occurred in the variation of frequency shifts with the inverse linear incompressibility (Fig.3.15), is consistent with the validity of the spectroscopically modified Pippard relation (Eq.2.56 through Eq.3.33) below T_c. As a result, correlation between the $A_g - 2$ vibrational mode frequencies and the inverse linear incompressibility ($1/K_1$ and $1/K_3$) becomes significant as approaching T_c for the α-β transition in quartz. For the vibrational $A_g - 2$ mode, isobaric mode Grüneisen parameter (γ_p) was obtained due to the inverse linear incompessibility ($1/K_1$ and $1/K_3$) and isothermal compressibility (κ_T), as stated in the Table 3.8. Grüneisen parameter obtained from $1/K_3$ is nearly half the value of the γ_p due to $1/K_1$ and κ_T (Table 3.8).

Due to the observed anomalous behavior of various modes A_u, B_u, A_g, B_g (with peak positions from 1 to 7) [19] in the α phase, their frequency shifts can be correlated

to the linear inverse incompressibility ($1/K_1$ and $1/K_3$) as in this study and also the shear moduli C_{S1} and C_{S3} ($C_{S1} = (C_{11} + C_{33} - 2C_{13})/4$ and $C_{S3} = (C_{11} - C_{12})/2 = C_{66}$) which are the linear combinations of elastic constants of α phase. This correlation leads to the linear variation of the frequency shifts with the elastic features in relation to the isobaric mode Grüneisen parameter γ_p for the α phase as expected.

3.4 Variation of the piezoelectric resonance frequency (υ) with the temperature associated with the anomalous strain (ΔL) close to the incommensurate phase of quartz

In the previous part, we related the resonant frequency shifts as an order parameter to the elastic properties for the α-β transition in quartz by starting with the temperature dependence of frequency shifts [5] which was also stated experimentally [25]. That brought the same possibility for the incommensurate (INC) phase which can also be descried by the correlation between the resonant frequency shifts and elastic properties, in this study mainly strain, of the α phase of quartz in a narrow temperature interval for the INC-β transition.

Variation of the piezoelectric resonance frequency with temperature was analyzed according to a power law formula due to its critical behavior by using the experimental data [34] close to the INC-β transition in quartz. The piezoelectric resonance frequency was also related to the anomalous strain as an order parameter using the observed data [70] in the vicinity of this transition.

In the previous parts we showed that the α-β transition in quartz can be describe by the free energy expansion of Landau theory in terms of order parameter (Section 2.3, 3.1 and 3.2). For the INC-β transition, free energy can be expanded in terms of the INC phase order parameter η as

$$F_{INC} = a\eta^2 + b\eta^4 + c\eta^6 - E\eta \tag{3.36}$$

in the presence of the electric field E, where $a = \alpha(T - T_c)$, with the α, b and c constants. The critical temperature T_c can also be denoted as T_i for the INC-β transition. According to the Cohran's soft mode theory [79] and experimental Raman lattice mode studies [22], soft mode frequency squared (υ^2) is in a linear relation with the order parameter (η) close to the α-β transition in quartz. Since INC phase occurs in a considerably small temperature range ($571.10 < T(^\circ C) < 572.55$) [34], its order parameter can be related to the piezoelectric resonance frequency of α as

$$\upsilon^2 \propto \eta \tag{3.37}$$

near the INC-β transition in quartz. Due to the critical behavior of order parameter in

the vicinity of the transition temperature T_c, it can be represented by the relation

$$\eta(T) = \eta_0 + A(T_c - T)^{\beta} \tag{3.38}$$

with the positive critical exponent β, amplitude A and the order parameter η_0 at the transition temperature. This power law representation of the order parameter was previously suggested for the α-β transition in quartz because of its critical behavior close to the T_c [6, 75]. As a result, temperature dependence of the piezoelectric resonant frequency can be analyzed according to

$$\upsilon^2 = \upsilon_0^2 + k(T - T_c)^{\beta} \tag{3.39}$$

by combining Eqs. 3.37 and 3.38 to describe the temperature dependence of the order parameter (η) where β is the critical exponent for the order parameter, υ_0 is the resonance frequency at the transition temperature ($T = T_c$ and $\beta > 0$) and k is the amplitude. To analyze the temperature dependence of the experimental piezoelectric resonance frequency [34], a power law formula can be expressed from the Eq.3.39 in the form of

$$ln(\upsilon^2 - \upsilon_0^2) = lnk + \beta ln(T - T_c) \tag{3.40}$$

close to the transition temperature (T_c) for the INC-β transition in quartz. Values of υ_0 (at $T = T_c$), k and β were obtained from the analysis of the piezoelectric resonance frequency data from the cooling cycle [34] as a function of temperature as plotted in Fig.3.16 for the INC-β transition in quartz with the parameters determined (Table 3.9).

For the analysis of correlation between the order parameter and elastic parameters, as previously stated, the relation between the anomalous strain (ΔL) and the mean value of the order parameter (squared) [70]

$$\Delta L \propto \langle \eta^2 \rangle \tag{3.41}$$

was used, where

$$\Delta L = L(T) - L_B(T) \tag{3.42}$$

with the background strain $L_B(T)$. By assuming $\langle \eta^2 \rangle = \eta^2$, anomalous strain ($\Delta L$) can also be related to the piezoelectric resonance frequency (υ) through the temperature dependence of order parameter (Eq.3.39) by means of equations 3.37 and 3.41

as

$$\Delta L^{1/2} \propto \upsilon^2 \tag{3.43}$$

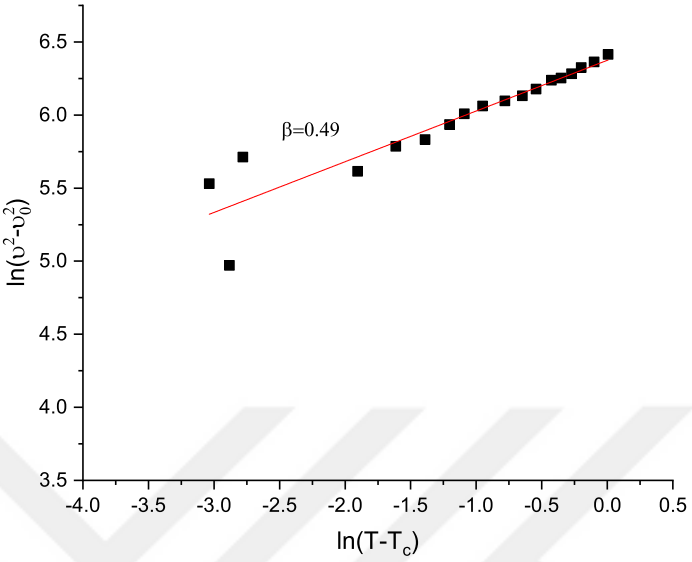

Figure 3.16: Temperature dependence of the piezoelectric resonance frequency (υ) in the log-log scale according to Eq. 3.40 using the experimental data of cooling run [34] close to the INC-β transition in quartz.

Table 3.9: Power law parameters according to Eq. 3.40 using the experimental data of the piezoelectric resonance frequency [34] close to the INC-β transition in quartz.

Quartz	T_c ($^\circ C$)	β	k[$kHz^2/^\circ$C]$^\beta$	υ_0(kHz)	Temperature interval ($^\circ C$)
INC-β transition	571.1	0.49	1.623	140.1	571.10<T<572.55

Since we assumed the strain as an order parameter (Eq.3.37), temperature dependence of anomalous strain (ΔL) and piezoelectric resonance frequency (υ) should exhibit similar critical behavior close to the INC-β transition in quartz. In the normalized forms, piezoelectric resonance frequency $(\upsilon^2 - \upsilon_0^2)/\upsilon_0^2$ in relation to the anomalus stain $\Delta L(T)/L_B(T)$ can be written as

$$\frac{(\upsilon^2 - \upsilon_0^2)}{\upsilon_0^2} = a_0(T) + a_1(T)\left[\frac{\Delta L(T)}{L_B(T)}\right]^{1/2} \tag{3.44}$$

with the temperature dependent parameters a_0 and a_1, where the background strain with the temperature dependence [70] is given by

$$L_B(T) = b_0 + b_1 T \tag{3.45}$$

with the constants b_0 and b_1 (Table 3.10). Variation of the observed piezoelectric resonance frequency [34] with the anomalous strain [70] obtained according to the Eq.3.44 with the temperature dependent background strain (Eq.3.45) linearly as in Figure 3.17 by assuming initially a_0 and a_1 as constants in the given temperature interval (Table 3.10) for the INC-β transition in quartz.

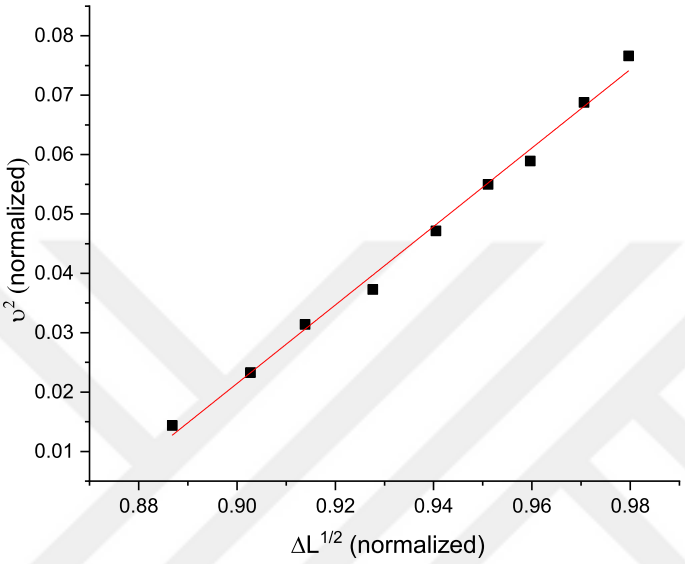

Figure 3.17: The normalized piezoelectric resonance frequency [34] in relation to the normalized anomalous strain [70] close to the INC-β transition in quartz in accordance with the Eq.3.44.

Table 3.10: Values of the parameters of a_0 and a_1 (Eq. 3.44), b_0 and b_1 (Eq.3.45) within the temperature intervals indicated by using the experimental data for the piezoelectric resonance frequency [34] and the anomalous strain [70] for the INC-β phase transition in quartz [3].

Quartz	a_0	a_1	Temperature interval (K)	$b_0\,(cm)$	b_1x$10^{-5}\,(cm/K)$	Temperature interval (K)
INC-β transition	-0.573	0.661	842.23< T <846.17	1.00834	1.53837	$T - T_0 > 15K$, $T_0 = 845.7K$ [70]

Then by taking into account the temperature dependence of a_0 and a_1, the relation between the piezoelectric resonance frequency (υ) and the anomalous strain (ΔL)

can be written in the linear form of

$$\frac{\upsilon^2\ (normalised)}{\Delta L^{1/2}(normalised)} = a_0^{'} + a_1^{'}T \tag{3.46}$$

at their various temperatures (Fig.3.18) with the constants $a_0^{'}$ and $a_1^{'}$ in the given temprature interval (Table 3.11) for the INC-β phase transition in quartz.

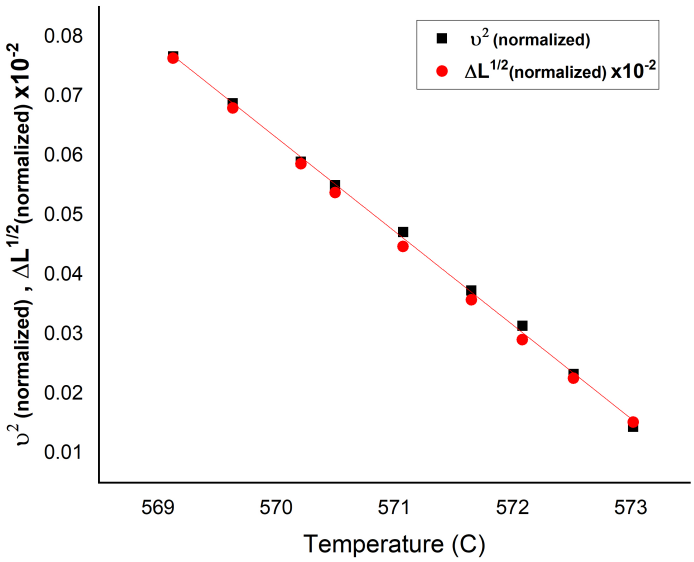

Figure 3.18: Piezoelectric resonance frequency (normalized) (υ^2) fitted to the anomalous strain (normalized) ($\Delta L^{1/2}$) as a function of temperature using Eq.3.44 through Eq.3.46 in the vicinity of the INC-β transition in quartz.

Table 3.11: Fitting parameters of the normalized piezoelectric resonance frequency (υ^2) in relation to the square root of the normalized anomalous strain ($\Delta L^{1/2}$) according to Eq.3.46 for the INC-β transition in quartz.

Quartz	$T_c(^\circ C)$	$a_0^{'}$	$a_1^{'}$	Temperature Interval (K)
INC-β transition	574.59	8.9734	-0.0156	$842.23 < T < 846.17$

Temperature dependence of the piezoelectric resonance frequency was analyzed according to the power law formula (Eq.3.39 through Eq.3.40) close to the INC-β transition in quartz. As a result of this analysis, critical exponent of the order parameter was obtained as $\beta = 0.49$ (Table 3.9) which is quite close to the critical exponent of the Landau phenomenological model $\beta = 0.5$ (calculated in Section 2.4) for a second order transition in a quite small temperature interval ($571.10 < T(^\circ C) < 572.55$)

for the INC-β transition in quartz. Our critical exponent value β is also comparable with the critical exponent value of Young $\beta = 1/3$ [80] obtained from the variations of atomic position with temperature and the experimental one from the ultrasound scattering with the value of $\beta = 0.34 \pm 0.02$ [75] whose order parameter is mainly related to the rotations of SiO_4 structure as in this case.

By using the order parameter relations in Eq.3.37 and Eq.3.43, the relation between piezoelectric resonance frequency (υ) and the anomalous strain (ΔL) was analyzed according to Eq.3.44 in the vicinity of INC-β transition in quartz. This analysis gives linear variation between these two parameters as in Fig.3.17 and both parameters decrease with increasing temperature in the α and INC phases toward the transition temperature ($T_c = 573°C$). For our analysis, experimental data of anomalous strain were shifted by about $3°C$ due to match of its transition temperature $T = 845.70\,K\,(T_c = 571.55°C)$ [70] to the transition temperature of the observed piezoelectric resonance frequency as $T_c = 573°C$ [34] according to Eq.3.44. Due to its anomalous behavior in the vicinity of INC-β transition in quartz, anomalous strain (ΔL) can be considered as an order parameter which leads to a power law as $\Delta L \propto (T^* - T)^{1/3}$ with a pseudo-critical exponent of the value 0.32 ± 0.02 [70] and an arbitrary parameter T^* . This pseudo-exponent obtained experimentally also indicates the long range order according to Eq.3.41 as $\beta = 0.16 \pm 0.01 \approx 1/6$ [70]. In comparison with the previously stated critical exponents $\beta = 1/3$ [80] and $\beta = 0.34 \pm 0.02$ [75], our critical exponent value $\beta = 0.49$ indicates that INC-β transition in quartz is a nearly second order transition as predicted by the Landau phenomenological model.

In the first part, for the analysis of the relation between the observed piezoelectric resonance frequency [34] and the anomalous strain [70] according to Eq. 3.44, a_0 and a_1 (Table 3.10) were assumed to be constant and gave a linear relation (Fig.3.17). But, both coefficients are the temperature dependent (3.44) as initially assumed. Therefore, normalized υ^2 fitted to the normalized $\Delta L^{1/2}$ at various temperatures (Eq.3.46) with the coefficients $a_0^{'}$ and $a_1^{'}$ in a given temperature interval of INC-β transition in quartz, Table3.11 gives the temperature dependence of a_0 and a_1 by multiplying $a_0^{'}$ and $a_1^{'}$ with the temperature dependence of normalized anomalous strain. As a result, linear variation of piezoelectric resonance frequency and anomalous strain with temperature was obtained in the vicinity of INC-β transition in quartz which is applicable

to the other crystals with INC phase.

3.5 Calculation of the damping constant (Γ_{sp}) and the relaxation time (τ_{LA}^{-1}) of the LA mode in the incommensurate phase of quartz

The variation of the damping constant (linewidth) for the longitudinal acoustic (LA) mode with the temperature in the INC phase of quartz was calculated by using pseudo-spin phonon coupled (PS) model and energy fluctuation (EF) model. Experimental data for the linewidth (Γ_{sp}) at $P = 0$ and $P = 80.5\,MPa$ from the Brillouin spectra of the LA mode [81] were used for this calculation. Temperature dependence of the linewidth was analyzed by a power law formula which was also adjusted for the observed temperature dependence of the frequency shifts [81] ($\Delta\upsilon_{LA}$) in the vicinity of the INC phase of quartz. From this analysis, the values of the critical parameters for both Γ_{LA} and $\Delta\upsilon_{LA}$ were extracted. Variation of the inverse relaxation time (τ_{LA}^{-1}) of the LA mode with the temperature was established and it was used to determine the activation energy values (E_a) at $P = 0$ and $P = 80.5\,MPa$ in the incommensurate phase of quartz.

Linewidth (Γ_{sp}) calculations by the PS and EF models

The damping constant of the LA mode was calculated as a function of temperature according to PS and EF models by using the experimental Brillouin spectra data for the piezoelectric frequency shifts ($\Delta\upsilon_{LA}$) [81] in the INC phase of quartz at $P = 0$ and $P = 80.5\,MPa$. As stated in the previous section (Section 3.4) and it was used for those calculations, piezoelectric frequency shifts ($\Delta\upsilon_{LA}$) can be considered as an order parameter according to $(\Delta\upsilon_{LA})^2 \propto Q$ in the INC phase of quartz where Q is the order parameter.

On the basis of the spin-phonon coupling, temperature dependence of the linewidth can be expressed by the pseudo-spin phonon coupled (PS) model (Section 3.5) with the order parameter Q close to the critical temperature T_c as

$$\Gamma_{sp} = \Gamma_0{}' + A'(1-Q^2)ln\left(\frac{T_c}{T - T_c(1-Q^2)}\right) \tag{3.47}$$

where Γ_0' and A' are background damping constant and the magnitude, respectively.

Γ_{sp} (Eq.3.47) of the PS model was fitted to the observed linewidth data Γ_{LA} [81]

at $P = 0$ (Fig.3.19) and $P = 80.5\,MPa$ (Fig.3.20) for the INC phase of quartz and the background parameters $\Gamma_0^{'}$ and $A^{'}$ were determined at $P = 0$ (Table 3.12) and $P = 80.5\,MPa$ (Table 3.13) for the given temperature intervals. For zero pressure, transition temperatures T_c and T_i (Table 3.12) were obtained from the almost minimum and maximum values of the observed transverse acoustic mode linewidth Γ_{TA} [81], respectively, due to the coupling of soft modes in the INC phase of quartz [31]. At $P = 80.5\,MPa$, T_c is the critical temperature, $T_{i1}(= T_c + 6.18\,K)$ and $T_{i3}(= T_c + 4.36\,K)$ (Table 3.13) are the transition temperatures in the INC phase [81].

Variations of the damping constant of the LA mode (Γ_{LA}) with the temperature was also calculated by using the observed data of the frequency shifts as an order parameter and the fitted parameters were determined (Tables 3.12 and 3.13) according to the PS model (Eq.3.47) at $P = 0$ and $P = 80.5\,MPa$, respectively, close to the INC phase of quartz as shown in Figures 3.19 and 3.20 (squares).

By taking into account the energy fluctuations due to the spin-phonon interactions, temperature dependence of the linewidth can also be analyzed by energy fluctuation (EF) model (Section 3.5) with the order parameter Q close to the critical temperature T_c as

$$\Gamma_{sp} = \Gamma_0 + A\left(\frac{T(1-Q^2)}{T - T_c(1-Q^2)}\right)^{1/2} \tag{3.48}$$

where Γ_0 and A are background damping constant and magnitude, respectively. The same steps in the analysis by PS model is followed for the analysis of the temperature dependence of the damping constant for the LA mode by the EF model.

Γ_{sp} (Eq.3.48) of the EF model was fitted to the observed linewidth data Γ_{LA} [81] at $P = 0$ (Fig.3.21) and $P = 80.5\,MPa$ (Fig.3.22) for the INC phase of quartz and the background parameters Γ_0 and A were determined at $P = 0$ (Table 3.12) and $P = 80.5\,MPa$ (Table 3.13) for the given temperature intervals. Variations of damping constant of the LA mode Γ_{LA} with temperature was calculated by using the observed data of frequency shifts as an order parameter and the fitted parameters were determined (Tables 3.12 and 3.13) according to EF model (Eq.3.48) at $P = 0$ and $P = 80.5\,MPa$ close to the INC phase of quartz as shown in Figures 3.21 and 3.22 (squares).

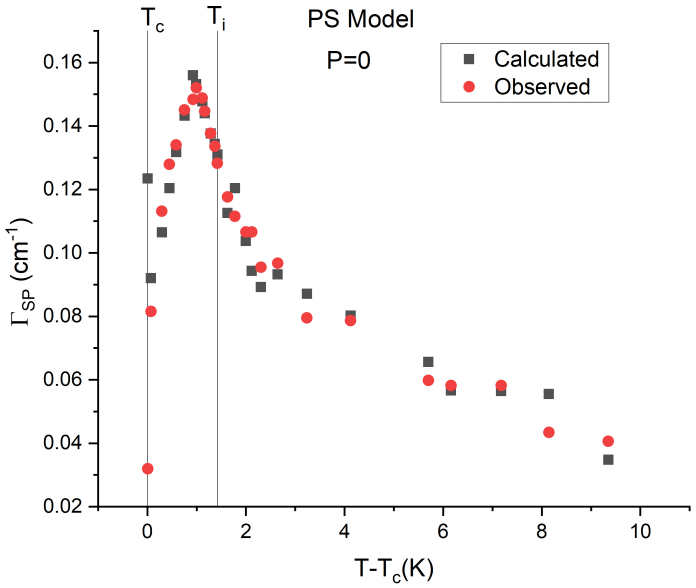

Figure 3.19: Variation of the linewidth of the LA mode (Eq.3.47) according to the PS model with the temperature at $P = 0$. The observed Γ_{LA} data [81] are also shown in the INC phase of quartz.

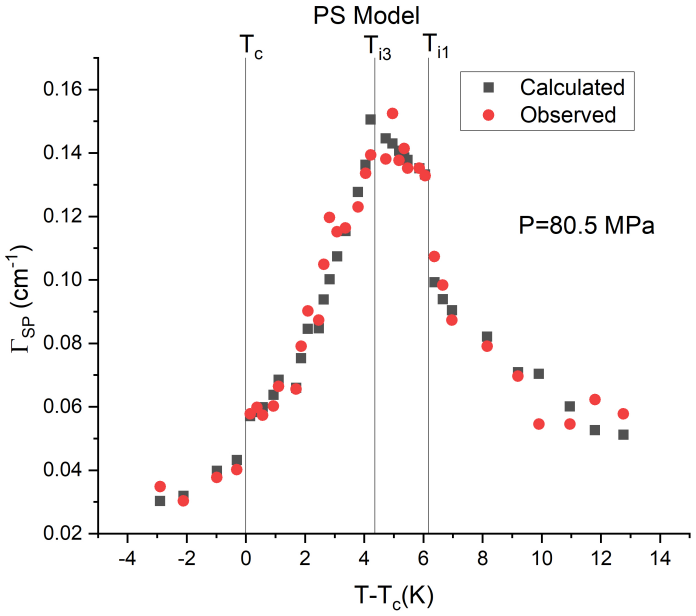

Figure 3.20: Variation of the linewidth of the LA mode (Eq.3.47) according to the PS model with the temperature at $P = 80.5\,MPa$. The observed Γ_{LA} data [81] are also shown in the INC phase of quartz.

Table 3.12: Values of the transition temperatures (T_c and $T_i = T_c + 1.43\,K$), background damping constants (Γ_0 and $\Gamma_0^{'}$) and the amplitudes (A and $A^{'}$) of the LA mode in the temperature intervals ($T_0 = 846.93\,K$) indicated according to the PS and EF models for the incommensurate phase of quartz ($P = 0$)

Models	$T_c(K)$	$T_i(K)$	P = 0	$T_c < T < T_0$	$T_0 < T < T_i$	$T > T_i$
PS (Eq.3.47)	846	847.43	$\Gamma_0^{'}(cm^{-1})$	0.176	0.141	0.167
			$A'(cm^{-1})$	-0.167	0.145	0.537
EF (Eq.3.48)	846	847.43	$\Gamma_0(cm^{-1})$	0.265	0.067	-0.064
			$A(cm^{-1})$	-0.176	0.147	0.446

Table 3.13: Values of the transition temperatures T_c, $T_{i1} = T_c + 6.18\,K$ and $T_{i3} = T_c + 4.36\,K$, background damping constants (Γ_0 and $\Gamma_0^{'}$) and the amplitudes (A and $A^{'}$) of the LA mode in the temperature intervals ($T_0 = 848.82\,K$) indicated according to the PS and EF models for the incommensurate phase of quartz ($P = 80.5MPa$)

Models	$T_c(K)$	$T_{i1}(K)$	$T_{i3}(K)$	P = 80.5 MPa	$T_0 < T < T_c$	$T_c < T < T_{i3}$	$T_{i3} < T < T_{i1}$	$T > T_{i1}$
PS(Eq.3.47)	851.72	857.90	856.08	$\Gamma_0^{'}x10^{-4}(cm^{-1})$	3.487	2425.9	1337.4	1070.3
				$A'(cm^{-1})$	0.088	-0.263	0.048	0.257
EF(Eq.3.48)	851.72	857.90	856.08	$\Gamma_0(cm^{-1})$	-0.045	0.379	0.109	-0.007
				$A(cm^{-1})$	0.091	-0.274	0.050	0.223

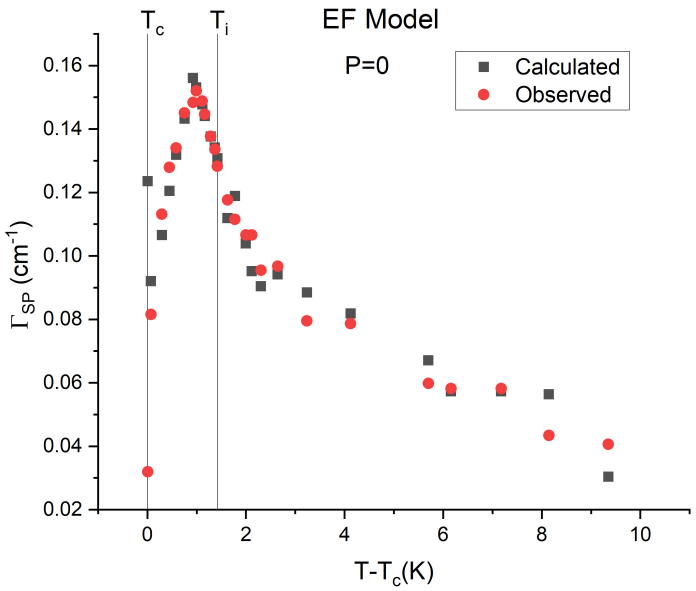

Figure 3.21: Variations of the linewidth of the LA mode (Eq.3.48) by the EF model at $P = 0$ with the temperature. The observed Γ_{LA} data are also shown [81] in the INC phase of quartz.

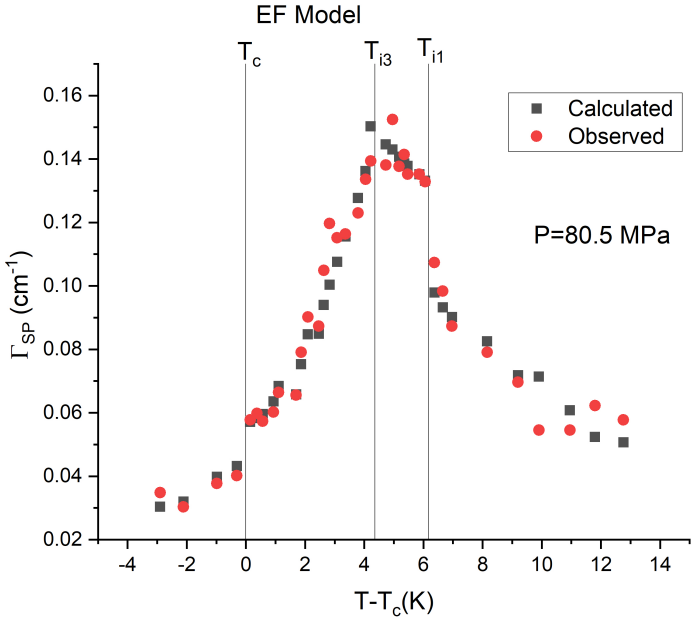

Figure 3.22: Variations of the linewidth of the LA mode (Eq.3.48) by the EF model at $P = 80.5\,MPa$ with the temperature. The observed Γ_{LA} data are also shown [81] in the INC phase of quartz.

Critical behavior of linewidth (Γ_{LA}) and frequency shifts ($\Delta\upsilon_{LA}$) close to the INC phase

Critical behavior of linewidth (Γ_{LA}) and frequency shifts ($\Delta\upsilon_{LA}$) close to the INC phase was analyzed by using a power law formula and observed data [81] of Brillouin spectra. Variation of the damping constant with temperature in the vicinity of the critical temperature (T_c) can be obtained by a power law formula,

$$\Gamma(T) = \Gamma^{'}(0)\left(\frac{T - T_c}{T_c}\right)^{-\eta} \tag{3.49}$$

with the critical exponent η of the damping constant and the amplitude $\Gamma^{'}(0)$ of the linewidth. Due to the critical behavior of the order parameter in the vicinity of the critical temperature (T_c), its temperature dependence can be explained by a power law formula (Section 2.4) which is related to the frequency shifts ($\Delta\upsilon$) according to $(\Delta\upsilon)^2 \propto Q$ as an order parameter. Hence, temperature dependence of the frequency shifts can be written in the form of a power law formula,

$$(\Delta\upsilon)^2 = (\Delta\upsilon_0)^2 + A\left(\frac{T - T_c}{T_c}\right)^{\beta} \tag{3.50}$$

where $\Delta\upsilon_0$ is the value of frequency shifts ($\Delta\upsilon$) at $T = T_c$, A is the amplitude and β is the critical exponent of the order parameter below the transition temperature T_i in the INC phase.

For $T > T_i$, frequency shifts as a function of temperature can be expressed as

$$(\Delta\upsilon)^2 = (\Delta\upsilon_0)^2 + a\left(\frac{T - T_c}{T_c}\right) \tag{3.51}$$

with the value of frequency shifts at $T = T_c$, $\Delta\upsilon_0$, and the amplitude a as before.

Variations of the damping constant with the temperature were studied by means of a power law formula (Eq. 3.49) by using the experimental linewidth data for the LA mode (Γ_{LA}) at $P = 0$ (Fig.3.23a) and $P = 80.5\,MPa$ (Fig.3.23b) close to the transition temperature T_c. Critical parameters η and $\Gamma^{'}(0)$ were obtained from the analyses for both pressures in the given temperature intervals (Table3.14) with the temperature T_{max} at which the maximum value of linewidth Γ_{max} occurs above T_c for the INC phase of quartz.

Variations of frequency shifts of the LA mode ($\Delta\upsilon_{LA}$) with temperature were also investigated by using the observed data [81] below (Eq3.50) and above (Eq3.51) the transition temperature (T_i) at $P = 0$ (Fig.3.24a) and $P = 80.5\,MPa$ (Fig.3.24b) close to the INC phase of quartz. Critical exponent of the order parameter β, amplitude A and coefficient a with the $\Delta\upsilon_0$ (the frequency shift at the transition temperature) were obtained from the analysis for both pressures in the given temperature intervals (Table3.15) for the INC phase of quartz.

Table 3.14: Values of the transition temperatures T_c, T_i ($P = 0$), T_{i1} ($P = 80.5MPa$), and T_{i3} ($P = 80.5MPa$) and the temperature T_{max} at the maximum value of the linewidth Γ_{LA} of the observed LA mode [81]. Also, values of the critical exponent η and the amplitude $\Gamma'(0)$ are given within the temperature intervals indicated ($P = 0$ and $P = 80.5MPa$) according to Eq.3.49 for the incommensurate phase of quartz.

Linewidth	Pressure (MPa)	$T_c(K)$	$T_i(K)$	$T_{i1}(K)$	$T_{i3}(K)$	$T_{max}(K)$	η	$\Gamma'(0)x10^{-2}$ (cm^{-1})	Temperature Interval (K)
$\Gamma_{LA}(cm^{-1})$	0	846	847.43	-	-	846.99	-0.28	100.34	$T_c < T < T_{max}$
							0.55	0.390	$T > T_{max}$
	80.5	851.72	-	857.90	856.08	856.68	-0.45	139.65	$T_c < T < T_{max}$
							1.3	0.020	$T > T_{max}$

Table 3.15: Values of the transition temperatures T_c, T_i ($P = 0$), T_{i1} ($P = 80.5MPa$), and T_{i3} ($P = 80.5MPa$) for the frequency shifts $\Delta\upsilon$ of the observed LA mode [81]. Also, values of the critical exponent β for the order parameter, amplitude A, the frequency shift $\Delta\upsilon_0$ at the transition temperature and the coefficient a within the temperature intervals indicated ($P = 0$ and $P = 80.5MPa$) according to Eqs.3.50 and 3.50, are given for the incommensurate phase of quartz.

Frequency Shifts	Pressure (MPa)	$T_c(K)$	$T_i(K)$	$T_{i1}(K)$	$T_{i3}(K)$	β	A (cm^{-2})	$\Delta\upsilon_0$ (cm^{-1})	a (cm^{-2})	Temperature Interval (K)
$\Delta\upsilon_{LA}$ (cm^{-1})	0	846	847.43	-	-	1.1	188.49	0.75	-	$T_c < T < T_i$
						-	-	0.86	7.756	$T > T_i$
	80.5	851.72	-	857.9	856.08	2.49	41655	0.73	-	$T_c < T < T_{i1}$
						-	-	0.79	11.767	$T > T_{i1}$

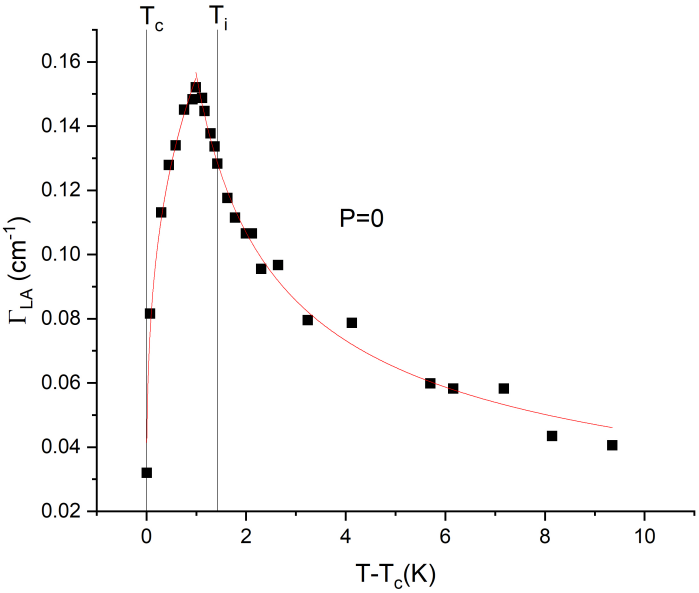

(a)

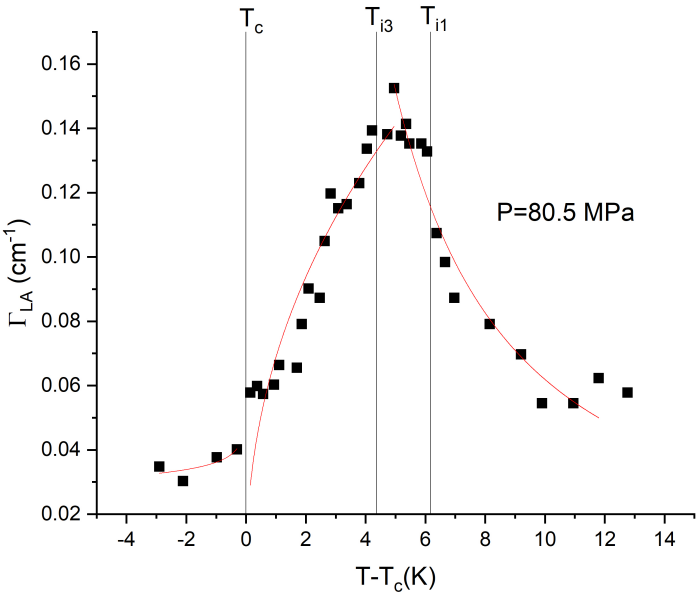

(b)

Figure 3.23: Analysis of the temperature dependence of the damping constant Γ_{LA} at $P = 0$ (a) and $80.5\,MPa$ (b) according to the power law formula (Eq.3.49) for the LA mode using the observed data [81]. Solid lines represent the best fits to the experimental data [81].

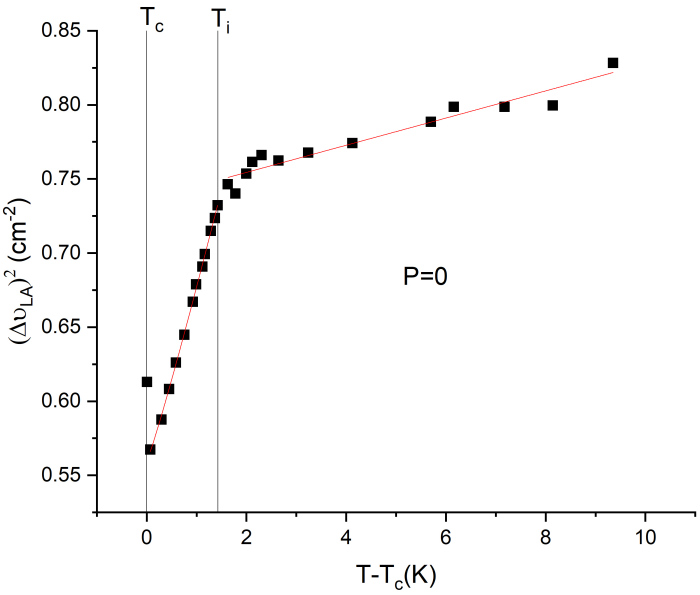

(a)

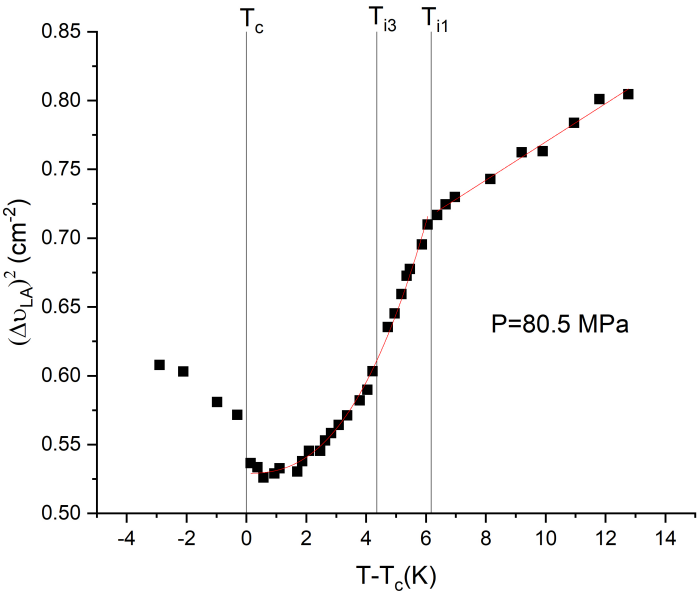

(b)

Figure 3.24: Frequency shifts ($\Delta\upsilon_{LA}$) squared as a function of temperature according to Eqs.3.50 and 3.51 below and above the transition temperature T_i at $P = 0$ and T_{i1} at $P = 80.5MPa$ respectively, which were fitted to the experimental $\Delta\upsilon_{LA}$ of the LA mode [81] in the commensurate phase of quartz. Solid lines represent the best fits to the experimental data [81].

Inverse relaxation time (τ_{LA}^{-1}) calculation

As stated in Section 2.8, inverse relaxation time of phonon modes can be expressed in terms of the frequency shifts and damping constant (linewidth) Γ as

$$\tau^{-1} = \frac{\upsilon^2}{\Gamma} \tag{3.52}$$

According to the Arrhenius law, temperature dependence of the relaxation time can be expressed as

$$\tau = \tau_0 exp\left(-\frac{E_a}{k_B T}\right) \tag{3.53}$$

where τ_0, E_a and k_B are the attempt relaxation time, activation energy and the Boltzmann constant respectively. Eq.3.53 can also be written in the logarithmic form

$$ln\tau = ln\tau_0 - \frac{E_a}{k_B T} \tag{3.54}$$

Variations of inverse relaxation time (τ^{-1}) with temperature were calculated by using observed linewidth (Γ_{LA}) and frequency shifts ($\Delta\upsilon_{LA}$) [81] of the LA mode according to Eq.3.52 at $P = 0$ (Fig.3.25a) and $P = 80.5MPa$ (Fig.3.25b) in the incommensurate phase of quartz. T_i ($P = 0$), T_{i1} ($P = 80.5MPa$), and T_{i3} ($P = 80.5MPa$) are the transition temperatures of given pressure conditions (Table 3.16). By using this temperature dependence by means of Eq.3.54, activation energy E_a was determined with the sufficiently small attempt relaxation time (τ_0) at $P = 0$ (Fig.3.26a) and $P = 80.5MPa$ (Fig.3.26b) within the given temperature intervals (Table 3.16) for the INC phase of quartz. Above the transition temperatures T_i ($P = 0$) and T_c ($P = 80.5MPa$), temperature dependence of inverse relaxation time (τ^{-1}) was also predicted according to the linear relations

$$\tau_{LA}^{-1} = a + b(T - T_i) \tag{3.55}$$

for $P = 0$ and

$$\tau_{LA}^{-1} = a + b(T - T_c) \tag{3.56}$$

for $P = 80.5MPa$ above the incommensurate phase of quartz. Values of a and b were determined by fitting Eqs. 3.55 and 3.55 to the calculated (τ^{-1}) (Fig.3.25) and they are given in Table 3.16.

Table 3.16: Values of the activation energy E_a (Eq.3.53) and the coefficients a and b (Eqs.3.55 and 3.56) of the LA mode with the values of $T_c(K)$, $T_i(K)$, $T_{i1}(K)$, $T_{i3}(K)$ and $T_0(K)$ for the pressures within the temperature intervals indicated in the incommensurate phase of quartz.

LA mode	Pressure (MPa)	$T_c(K)$	$T_i(K)$	$T_{i1}(K)$	$T_{i3}(K)$	$T_0(K)$	a (s^{-1})	b (s^{-1}/K)	$E_a x 10^{-18}$ (J/mol)	E_a (eV/mol)	Temperature Interval (K)
Relaxation time $\tau_{LA}(s)$ Eq.3.53	0	846	847.43	-	-	846.85	5.74	1.71	14.8	92.5	$T_c < T < T_0$
									-4.95	-30.9	$T_0 < T < T_i$
									-1.46	-9.1	$T > T_i$
	80.5	851.72	-	857.9	856.08	849.92	5.78	1.39	0.001	0.0075	$T < T_0$
									-1.04	-6.5	$T_0 < T < T_c$
									-2.18	-13.6	$T_c < T < T_{i3}$
									-0.257	-1.6	$T_{i3} < T < T_{i1}$
									-0.843	-5.3	$T > T_{i1}$

Discussion

Temperature dependence of the damping constant (Γ_{sp}) of the LA mode was calculated by means of the Eq.3.47, PS model, (Figs. 3.19 and 3.20) and Eq.3.48,EF model, (Figs.3.21 and 3.22) in the incommensurate phase of quartz by using observed data [81] at pressures $P = 0$ and $P = 80.5\,MPa$. Fitted parameters given (Tables 3.12 and 3.13) with the close value of amplitudes A and $A^{'}$, indicates that PS and EF models are adequate to describe the observed behavior of the LA mode linewidth due to the pseudo-spin phonon coupling in the incommensurate phase of quartz.

Critical behavior of the damping constant (Γ_{LA}) and frequency shifts ($\Delta\upsilon_{LA}$) of the LA mode close to the transition temperature T_c were also investigated by power law formulas (Eqs.3.50 and 3.49), while the critical exponents η (Table 3.14) and β (Table 3.15) were determined in the given temperature intervals (Table 3.14 and 3.15) at pressures $P = 0$ and $80.5\,MPa$. Maximum value of $\Gamma_{LA}(max)$ was observed at T_{max} during the increase between T_c and T_i at $P = 0$ (Fig. 3.23a) and between $T_{i3}(K)$ and $T_{i1}(K)$ at $P = 80.5\,MPa$ (Fig. 3.23b) where the negative η values occur. Above T_{max}, positive η values are consistent with the abrupt decrease in Γ_{LA} with increasing temperature.

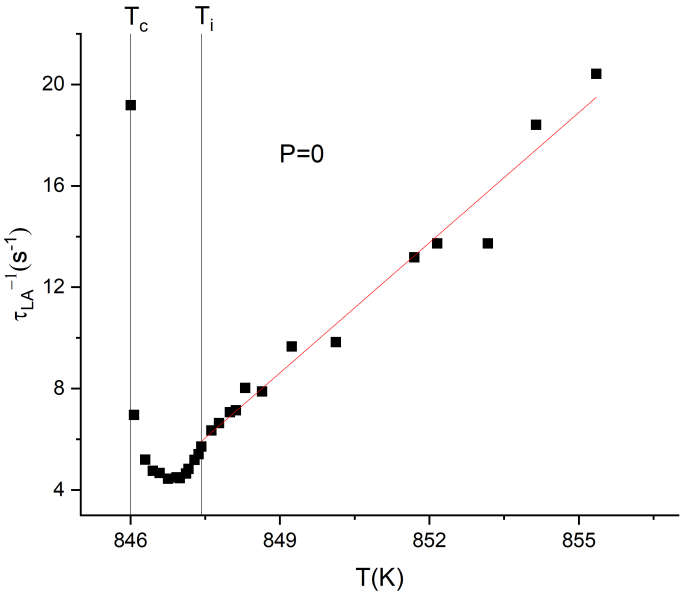

(a)

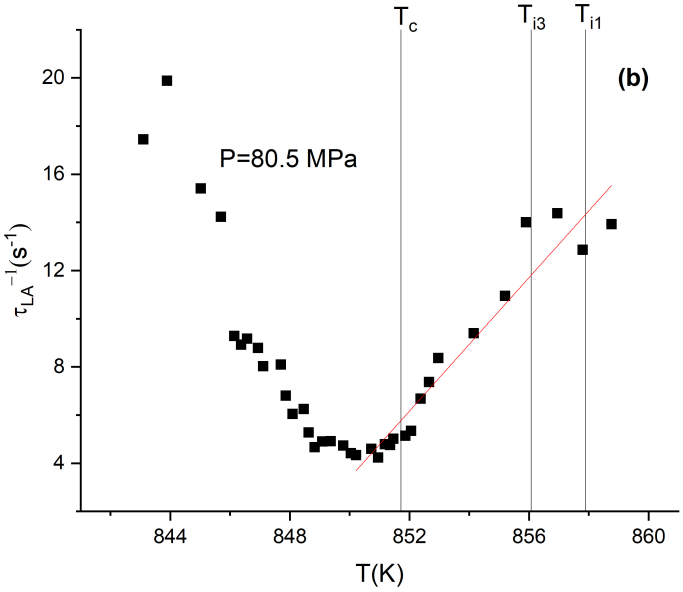

(b)

Figure 3.25: Inverse relaxation time (τ_{LA}^{-1}) calculated as a function of temperature for the LA mode according to Eq.3.52 where the observed data for the frequency shifts ($\Delta\upsilon$) and the linewidth (Γ_{LA}) of this mode [26] were used at the pressures of $\mathrm{P} = 0$ (a) and $80.5\mathrm{MPa}$ (b) in the incommensurate phase of quartz. Straight lines above T_i $(\mathrm{P} = 0)$ and $T_c(80.5\ \mathrm{MPa})$ denote the best fits to the τ^{-1} values.

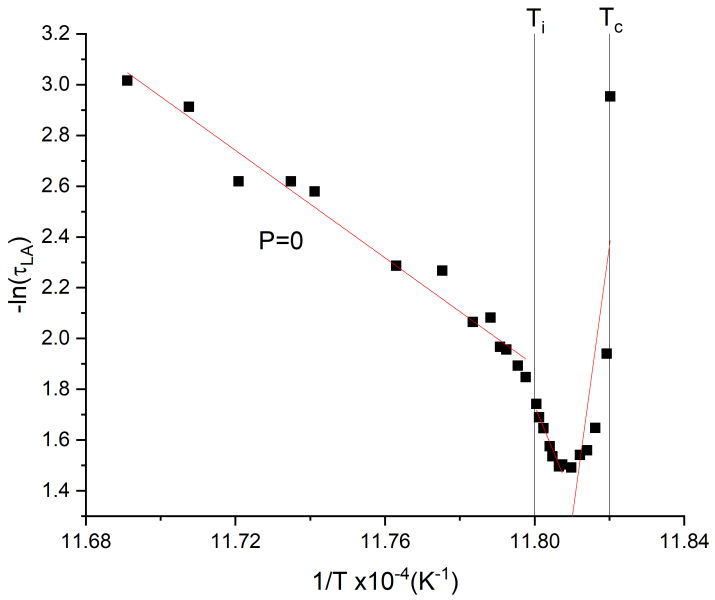

(a)

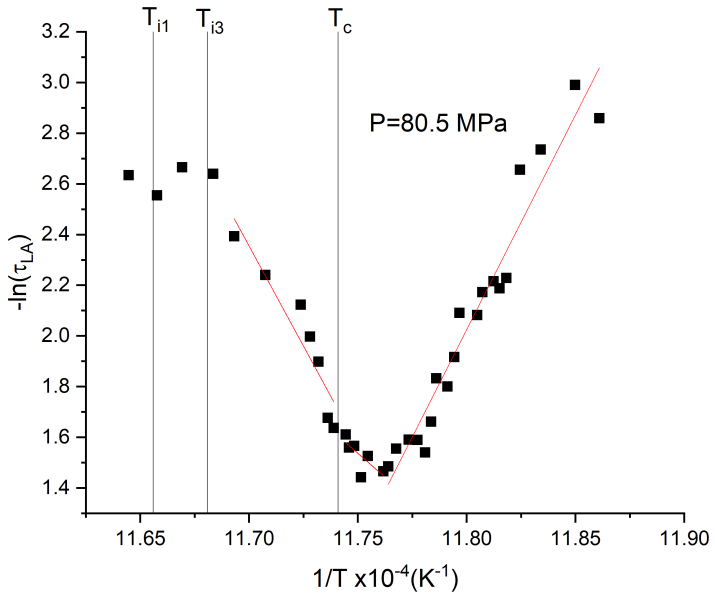

(b)

Figure 3.26: Relaxation time (τ_{LA}) in the logarithmic form of the LA mode as a function of the inverse temperature to determine the values of the activation energy (E_a) according to Eq.3.54 for $\mathrm{P} = 0$ (a) and $80.5\mathrm{MPa}$ (b) in the incommensurate phase of quartz. Solid lines represent best fits to the predicted values (τ_{LA}).

In the analysis of the $\Delta\upsilon_{LA}$, linear temperature dependence of $(\Delta\upsilon_{LA})^2$ above transition temperatures (Eq.3.51) T_i at $P = 0$ (Fig. 3.24a) and $T_{i1}(K)$ at $P = 80.5\,MPa$ (Fig. 3.24b) ,that obeys the Curie-law form, adequately represent the observed behavior of the LA mode [81] in the INC phase of quartz. In Fig. 3.24, as the temperature decreases, a rapid decrease of frequency shifts, in other words a strong softening, below transition temperatures T_i at $P = 0$ and $T_{i1}(K)$ at $P = 80.5\,MPa$ was observed in the INC phase as compared to that in the β phase. It has been interpreted as a result of the soft optic mode's coupling to LA mode that it condenses below T_i $(P = 0)$ [26].

Inverse relaxation time (τ_{LA}^{-1}) was also calculated as a function temperature by using observed linewidth (Γ_{LA}) and frequency shift $(\Delta\upsilon_{LA})$ data of the LA mode by Eq.3.52. As the temperature increases, τ_{LA}^{-1} exhibits first a sudden decrease at T_c $(P = 0)$ and below T_c $(P = 80.5\,MPa)$, then a smooth increase above T_i $(P = 0)$ and T_c through $T_{i3}(K)$ and $T_{i1}(K)$ $(P = 80.5\,MPa)$ occurs (Fig3.25). This critical behavior of τ_{LA}^{-1} (Fig3.25) is in agreement with Γ_{LA} (Fig3.23), especially for zero pressure as $\tau_{LA}^{-1} \propto \Gamma_{LA}$. For $P = 80.5\,MPa$, the minimum value of τ_{LA}^{-1} occurs below T_c at around $850\,K$ (Fig3.25b), whereas the corresponding Γ_{LA} has a maximum value between $T_{i3}(K)$ and $T_{i1}(K)$ at around $857\,K$ (Fig3.23b). Since frequency shifts $\Delta\upsilon_{LA}$ become dominant over the critical behavior, the inverse relaxation time τ^{-1} occurs under pressure, due to the ${\tau_{LA}}^{-1} \propto (\Delta\upsilon_{LA})^2$.

For the zero pressure case, frequency shifts Γ_{LA} which are expected to show the Landau-Khalatnikov type single relaxation behavior, indicate a linear temperature dependence as $\tau \approx 6.3x10^{-12}(T - T_i)^{-1}$ [81]. Variations of sound wave with temperature near the β-INC transition can be explained by single relaxation mechanism [81]. In this study, linear temperature dependence of the inverse relation time ${\tau_{LA}}^{-1}$ was constructed by $(T - T_i)$ at $P = 0$ (Eq.3.55) and $(T - T_c)$ at $P = 80.5\,MPa$ (Eq.3.55) with the coefficients a snd b (Table 3.16). In accordance with the close values of this coefficients, the Landau-Khalatnikov type single relaxation can also be observed at high pressures $P = 80.5\,MPa$ in the INC phase of quartz above the transition temperate as in zero pressure case.

Activation energy E_a (in the units of J/mol and eV/mol) was calculated from the variation of the relaxation time (τ_{LA}) of the LA mode with temperature accord-

ing to Eq.3.54 for the INC phase of quartz. Positive E_a values were obtained in the temperature intervals $846 < T(K) < 846.85$ ($P = 0$) and $T(K) < 849.92$ ($P = 80.5\,MPa$) whereas the E_a values were negative in all the other temperature ranges in the incommensurate phase of quartz. Except the value of $7.5meV$ below $849.92\,K$ ($P = 80.5\,MPa$), all other E_a values are too large compared to some other piezoelectric materials ferroelectric MOFs (metal organic frameworks) of $NH_4Zn(HCOO)_3$ and $ND_4Zn(DCOO)_3$ and $LiTaO_3$], with the values of $0.17eV$, $0.16eV$ [82] and $0.13eV$ [83] which could be the result of significantly small attempt relaxation time (τ_0) values which was obtained in the INC phase at $P = 0$ and $P = 80.5\,MPa$ according to Eq.3.53. Temperature dependence of inverse relaxation time can be expressed in the form of $\tau(T)^{-1} \propto (T - T_i)^{-1}$ [35] at $P = 0$ and $(T - T_c)^{-1}$ at $P = 80.5\,MPa$ since it is the the decay rate of the correlation function of the order parameter below T_c [84] or below T_i ($P = 0$) in the INC phase of quartz. As a result, Eq.3.52 can be rewritten in the form of

$$FWHM = A + BT + Cexp(-E_a/k_BT) \tag{3.57}$$

regarding the Γ or the linewidth [85] as also studied for MOFs [82] In this equation, A depends on structural and compositional defects, the BT term represents the influence of phonon-phonon anharmonic interactions and the last term defines thermally activated reorientational process, which can also be considered for the reorientational motion of the SiO_4 in the incommensurate phase of quartz.

3.6 Heat capacity (C_p) renormalization analysis with the renormalized critical exponents

Variation of heat capacity (C_p) with the temperature was calculated according to the renormalization-group (Section 2.4) expression with the first order corrected scaling term by using various experimental data [1, 32, 33] in the vicinity of the α-INC-β transition in quartz. Critical exponents of the heat capacity (C_p), order parameter (η) and isothermal compressibility (κ_T) , α, β and γ respectively, were also predicted with the renormalized forms in relation to the Rusbrooke's scaling law [37, 45] and Fisher renormalization [48, 49] for the α-INC-β transition in quartz.

Temperature dependence of heat capacity C_p for the α-INC-β transition in quartz according to the renormalization-group formula [47, 50] can be expressed in the form of

$$C_p = A^{\pm}|t|^{-\alpha}\left(1 + D^{\pm}|t|^{\Delta}\right) + B \tag{3.58}$$

with the reduced temperature

$$t = \frac{T - T_c}{T_c} \tag{3.59}$$

where α is the critical exponent and $\Delta = 0.5$ with the constants $A^{\pm}, D^{\pm}$ for above and below critical temperature T_c and B.

Critical exponent of the order parameter can be rewritten in the renormalized form according to Fisher renormalization [48, 49] as

$$\alpha_R = -\frac{\alpha}{1 - \alpha} \tag{3.60}$$

due to the singular behavior of the heat capacity C_p asymptotically close to the transition.

Heat capacity renormalization formula (Eq.3.58) was fitted to the experimental data from DSC (Differential Scanning Calorimetry) [1, 32] (Figs.3.27 and 3.28) and ac calorimetry measurements [33] (Figs.3.27 and 3.28) for the α-INC-β transition in quartz and parameters for Eq.3.58 were determined within the temperature intervals and transition temperatures given in Tables 3.17 and 3.18. Temperature dependence of heat capacity C_p was investigated close to α-INC, INC-α, INC-β and β-INC transitions in a reversible manner for both type of measurements [1,32,33] and ac calorime-

try [33] measurements were also used in the study of cooling and heating runs in quartz. Finally, renormalized critical exponent α_R values for the heat capacity C_p were calculated according to Fisher renormalization (Eq.3.60) for the α-INC-β transition within the temperature intervals are given in the Tables 3.17-3.19 by using the critical exponent α in the each temperature interval.

Table 3.17: Values of the critical exponent α and α_R (renormalized) (Eq.3.60) for the heat capacity C_p with the parameters A, B and D according to Eq.3.58 for the transitions within the temperature intervals indicated for quartz. Transition temperatures (T_c, T_c' and T_i) are also given from the observed C_p data [1, 32]. Quality of fits is also given for the transitions studied.

C_p $(Cal/K.g)$	Transition Temperature (K)		$-\alpha$	α_R	A $(Cal/K.g)$	B $(Cal/K.g)$	$-D$ $(Cal/K.g)$	Temperature Interval (K)	Quality of fit (R)
α-INC	T_c'	845.26	0.70	0.41	-113.56	0.54	32.26	845<T<845.26	0.99
INC-α	T_c	845.60	0.06	0.06	1.03	0.54	43.28	845.6<T<846	0.99
INC-β	T_i	847.12	0.09	0.08	-0.85	0.59	30.62	846<T<847.12	0.98
β-INC	T_i	847.12	0.50	0.33	-31.39	0.51	87.38	847.12<T<848	0.93

Table 3.18: Values of the critical exponent α and α_R (renormalized) (Eq.3.60) for the heat capacity C_p with the parameters A, B and D according to Eq.3.58 for the transitions within the temperature intervals indicated for the cooling run in quartz. Transition temperatures (T_c and T_i) are also given from the observed C_p data [33]. Quality of fits is also given for the transition studied.

C_p $(Cal/K.g)$	Transition Temperature (K)		α	$-\alpha_R$	$Ax10^{-3}$	B	$-D$	Temperature Interval (K)	Quality of fit (R)
α-INC	T_c	846.9	0.52	1.061	-2.7	-1.529	4139.94	846.0<T<846.9	0.98
INC-α			0.51	1.028	-1.6	-15.66	15659.08	846.9<T<848.0	0.98
INC-β	T_i	848	0.50	1.004	4.2	30.12	4681.42	847<T<848	0.70
β - INC			0.93	-	3.0	36.40	268.9	848<T<849	0.99

Table 3.19: Values of the critical exponents α and α_R (renormalized) (Eq.3.60) for the heat capacity C_p with the parameters A, B, and D according to Eq.3.58 for the transitions within the temperature intervals indicated for the heating run in quartz. Transition temperatures (T_c and T_i) are also given from the observed C_p data [33]. Quality of fits is given for the transition studied.

C_p $(Cal/K.g)$	Transition Temperature (K)		α	$-\alpha_R$	$Ax10^{-5}$	B	$-D$	Temperature Interval (K)	Quality of fit (R)
α-INC	T_c	847.7	0.52	1.074	2.0	1.59	38273.90	847.0<T<847.7	0.99
INC-α			0.50	1.012	141	15.29	-3195.36	847.7<T<848.0	0.83
INC-β	T_i	848.0	0.10	0.110	181140	5.77	12.82	847<T<848	0.99
β- INC			0.42	0.730	101364	14.63	-761.73	848<T<849	0.91

Discussion

Temperature variation of the heat capacity was investigated by means of renormaliztion expression with the first order corrected scaling term (Eq.3.58) by using the observed data [1, 32, 33] for the α-INC-β transition in quartz. Our fits to the experimental data [1, 32, 33] in Fig.3.27-3.30 seem reasonable and critical exponents obtained from these fits were used to obtain renormalized critical exponent (α_R) due to Fisher renormalization [48] according to Eq.3.60. While analysis of DSC measurements [1,32] gave negative critical exponent α with the positive renormalized α_R (Table 3.17), ac calorimetry measurements [33] gave positive critical exponent α with the negative renormalized α_R (Tables 3.18 and 3.19). Our analysis showed that for the given temperature intervals and transitions (Tables 3.18 and 3.19) heat capacity (C_p) diverges as observed experimentally [33] except β-INC ($\alpha = 0.93$) and INC-β ($\alpha = 0.10$) transitions. The renormalized critical exponents (α_R) deduced from experimental data [1, 32] with the values varying from ~ 0.1 to 0.41 (Table 3.17) refers to two types of transitions for the α-INC-β transition in quartz. While the renormalized critical exponent of α-INC (T_c') transition $\alpha_R = 0.41$ (Table 3.17) refers to a weakly first order transition, the values of $\alpha_R = 0.06$ and 0.08 (Table 3.17) indicate that INC-α (T_c) and INC-β (T_i) transitions are nearly a second order.

Analysis from the ac calorimetry measurements [33] also agrees with above results with the divergent heat capacity C_p within the temperature intervals. Transitions

(Tables 3.18 and 3.19) are as weakly first order β-INC transition $\alpha_R = 0.5$ (Table 3.18) and nearly second order INC-β $\alpha = 0.10$ (3.19) which, are also comparable to the values of $\alpha_R = 0.1$, 0.2 ($T_Q = 578°C$) and 0.4 ($T_Q = 577.1°C$) from earlier studies [86, 87].

Our nonzero α and α_R values (Tables 3.17-3.19) do not correspond to the mean field value $\alpha = \alpha^{'} = 0$ whereas the $\alpha_R(\sim 0.1)$ values for the INC-α and INC-β transitions (Table 3.17) agree with the the three dimensional Ising model values ($\alpha = 0.119 \pm 0.060$) [88, 89]. For the INC-α and INC-β transitions, critical behavior of the heat capacity can also be described by the negative critical exponents $\alpha = -0.06$ and $\alpha = -0.09$ (Table 3.17) in comparison with the values of $\alpha = -0.08 \pm 0.04$ and $\alpha^{'} = -0.02$ according to the Heisenberg (d=3, D=3) model [88, 89] and the inverted XY model (or helium analogy) [50] respectively.

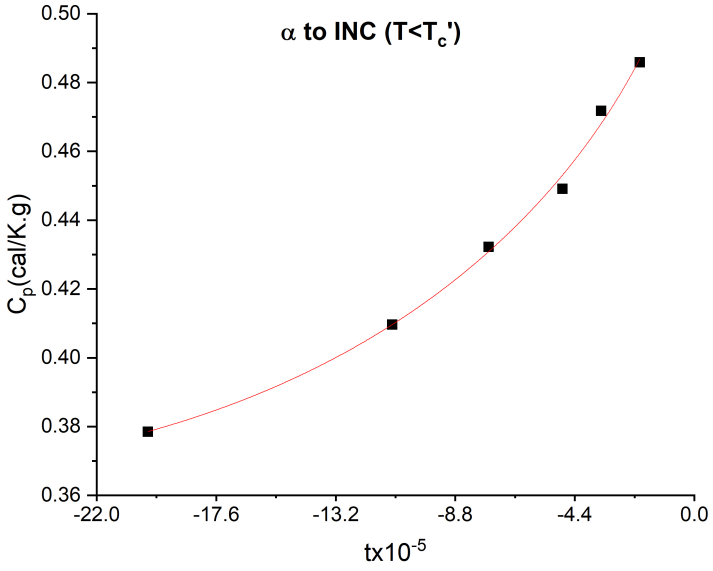

(a)

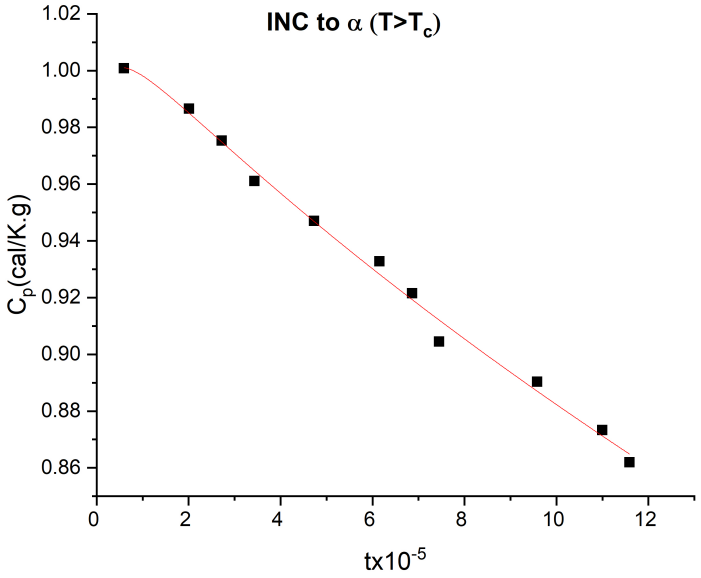

(b)

Figure 3.27: Variation of the heat capacity C_p with the reduced temperature t (Eq.3.59) according to Eq.3.58 for the transitions of α-INC for $T < T_c^{'}$ (a) and INC-α for $T > T_c$ (b) using the observed data [1, 32] in quartz with the critical temperatures $T_c^{'}$ and T_c (Table 3.17).

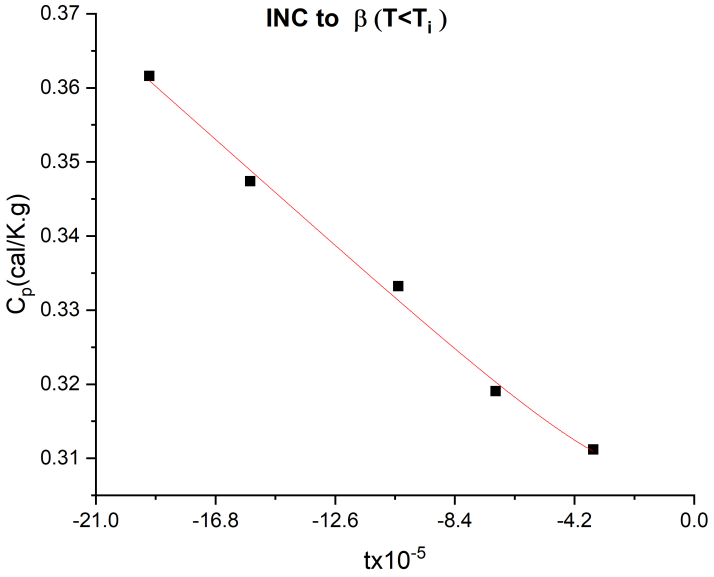

(a)

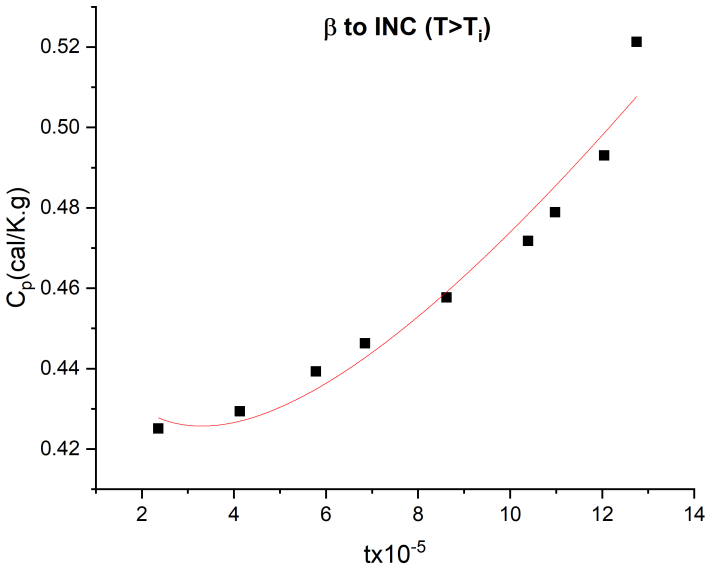

(b)

Figure 3.28: Variation of the heat capacity C_p with the reduced temperature t (Eq.3.59) according to Eq.3.58 for the transitions of INC-β for $T < T_i$ (a) and β-INC for $T > T_i$ (b) using the observed data [1, 32] in quartz. T_i is the critical temperature (Table 3.17).

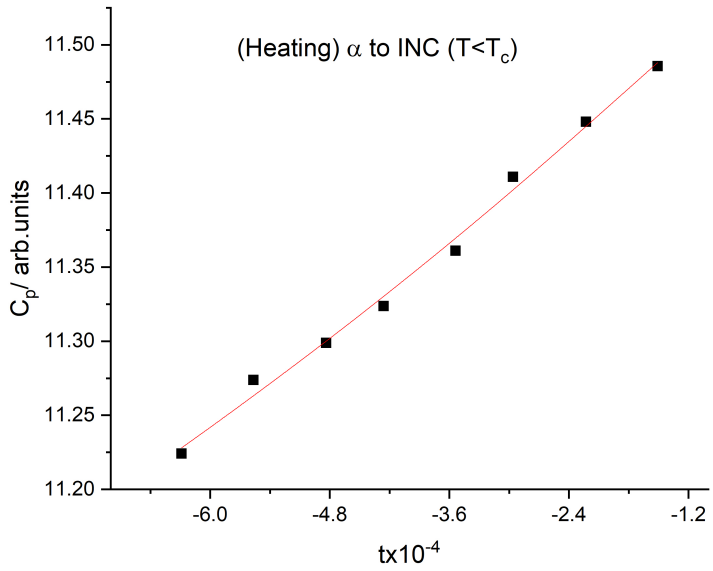

(a)

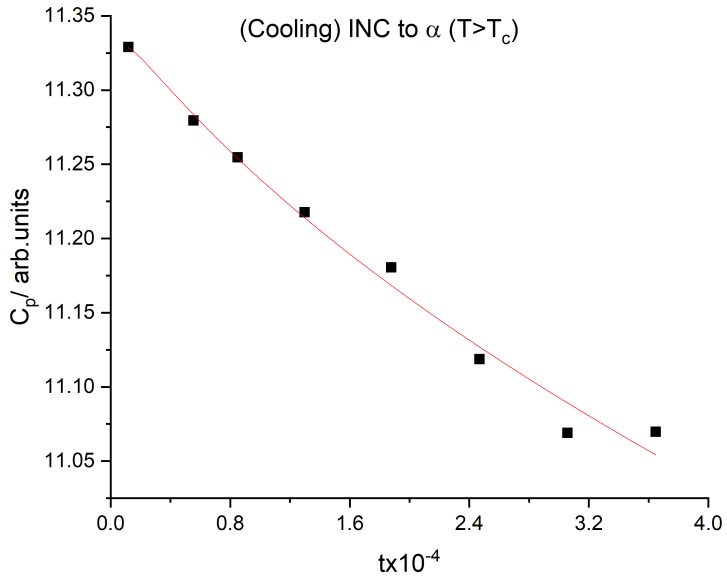

(b)

Figure 3.29: Variation of the heat capacity C_p with the reduced temperature t (Eq.3.59) according to Eq.3.58 for the transitions of α-INC for $T < T_c$ (a) and INC-α for $T > T_c$ (b) for heating and cooling runs, respectively, using the observed data [33] in quartz with the critical temperature T_c (Tables 3.18 and 3.19).

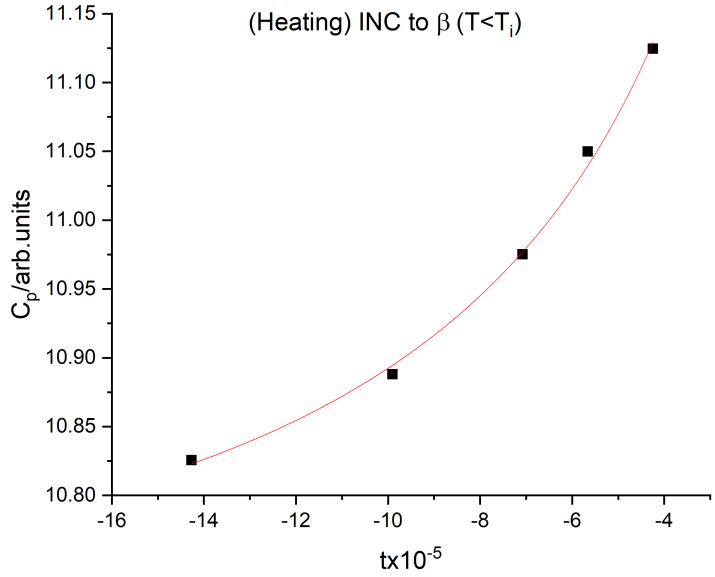

(a)

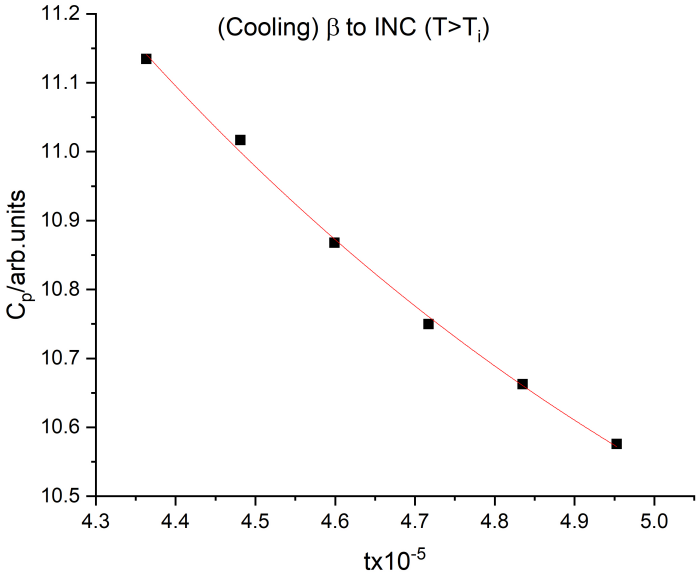

(b)

Figure 3.30: Variation of the heat capacity C_p with the reduced temperature t (Eq.3.59) according to Eq.3.58 for the transitions of INC-β for $T < T_i$ (a) and β-INC for $T > T_i$ (b) for heating and cooling runs, respectively, using the observed data [33] in quartz with the critical temperature T_i (Tables 3.18 and 3.19).

3.7 Landau mean field model with the coupling terms in the presence of the electric field

The temperature dependence of the order parameter (η) and the inverse susceptibility (${\chi_\eta}^{-1}$) of the α-INC-β transition in quartz were calculated by using free energy expansion of the Landau phenomenological model in the absence and presence of the electric field using approximations. For comparison they were fitted to experimental data ($E = 0$) from the literature [6]. We also predicted the temperature dependence of the order parameter (ξ) and the inverse susceptibility (${\chi_\xi}^{-1}$) of the incommensurate (INC) phase of quartz. In addition, $E-T$ phase diagram is obtained for the α-INC-β transition in quartz by using the literature data.

α-INC transition

The free energy expansion for the first order α-INC transition in terms of the order parameter η of the α phase in the presence of electric field (E) can be expressed in the form of

$$F_{\alpha-INC} = \frac{1}{2}a\left(T - T_c\right)\eta^2 + \frac{1}{4}b\eta^4 + \frac{1}{6}c\eta^6 + d\eta\xi + e\eta^2\xi^2 - E\eta^2 \tag{3.61}$$

where a, b and c are constants and, d and e are the coupling constants between the phases of α and INC for $a > 0, b < 0, c > 0, d < 0$ and $e > 0$. ξ is the order parameter of the INC phase and T_c is the transition temperature. By minimizing free energy (Eq.3.61) with respect to order parameter η as

$$\frac{\partial F_{\alpha-INC}}{\partial \eta} = 0 \tag{3.62}$$

one can obtain

$$a\left(T - T_c\right)\eta + b\eta^3 + c\eta^5 + d\xi + 2e\eta\xi^2 - 2E\eta = 0 \tag{3.63}$$

and by minimizing Eq.3.61 with respect to ξ

$$\frac{\partial F_{\alpha-INC}}{\partial \xi} = 0 \tag{3.64}$$

one gets

$$d\eta + 2e\eta^2\xi = 0 \tag{3.65}$$

The relation between the order parameters through Eq.3.65 can be constructed as

$$\xi = -\frac{d}{2e\eta} \tag{3.66}$$

Inserting Eq.3.66 into Eq.3.63 gives

$$a\left(T - T_c\right) + b\eta^2 + c\eta^4 - 2E = 0 \tag{3.67}$$

with the roots of

$$\eta_{1,2}^2 = \frac{-b \pm \sqrt{b^2 - 4c[a\left(T - T_c\right) - 2E]}}{2c} \tag{3.68}$$

For $a > 0, b < 0,\ c > 0$, real and positive order parameter (η) with a nonzero E-field η is given by

$$\eta = \sqrt{\frac{-b \pm \sqrt{b^2 - 4c[a\left(T - T_c\right) - 2E]}}{2c}} \tag{3.69}$$

For $E = 0$, the temperature dependence of the order parameter becomes

$$\eta = \sqrt{\frac{-b + \sqrt{b^2 + 4ac\left(T_c - T\right)}}{2c}} \tag{3.70}$$

For the analysis of the temperature dependence of the order parameter η in the presence of E-field, Eq.3.70 was first fitted to the observed order parameter data [6] from the X-ray measurements without E-field (Fig.3.31) for the α-β transition in quartz. The determined constants $a,\ b$ and c are given in Table 3.20. Electric field values with the transition temperatures T_c (α-INC transition) and T_i (INC-β transition) were obtained from the experimental $E-T$ phase diagram [90] as given in Table 3.21. Then, temperature dependence of the order parameter was calculated according to Eq.3.69 with the constants (Table 3.20) by using the experimental E-field and transition temperature T_c [90], (Table 3.21) within the temperature interval of $825 < T(K) < 850$ for the α-INC transition in quartz.

Table 3.20: Coefficients determined by using the experimental data for the α-β transition [6] according to Eq.(3.70) within the temperature interval indicated in quartz.

Transition	T_c	a	b	c	Temperature Interval (K)
α-β	847K	7.79	-2.64	0.07	$420 < T < 847$

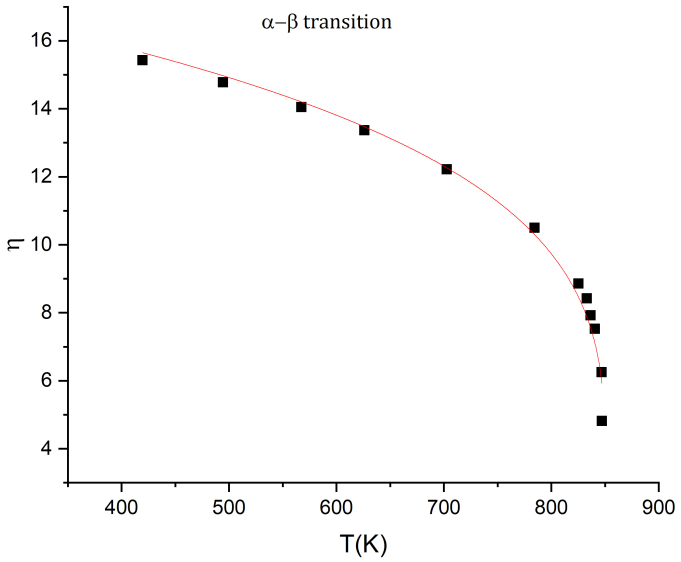

Figure 3.31: Temperature dependence of the order parameter η (Eq.3.70) and the observed data [6] for the α-β transition in quartz within the temperature interval $319 < T(K) < 847$.

Table 3.21: Observed electric (E) field values with the transition temperatures T_c (α-INC transition) and T_i (INC-β transition) from the $E - T$ phase diagram [90].

E(kV/cm)	$T_c(K)$	$T_i(K)$	$\Delta T\,(K)$
8	832.5	837	4.5
5	842.9	845.4	2.5
4	844	846.5	2.5
2	846.8	848.9	2.1
0	848	850.5	2.5

By using the relation between the order parameters in Eq.3.66 due to the coupling with the parameters $d < 0$ and $e > 0$, normalized order parameter of INC-β transition can be written as

$$\frac{\xi}{\xi_0} = -\frac{1}{\eta} \tag{3.71}$$

where $\xi_0 = d/2e$. Temperature dependence of the order parameter ξ of the INC phase in the normalized form, was calculated according to the Eq.3.66 through Eq.3.71 by using the calculated η values (Fig.3.32) for the INC phase of quartz in the presence of E-field (Table 3.21).

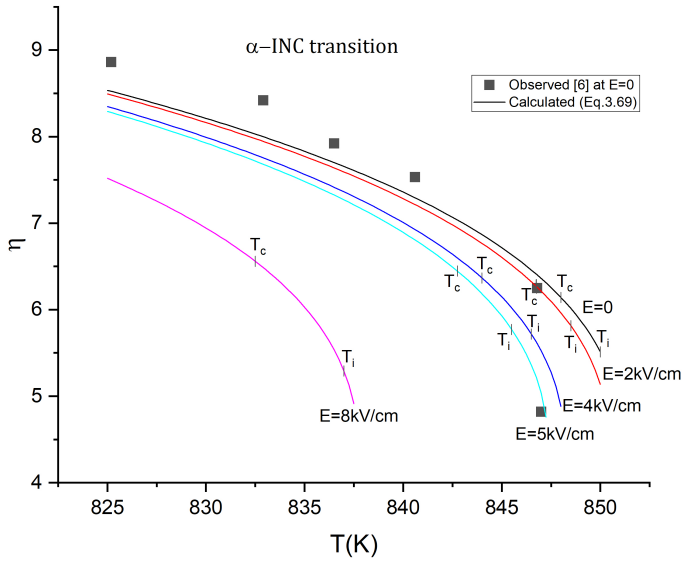

Figure 3.32: The order parameter calculated as a function of temperature for various electric fields (E) for the α-INC phase transitions in quartz. Observed η at $E = 0$ [6] are also shown within the temperature interval of $825 < T(K) < 850$.

The inverse susceptibility χ^{-1} of this transition is defined as

$$\chi_\eta^{-1} = \frac{\partial^2(F_{\alpha-INC})}{\partial\eta^2} \tag{3.72}$$

By using free energy in the presence of the E-field (Eq.3.61), inverse susceptibility of the α-INC transition can be obtained as

$$\chi_\eta^{-1} = 5c\eta^4 + 3b\eta^2 + a\,(T - T_c) + 2e\xi^2 - 2E \tag{3.73}$$

By inserting $\xi = -\frac{d}{2e\eta}$ (Eq.3.66) into Eq.3.73, and for $d < 0$ and $e > 0$, by taking $d = -1$ and $e = 1$, the inverse susceptibility can be written in the form of

$$\chi_\eta^{-1} = 5c\eta^4 + 3b\eta^2 + a\,(T - T_c) + \frac{1}{2\eta^2} - 2E \tag{3.74}$$

in terms of order parameter η.

Variation of the inverse susceptibility χ_η^{-1} of the order parameter η with temperature was obtained according to Eq.3.74 with the coefficients (Table 3.20) by using η values which were calculated from Eq.3.70 (Fig.3.34). For this calculations, the experimental E-field and transition temperature T_c [90] were also used for the α-INC transition in quartz.

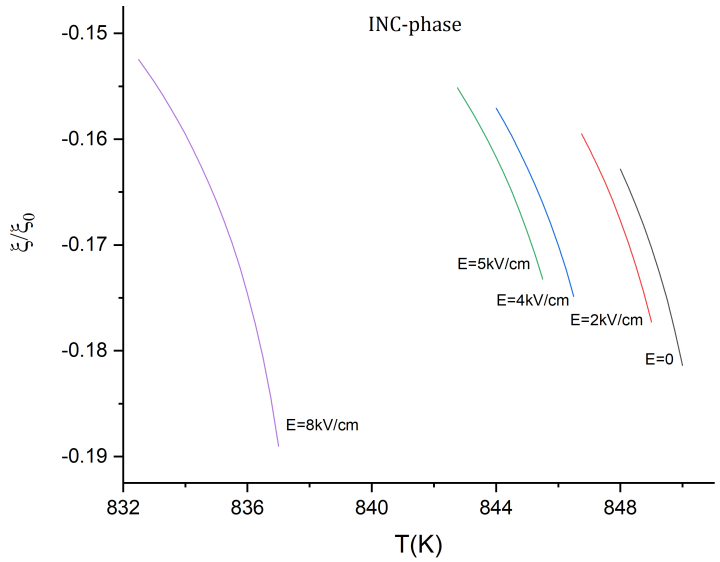

Figure 3.33: Temperature dependence of the order parameter ξ of the INC phase in the normalized form, which was calculated according to the Eq.3.66 within the temperature interval of $832.5 < T(K) < 850$ with the $E - T$ values [90] (Table 3.21).

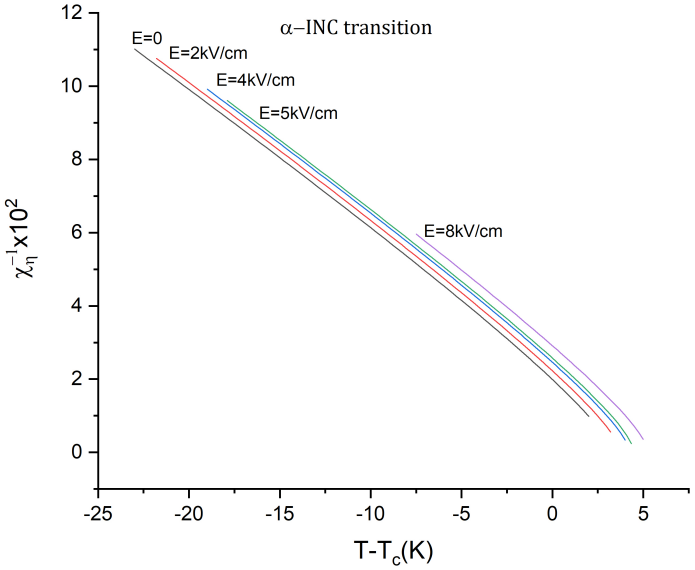

Figure 3.34: Temperature dependence of the inverse susceptibility χ_η^{-1} calculated from Eqs.3.69 and 3.74 in the presence of E-field.

Similarly, χ_ξ^{-1} can be derived according to

$$\chi_\xi^{-1} = \frac{\partial^2(F_{\alpha-INC})}{\partial\xi^2} \tag{3.75}$$

By taking the second derivative of $F_{\alpha-INC}$ (Eq.3.61) with respect to the order parameter ξ of the INC phase, we find

$$\chi_\xi^{-1} = 2e\eta^2 = \frac{d^2}{2e\xi^2} \tag{3.76}$$

using Eq.(3.66). The inverse susceptibility of the INC phase χ_ξ^{-1} was calculated in the normalized form with $\chi_0^{-1} = -d^2/2e$ as a function of temperature (Fig.3.35) according to Eq.(3.76)at constant electric fields indicated in Table 3.21 for the α-INC transition in quartz.

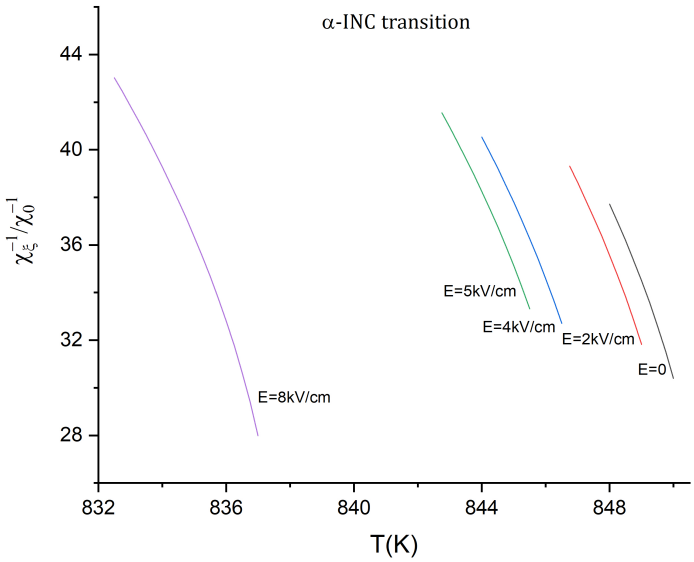

Figure 3.35: The inverse susceptibility χ_ξ^{-1} of the order parameter ξ in the incommensurate (INC) phase ($T_c < T < T_i$) as a function of temperature at constant electric fields for the α-INC transition in quartz. T_i denotes the transition temperature above which the β phase occurs in quartz.

INC-β transition

β phase of quartz is the disordered phase without any ordering parameter (order parameter is zero). By expanding the free energy for the second order INC- β transition

in terms of the order parameter ξ for the INC phase in the presence of the electric field (E), we can write

$$F_{INC-\beta} = \frac{1}{2}a_2\xi^2 + \frac{1}{4}a_4\xi^4 + \frac{1}{6}a_6\xi^6 + d\xi\eta + e\xi^2\eta^2 - E\xi^2 \tag{3.77}$$

where $a_2 = \alpha(T - T_i)$ and $\alpha > 0$, $a_2 < 0$, $a_4 > 0$ (second order transition), $a_6 > 0$. T_i is the transition temperature between INC and β phases where its relation to T_c is

$$T_i = T_c + \Delta T_1 \tag{3.78}$$

for $\Delta T_1 \cong 1.3K$ and $T_i \cong 848.3K$ in quartz [34].

Minimizing the free energy (Eq.3.77) with respect to ξ gives

$$a_2\xi + a_4\xi^3 + a_6\xi^5 + d\eta + 2e\xi\eta^2 - 2E\xi = 0 \tag{3.79}$$

By minimizing the free energy (Eq.3.77) with respect to η, we can obtain

$$\eta = -\frac{d}{2e\xi} \tag{3.80}$$

as in the α-INC transition case (Eq.3.66). Inserting Eq.(3.80) into Eq.(3.79), gives the quadratic equation

$$a_2 + a_4\xi^2 + a_6\xi^4 - 2E = 0 \tag{3.81}$$

with the roots of

$$\xi_{1,2}^2 = \frac{-a_4 \pm \sqrt{a_4^2 - 4a_6(a_2 - 2E)}}{2a_6} \tag{3.82}$$

for $a_2 < 0$, $a_4 > 0$ and $a_6 > 0$, it becomes

$$\xi = \sqrt{\frac{-a_4 + \sqrt{a_4^2 - 4a_6[a_2 - 2E]}}{2a_6}} \tag{3.83}$$

and for zero electric field as

$$\xi = \sqrt{\frac{-a_4 + \sqrt{a_4^2 - 4a_6\alpha(T - T_i)}}{2a_6}} \tag{3.84}$$

with $a_2 = \alpha(T - T_i)$. Constants of Eq.(3.84) (Table 3.22) was determined by fitting to the experimental data [6] for the second order transition. By using these Table 3.22 constants and Eq.(3.84), temperature dependence of the order parameter ξ was calculated as plotted in Fig.3.36 at constant electric fields for the INC-β transition. By using calculated ξ values of Fig.3.36 and Eq.(3.66) with $\eta_0 = -d/2e$, normalized order parameter η was obtained as a function of $T - T_i$ where T_i is the temperature of the INC-β transition in quartz (Table 3.21).

Table 3.22: Coefficients determined by using the experimental data for the INC-β transition [90] according to equations within the temperature interval indicated in quartz.

Transition	α	α_0	$\alpha_1 x10^{-2}$	$a_4 x10^{-16}$	$a_6 x10^{-2}$	Eqs.	Temperature Interval (K)
INC-β	3.65	-	-	1.0	2.5	3.84	$432.5 < T < 850.5$
	-	-2.42	9.0	-	-	3.94	

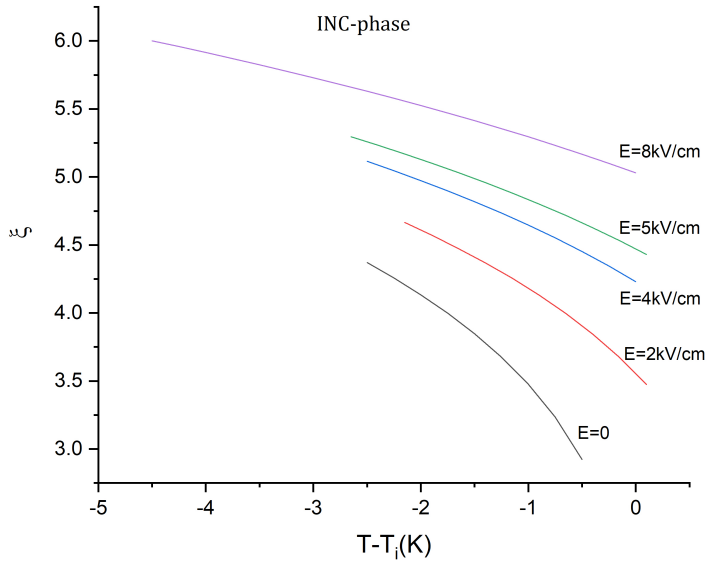

Figure 3.36: Temperature dependence of the order parameter ξ for the incommensurate (INC) phase according to Eq.(3.84) at constant electric fields in quartz. T_i indicates the temperature for the INC-β transition (Table 3.21)

The inverse susceptibility χ^{-1} of this transition is defined as

$$\chi_\xi^{-1} = \frac{\partial^2 F}{\partial \xi^2} \tag{3.85}$$

By taking the second derivative of the $F_{INC-\beta}$ (Eq.3.77) with respect to ξ, the inverse susceptibility χ_ξ^{-1} can be obtained as

$$\chi_\xi^{-1} = a_2 + 3a_4\xi^2 + 5a_6\xi^4 + 2e\eta^2 - 2E \tag{3.86}$$

By inserting $\eta = -\frac{d}{2e\xi}$ (Eq.3.66) into Eq.3.86, for $d < 0$ and $e > 0$, by taking $d = -1$ and $e = 1$ as before, the inverse susceptibility in terms of the order parameter ξ of the

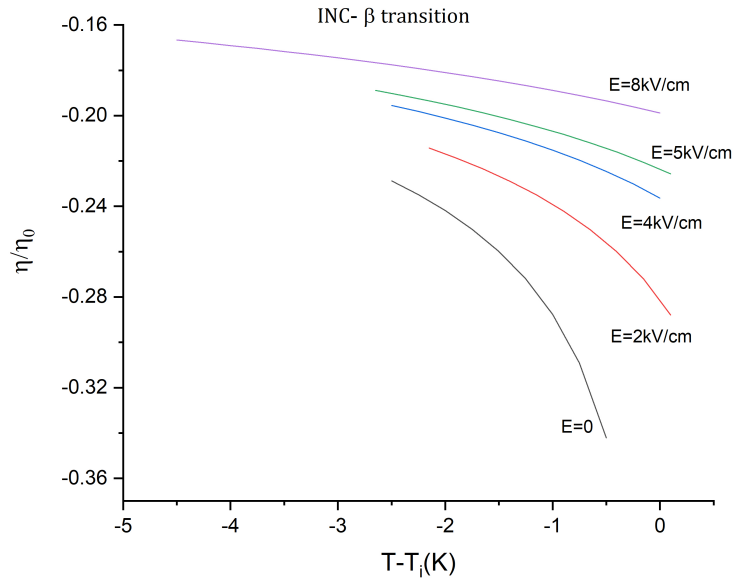

Figure 3.37: Order parameter η of the α phase as a function of the temperature in the incommensurate (INC) phase for the INC-β transition at constant electric fields according to Eq. (3.66).

INC phase can be written as

$$\chi_{\xi}^{-1} = a_2 + 3a_4\xi^2 + 5a_6\xi^4 + \frac{1}{2\xi^2} - 2E \tag{3.87}$$

By defining χ_{η}^{-1} as

$$\chi_{\eta}^{-1} = \frac{\partial^2(F_{INC-\beta})}{\partial\eta^2} \tag{3.88}$$

we obtain from Eq.(3.73),

$$\chi_{\eta}^{-1} = 2e\xi^2 = \frac{d^2}{2e\eta^2} \tag{3.89}$$

through Eq.(3.66).

Variations of the inverse susceptibilities χ_{ξ}^{-1} and χ_{η}^{-1} with $T - T_i$ (Eqs. 3.87 and 3.89) were also calculated as shown in Figs. 3.38 and 3.39, respectively for the INC-β transition at constant electric fields with T_i which is the transition temperature of the INC-β transition in quartz (Table 3.21).

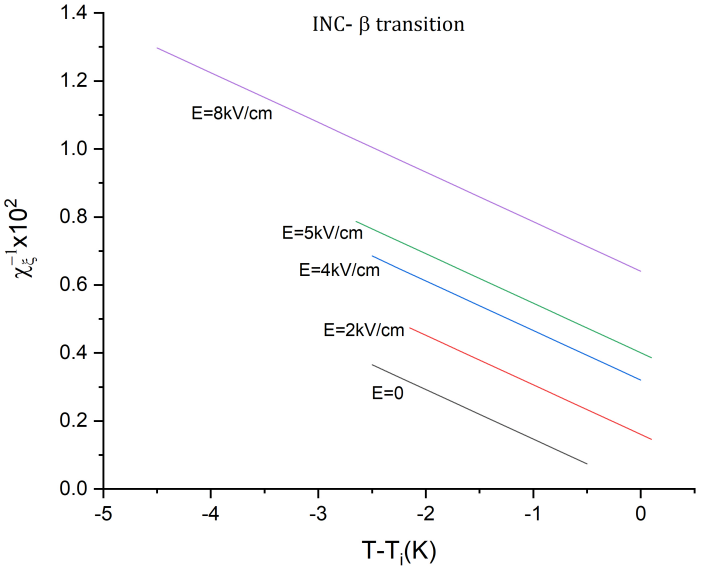

Figure 3.38: Inverse susceptibility susceptibility calculated from Eq.(3.87) in the incommensurate (INC) phase for the INC-β transition at constant electric fields in quartz.

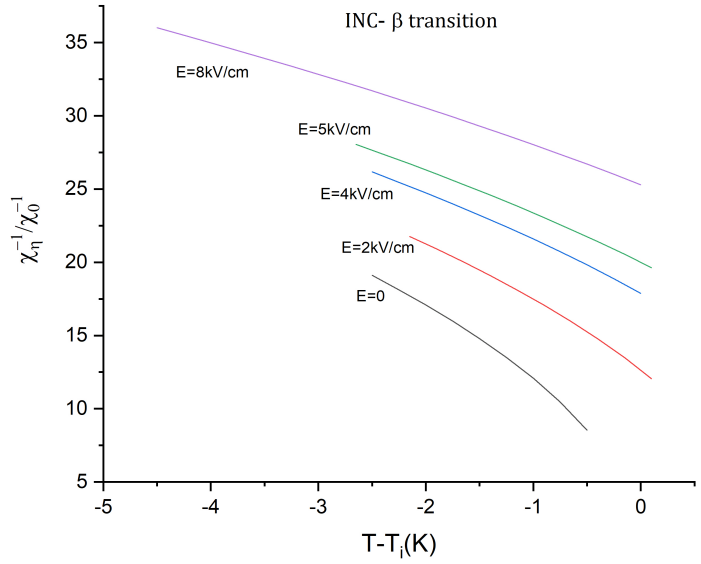

Figure 3.39: Inverse susceptibility χ_η^{-1} calculated as a function of the temperature at constant electric fields according to Eq.(3.89) for the INC-β transition in quartz. T_i denotes the temperature for the INC-β transition (Table 3.21).

Phase line equations

We obtain the phase line equations under the electric field and the temperature ($E-T$) for the transition of the α-INC (first order) and INC-β (second order) in quartz.

α-INC transition

In order to describe the fist order α-INC transition, we have the same free energy for the α and the incommensurate (INC) phases along the transition line. This can be obtained by equating

$$F_{\alpha-INC} = F_{INC-\beta} \tag{3.90}$$

which gives from Eqs.(3.61) and (3.73),

$$\frac{1}{2}a\left(T-T_c\right)\eta^2 + \frac{1}{4}b\eta^4 + \frac{1}{6}c\eta^6 - E\eta^2 = \frac{1}{2}a_2\xi^2 + \frac{1}{4}a_4\xi^4 + \frac{1}{6}a_6\xi^6 - E\xi^2 \tag{3.91}$$

where

$$a_2 = \frac{1}{2}[\alpha_0(T-T_i) + \alpha_1(T-T_i)^2] \tag{3.92}$$

By using the solutions of η^2 (Eq.3.69) and ξ^2 (Eq.3.83) in Eq.(3.91) in the presence of the electric field E, we obtain the phase line equation ($E-T$) in terms of the coefficients a, b, c (Table 3.20) and α_0, α_1, a_4, a_6 (Table 3.23) which can be determined for the α-INC transition in quartz.

INC-β transition

For the second order INC-β transition, we use directly the free energy of $F_{INC-\beta}$ (Eq.3.73) in terms of ξ^2 by means of Eq.(3.66) which gives

$$F_{INC-\beta} = [\frac{1}{2}a_2 - E]\xi^2 + \frac{1}{4}a_4\xi^4 + \frac{1}{6}a_6\xi^6 + d\xi\eta + e\xi^2\eta^2 \tag{3.93}$$

Using the condition for the second order transition according to which the coefficients of the quadratic term in the free energy expansion should be equal to zero, we get the phase line equation for the INC-β transition in quartz simply as

$$\frac{1}{2}[\alpha_0(T-T_i) + \alpha_1(T-T_i)^2] - E = 0 \tag{3.94}$$

with the coefficients α_0 and α_1 (Table 3.22) which were determined by fitting Eq.(3.94) to the experimental data [90] for the INC-β transition in quartz.

The $E-T$ phase diagram was obtained according to the phase line equations, Eqs. (3.91) and (3.94) for the transitions of α-INC and the INC-β, respectively,and fitted to the experimental data [90] in quartz (Fig.3.40).

Table 3.23: Coefficients determined by using the experimental data for the α-INC transition [90] according to Eq.(3.91) with the values of $a,\ b$ and c (Table 3.20) within the temperature interval indicated in quartz.

Transition	$\alpha_0 x10^3$	$\alpha_1 x10^{-3}$	$a_4 x10^3$	$a_6 x10^{-4}$	Temperature Interval (K)
α-INC	-12.69	1.21	17.21	-3.42	$425 < T < 847$

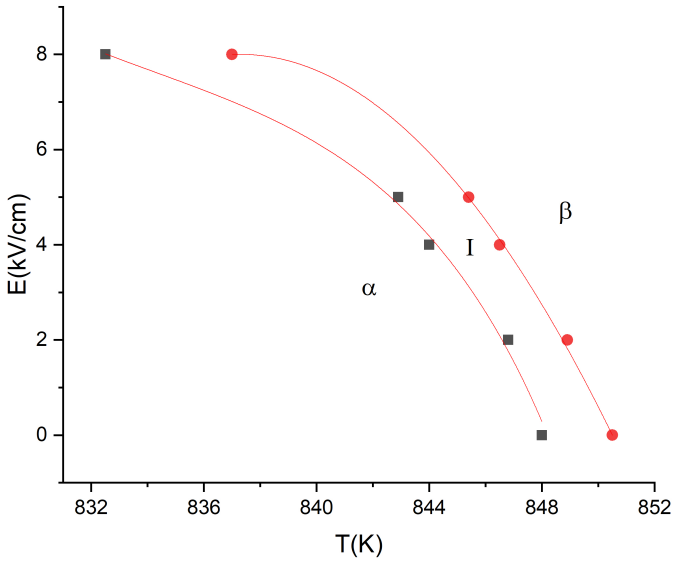

Figure 3.40: The $E-T$ phase diagram according to the phase line equations, Eqs. (3.91) and (3.94) for the transitions of α-INC (α-I) and the INC-β (I-β), respectively, which were fitted (solid lines) to the experimental data [90] in quartz.

Landau phenomenological model with the coupling terms in the presence of the electric field was used to calculate the order parameters η (α-phase) and ξ (INC phase) and their inverse susceptibilities (χ_η^{-1} and χ_ξ^{-1}) as a function of temperature at constant electric fields. Our predictions for the order parameters and the susceptibilities are satisfactory.

On the basis of the Landau phenomenological model, the electric field-temperature ($E - T$) phase diagram was constructed by fitting the phase line equations to the experimental data from the literature which explains adequately the first order α-INC and the second order INC-β transitions in quartz.

CHAPTER 4

CONCLUSIONS

In this dissertation, the incommensurate (INC) phase that is the intermediate phase between the α and β phases of quartz was investigated extensively in the vicinity of the α-INC-β transition by using experimental data from the literature mainly by the Landau phenomenological model.

In Section 3.1, variations of the tilt angle (ϕ) and its inverse susceptibility (χ_{ϕ}^{-1}) with temperature were calculated in the vicinity of the α-INC-β transition ($T_c = 846\,K$) according the Landau phenomenological model with the even order terms up to the sixth order. Calculated tilt angle as an order parameter was fitted to the experimental data [24] and temperature dependence of the tilt angle susceptibility was predicted according to this fit. Our results indicate that the observed behavior of the α-β transition in quartz is adequately described by the Landau mean field model in this study. Other types of quartz with the similar structural phase transition regime as tridymite and crystobalite can also be analyzed by this method.

In Section 3.2, temperature dependence of thermodynamic properties was analyzed in the vicinity of the α-β transition in quartz according to the Landau model including the cubic term for the first order transition. The order parameter(Q), inverse susceptibility (χ^{-1}), entropy (S), heat capacity (C_p) and strain (V_s) were calculated as a function of temperature in relation to the observed excess heat capacity ΔC_p data [18] close to the α-INC-β transition in quartz. Our calculations suggest that Landau mean field model with the cubic term sufficiently describes the first order behavior of the α-INC-β transition. Besides quartz, Landau model of the previous study was used to calculate the thermal and magnetic properties of the metal organic frameworks, (chiral HyFe and HyMn), [91] which indicates that the Landau model with the cubic

terms can also be used to describe the thermal properties of some other materials and crystalline systems.

In Section 3.3, elastic constants, which show anomalous behavior in the vicinity of transition, were correlated to the piezoelectric resonance frequency shifts on the basis of the spectroscopically modified Pippard relation close to the α-β transition in quartz. The linear relation was obtained between the resonance frequency shifts of the $A_g - 2$ mode and inverse incompressibility $(1/K)$ by using the observed data [19], which leads to the calculation of the isobaric mode Grüneisen parameter (γ_p). Similar relation can be obtained for the other quartz forms such as tridymite and crystobalite whose phase diagram show similarities with quartz.

In Section 3.4, temperature dependence of the piezoelectric resonance frequency as an order parameter was analyzed close to the INC-β transition in quartz according to a power law formula by using experimental data from literature [34] which gave critical exponent value ($\beta = 0.5$) similar to the Landau model. Piezoelectric resonance frequency was also related to the anomalous strain over its temperature dependent critical behavior close to the α-INC-β transition in quartz. The linear relation between the piezoelectric resonance frequency (υ^2) and the anomalous strain ($\Delta L^{1/2}$) was obtained in this study. It indicates that they can both define satisfactorily the α-β transition through the INC phase in quartz. This analysis is also applicable to some other crystals with the INC phases like $NaNO_2$, $AlPO_4$ (Berlinite) and $LiAlSiO_4$ (β-Eucryptite).

In Section 3.5, variation of the damping constant (Γ_{LA}) of the LA mode with the temperature was calculated by means of the pseudospin-phonon (SP) coupled and the energy fluctuations (EF) models by using the observed data [81] from literature at $P = 0$ and $P = 80.5\,MPa$ in the INC phase of quartz. Our results for both models are adequate to describe the observed behavior of the linewidth of the LA mode in the phase of interest. Observed data of the Γ_{LA} and $\Delta\upsilon_{LA}$ (Brillouin frequency shifts) [81] were analyzed according to the power law formula close to the α-INC and INC-β transitions in quartz by determining their critical exponents η and β, respectively. We find that their determined values can adequately describe the phase transition close to the INC phase. Finally, temperature dependence of the inverse relaxation time (τ_{LA}^{-1})

and the activation energy (E_a) were predicted from the Γ_{LA} and $\Delta\upsilon_{LA}$ in the INC phase of quartz which can be compared to the experimental results. This explains the order-disorder transition mechanisms of the INC phases.

In Section 3.6, the temperature dependence of the heat capacity (C_p) was analyzed according to the renormalization group expression with the first order corrections to the scaling term in the vicinity of the α-INC-β transition in quartz by using experimental data [1, 32, 33]. Critical exponent (α) of the specific heat, which was subtracted from this study was used to calculate the renormalized critical exponent (α_R) by Fisher renormalization close to the INC phase of quartz. Both α and α_R values obtained in this study sufficiently explain the weakly first order and nearly second order behavior of the α-INC-β transition in quartz. Critical exponent (α) of the specific heat can also be studied in relation to the other critical exponents β and γ of the order parameter and isothermal compressibility, respectively, according to Fisher renormalization and Rusbrooke's scaling law [37, 45] for the INC phase of quartz and related materials.

In Section 3.7, variations of the order parameter (η) and its inverse susceptibility (${\chi_\eta}^{-1}$) with temperature were calculated on the basis of free energy expansion of the Landau model including coupling terms in the absence and presence of the electric field for the α-INC-β transition in quartz, in comparison to experimental data [6] at $E = 0$. The temperature dependence of the order parameter (ξ) of the INC phase and its inverse susceptibility (${\chi_\xi}^{-1}$) was also predicted according to the Landau model studied. $E-T$ phase diagram of the α-INC and INC-β was also constructed by using the Landau model including coupling terms in the presence of the electric field.

Several materials with the INC phases such as $NaNO_2$ [92] and Thiourea [93] can be compared to the INC phase of quartz [32] in relation to the coupling mechanism of the order parameter to another degree of freedom as suggested [73]. Ferroelectric-paraelectric phase transition in $NaNO_2$ through its INC phase was studied by using the mean field models [94, 95] as we did in previous sections for the INC phase of quartz [2,5]. The power law analysis is also applicable for the INC phases of $NaNO_2$ [92] and Thiourea [93] which occur between the ferroelectric-paraelectric phases in a narrow temperature interval.

On the basis of our analysis for quartz in this study, order-disorder transitions of

various materials particularly close to their INC (incommensurate) phases can be described by using temperature and pressure dependence of (experimentally measurable macroscopic parameters) the frequency shifts and strain in relation to the susceptibility (microscopic order parameter). Tridymite and crystobalite whose phase diagrams are analogous to quartz [32] can be analyzed from this point of view. Analysis of this study can also be used to describe the phase transitions of the crystals with the INC phases and similar crystalline structures to quartz such as $NaNO_2$ [92], $AlPO_4$ (Berlinite) [61] and $LiAlSiO_4$ (β-Eucryptite) [96].

REFERENCES

[1] G. Dolino, J. Bachheimer, and C. Zeyen, "Observation of an intermediate phase near the α-β transition of quartz by heat capacity and neutron scattering measurements," *Solid State Communications*, vol. 45, no. 3, pp. 295 – 299, 1983.

[2] H. Yurtseven, U. Ipekoğlu, and S. Ateş, "Calculation of the tilt angle and susceptibility for the α-β transition in quartz using a mean field model," *Modern Physics Letters B*, vol. 31, no. 09, p. 1750092, 2017.

[3] S. Ateş and H. Yurtseven, "Temperature dependence of the piezoelectric resonance frequency in relation to the anomalous strain near the incommensurate phase of quartz," *Ferroelectrics*, vol. 571, 2021.

[4] H. Yurtseven and S. Ateş, "Resonant frequency shifts related to the elastic constants near the α-β transition in quartz," *Journal of Molecular Structure*, vol. 1179, pp. 421 – 424, 2019.

[5] S. Ateş and H. Yurtseven, "Landau mean-field model with the cubic term for the α-β transition in quartz," *Bulletin of Materials Science*, vol. 43, no. 156, pp. 1–10, 2020.

[6] G. Dolino, "The α-inc-β transitions of quartz: A century of research on displacive phase transitions," *Phase Transitions*, vol. 21, no. 1, pp. 59–72, 1990.

[7] G. Jaeger, "The ehrenfest classification of phase transitions: Introduction and evolution," *Archive for History of Exact Sciences*, vol. 53, pp. 51–81, 05 1998.

[8] M. J. Buerger, E. R. Smoluchowski, and J. E. Mayer, *Phase Transformations in Solids*. Wiley, 1951.

[9] H. K. Heinisch, R. Roy, and L. E. Cross, *Phase transitions (eds)*. Oxford: Pergamon Press, 1973.

[10] J. C. Tolédano and P. Tolédano, *The Landau Theory of Phase Transitions*. World Scientific, 1987.

[11] *Phase Diagram of Silica Polymorphs*. http://www.quartzpage.de, accessed: 11.19.2020.

[12] A. Putnis, *An Introduction to Mineral Sciences*. Cambridge University Press, 1992.

[13] B. E. Douglas and S. M. Ho, *Crystal Structures of Silica and Metal Silicates*. Springer, 2006.

[14] H. Le Chatelier, "Sur la dilatation du quartz," *Bulletin de la Société française de Minéralogie, volume 13, 3, 1890.*, 1890.

[15] M. Matsuura, H. Yao, K. Gouhara, I. Hatta, and N. Kato, "Heat capacity in α-β phase transition of quartz," *Journal of the Physical Society of Japan*, vol. 54, no. 2, pp. 625–629, 1985.

[16] J. M. Branlund and A. M. Hofmeister, "Thermal diffusivity of quartz to 1,0003 °C: effects of impurities and the α-β phase transition," *Physics and Chemistry of Minerals*, vol. 34, pp. 581–595, 2007.

[17] J. P. Bachheimer, "An anomaly in the β phase near the α-β transition of quartz," *J. Physique Lett.*, vol. 41, no. 23, pp. 559–561, 1980.

[18] M. A. Carpenter, E. K. H. Salje, A. Graeme-Barber, B. Wruck, M. T. Dove, and K. S. Knight, "Calibration of excess thermodynamic properties and elastic constant variations associated with the alpha -beta phase transition in quartz," *American Mineralogist*, vol. 83, pp. 2–22, 1998.

[19] I. Ohno, K. Harada, and C. Yoshitomi, "Temperature variation of elastic constants of quartz across the α-β transition," *Physics and Chemistry of Minerals*, vol. 33, pp. 1–9, 2006.

[20] R. E. A. McKnight, T. Moxon, A. Buckley, P. A. Taylor, T. W. Darling, and M. A. Carpenter, "Grain size dependence of elastic anomalies accompanying the α-β phase transition in polycrystalline quartz," *Journal of Physics: Condensed Matter*, vol. 20, p. 075229, jan 2008.

[21] M. Midorikawa, K. Gouhara, and Y. Ishibashi, "Dilatometric and dielectric studies of an incommensurate transition in quartz," *Journal of the Physical Society of Japan*, vol. 53, no. 8, pp. 2431–2433, 1984.

[22] S. M. Shapiro, D. C. O'Shea, and H. Z. Cummins, "Raman scattering study of the alpha-beta phase transition in quartz," *Phys. Rev. Lett.*, vol. 19, pp. 361–364, Aug 1967.

[23] E. K. H. Salje, A. Ridgwell, B. Guttler, B. Wruck, M. T. Dove, and G. Dolino, "On the displacive character of the phase transition in quartz: a hard-mode spectroscopy study," *Journal of Physics: Condensed Matter*, vol. 4, pp. 571–577, jan 1992.

[24] M. G. Tucker, M. T. Dove, and D. A. Keen, "Simultaneous analysis of changes in long-range and short-range structural order at the displacive phase transition in quartz," *Journal of Physics: Condensed Matter*, vol. 12, pp. L723–L730, nov 2000.

[25] A. N. Nikitin, G. V. Markova, A. M. Balagurov, R. N. Vasin, and O. V. Alekseeva, "Investigation of the structure and properties of quartz in the α-β transition range by neutron diffraction and mechanical spectroscopy," *Crystallography Reports*, vol. 52, pp. 428–435, 2007.

[26] Berge, B., Dolino, G., Vallade, M., Boissier, M., and Vacher, R., "Incommensurate phase of quartz. - ii : Brillouin scattering studies," *J. Phys. France*, vol. 45, no. 4, pp. 715–724, 1984.

[27] E. Gregoryanz, R. J. Hemley, H. K. Mao, and P. Gillet, "High-pressure elasticity of α-quartz: Instability and ferroelastic transition," *Phys. Rev. Lett.*, vol. 84, pp. 3117–3120, Apr 2000.

[28] T. Shigenari, Y. Limura, and Y. Takagi, "On the static nature of the 'opalescence' near the α-β transition in a quartz crystal," *Optics Communications*, vol. 31, no. 1, pp. 57 – 60, 1979.

[29] S. M. Shapiro and H. Z. Cummins, "Critical opalescence in quartz," *Phys. Rev. Lett.*, vol. 21, pp. 1578–1582, Dec 1968.

[30] G. Dolino, "Angular and polarization properties of light scattering at the α-β phase transition of quartz," *Physica Status Solidi (a)*, vol. 60, no. 2, pp. 391–401, 1980.

[31] T. Aslanian and A. Levanyuk, "On the possibility of the incommensurate phase near α-β transition point in quartz," *Solid State Communications*, vol. 31, no. 8, pp. 547 – 550, 1979.

[32] G. Dolino, J. P. Bachheimer, B. Berge, and C. M. E. Zeyen, "Incommensurate phase of quartz : I. elastic neutron scattering," *J. Phys. France*, vol. 45, no. 2, pp. 361–371, 1984.

[33] H. Yao and I. Hatta, "Phase transitions of quartz studied by a.c. calorimetry," *Thermochimica Acta*, vol. 266, pp. 301 – 308, 1995. Transition Phenomena in Condensed Matter.

[34] S. Ishibashi, K. Abe, M. Suzuki, Y. Sasaki, and T. Shigenari, "Acoustic phonon dispersion of SiO_2 (quartz) near the incommensurate phase transition," *Physica B: Condensed Matter*, vol. 219-220, pp. 593 – 595, 1996. Phonons 95.

[35] T. Ochiai, M. Ohya, T. Nishikawa, Y. Sasaki, K. Abe, and T. Shigenari, "Piezoelectric properties in α-, incommensurate- and β-phases of quartz SiO_2," *Japanese Journal of Applied Physics*, vol. 37, pp. 2606–2607, may 1998.

[36] M. Kardar, *Thermodynamics*, p. 1–34. Cambridge University Press, 2007.

[37] P. Papon, J. Leblond, and P. Meijer, *The physics of phase transitions: Concepts and applications*. Springer, 01 2006.

[38] R. Winter, *Condensed Matter Physics, Order of phase transitions*. https://users.aber.ac.uk/ruw/teach/334/phtr-order.php, accessed: 12.03.2020.

[39] V. A. Blatov, A. A. Golov, C. Yang, Q. Zeng, and A. A. Kabanov, "Network topological model of reconstructive solid-state transformations," *Scientific Reports*, vol. 9, p. 6007, 2019.

[40] "Chapter 2 - Classification of phase transformations," in *Phase Transformations* (S. Banerjee and P. Mukhopadhyay, eds.), vol. 12 of *Pergamon Materials Series*, pp. 87 – 123, Pergamon, 2007.

[41] L. Landau, "On the theory of phase transitions," *Zh. Eksp. Teor. Fiz.*, vol. 7, pp. 19–32, 1937.

[42] P. Tolédano and V. Dmitriev, *Reconstructive Phase Transitions*. World Scientific, 1996.

[43] L. Landau, "Theory of the superfluidity of helium II," *Phys. Rev.*, vol. 60, pp. 356–358, Aug 1941.

[44] Perez-Mato, J M , Aroyo, M I , and Orobengoa, D , "Symmetry considerations in structural phase transitions," *EPJ Web of Conferences*, vol. 22, p. 00008, 2012.

[45] J. P. Casquilho and P. I. C. Teixeira, *Phase transitions and critical phenomena*, p. 269–297. Cambridge University Press, 2014.

[46] H. E. Stanley, "Scaling, universality, and renormalization: Three pillars of modern critical phenomena," *Rev. Mod. Phys.*, vol. 71, pp. S358–S366, Mar 1999.

[47] K. G. Wilson and J. Kogut, "The renormalization group and the ϵ expansion," *Physics Reports*, vol. 12, no. 2, pp. 75 – 199, 1974.

[48] M. E. Fisher, "Renormalization of critical exponents by hidden variables," *Phys. Rev.*, vol. 176, pp. 257–272, Dec 1968.

[49] J. P. Hill, B. Keimer, K. W. Evans-Lutterodt, R. J. Birgeneau, and C. W. Garland, "Extended Fisher renormalized tricritical behavior of the nematic–smectic-a transition in liquid-crystal mixtures," *Phys. Rev. A*, vol. 40, pp. 4625–4629, Oct 1989.

[50] F. J. Wegner, "Corrections to scaling laws," *Phys. Rev. B*, vol. 5, pp. 4529–4536, Jun 1972.

[51] W. Cochran, "Crystal stability and the theory of ferroelectricity," *Advances in Physics*, vol. 9, no. 36, pp. 387–423, 1960.

[52] A. J. Hughes and A. W. Lawson, "Cylindrical approximation and the α-β quartz transition," *The Journal of Chemical Physics*, vol. 36, no. 8, pp. 2098–2100, 1962.

[53] D. Cuffari and A. Bongiorno, "Calculation of mode Grüneisen parameters made simple," *Phys. Rev. Lett.*, vol. 124, p. 215501, May 2020.

[54] G. Dolino, B. Berge, M. Vallade, and F. Moussa, "Origin of the incommensurate phase of quartz: I. inelastic neutron scattering study of the high temperature β phase of quartz," *J. Phys. I France*, vol. 2, no. 7, pp. 1461–1480, 1992.

[55] M. Matsushita, "Anomalous temperature dependence of the frequency and damping constant of phonons near T_λ in ammonium halides," *The Journal of Chemical Physics*, vol. 65, no. 1, pp. 23–28, 1976.

[56] I. Laulicht and N. Luknar, "Internal-mode line-broadening by proton jumps in KH_2PO_4," *Chemical Physics Letters*, vol. 47, no. 2, pp. 237 – 240, 1977.

[57] G. Lahajnar, R. Blinc, and S. Zumer, "Proton spin-lattice relaxation by critical polarization fluctuations in KH_2PO_4," *Physics of condensed matter*, vol. 18, no. 4, pp. 301–316, 1974.

[58] G. Schaack and V. Winterfeldt, "Temperature behaviour of optical phonons near T_c in triglycine sulphate and triglycine selenate," *Ferroelectrics*, vol. 15, no. 1, pp. 35–41, 1977.

[59] B. Lawn, D. Marshall, R. Raj, G. Hirth, T. Page, and J. Yeomans, "Precipitous weakening of quartz at the α-β phase inversion," *Journal of the American Ceramic Society*, vol. 104, no. 1, pp. 23–26, 2021.

[60] B. Berge, J. P. Bachheimer, G. Dolino, M. Vallade, and C. M. E. Zeyen, "Inelastic neutron scattering study of quartz near the incommensurate phase transition," *Ferroelectrics*, vol. 66, no. 1, pp. 73–84, 1986.

[61] G. van Tendeloo, J. van Landuyt, and S. Amelinckx, "The $\alpha \rightarrow \beta$ phase transition in quartz and alpo4 as studied by electron microscopy and diffraction," *Physica Status Solidi (a)*, vol. 33, no. 2, pp. 723–735, 1976.

[62] A. Wright and M. Lehmann, "The structure of quartz at 25 and 590°C determined by neutron diffraction," *Journal of Solid State Chemistry*, vol. 36, no. 3, pp. 371 – 380, 1981.

[63] J. Ericksen, "On the theory of the α-β phase transition in quartz," *Journal of Elasticity and the Physical Science of Solids*, vol. 63, pp. 61–86, 2001.

[64] J. Etchepare, M. Merian, and L. Smetankine, "Vibrational normal modes of SiO_2. I. α and β quartz," *The Journal of Chemical Physics*, vol. 60, no. 5, pp. 1873–1876, 1974.

[65] R. S. Mulliken, "Report on notation for the spectra of polyatomic molecules," *The Journal of Chemical Physics*, vol. 23, no. 11, pp. 1997–2011, 1955.

[66] R. S. Mulliken, "Erratum : Report on notation for the spectra of polyatomic molecules," *The Journal of Chemical Physics*, vol. 24, no. 5, pp. 1118–1118, 1956.

[67] Y. Tezuka, S. Shin, and M. Ishigame, "Observation of the silent soft phonon in β-quartz by means of hyper-raman scattering," *Phys. Rev. Lett.*, vol. 66, pp. 2356–2359, May 1991.

[68] H. Ogi, T. Ohmori, N. Nakamura, and M. Hirao, "Elastic, anelastic, and piezoelectric coefficients of α-quartz determined by resonance ultrasound spectroscopy," *Journal of Applied Physics*, vol. 100, no. 5, p. 053511, 2006.

[69] H. Kimizuka, S. Ogata, J. Li, and Y. Shibutani, "Complete set of elastic constants of α-quartz at high pressure: A first-principles study," *Phys. Rev. B*, vol. 75, p. 054109, Feb 2007.

[70] E. Banda, R. Craven, R. Parks, P. Horn, and M. Blume, "α-β transition in quartz: Classical versus critical behavior," *Solid State Communications*, vol. 17, no. 1, pp. 11 – 14, 1975.

[71] M. H. Müser and K. Binder, "Molecular dynamics study of the α-β transition in quartz: elastic properties, finite size effects, and hysteresis in the local structure," *Physics and Chemistry of Minerals*, vol. 28, pp. 746–755, 2001.

[72] M. Gambhir, M. T. Dove, and V. Heine, "Rigid unit modes and dynamic disorder: SiO_2 cristobalite and quartz," *Physics and Chemistry of Minerals*, vol. 26, pp. 484–485, 1999.

[73] A. P. Levanyuk and D. G. Sannikov, "Thermodynamic theory of phase transitions accompanied by the formation of the non-commensurate superstructure in $NaNO_2$," *Soviet Phys.—Solid State*, vol. 18, p. 1122, 1976.

[74] G. Dolino and P. Bastie, "Phase transitions of quartz," *Key Engineering Materials*, vol. 101, pp. 285–310, 3 1995.

[75] U. T. Höchli and J. F. Scott, "Displacement parameter, soft-mode frequency, and fluctuations in quartz below its $\alpha - \beta$ phase transition," *Phys. Rev. Lett.*, vol. 26, pp. 1627–1629, Jun 1971.

[76] B. S. Hemingway, "Quartz; heat capacities from 340 to 1000 K and revised values for the thermodynamic properties," *American Mineralogist*, vol. 72, pp. 273–279, 04 1987.

[77] K. Kihara, "An X-ray study of the temperature dependence of the quartz structure," *European Journal of Mineralogy*, vol. 2, pp. 63–78, 02 1990.

[78] A. P. Levanyuk, S. A. Minyukov, and M. Vallade, "Fluctuation-induced first-order phase transitions near mean-field tricritical points in solids," *Journal of Physics: Condensed Matter*, vol. 5, pp. 4419–4428, jun 1993.

[79] W. Cochran, "Crystal stability and the theory of ferroelectricity part ii. piezoelectric crystals," *Advances in Physics*, vol. 10, no. 40, pp. 401–420, 1961.

[80] R. A. Young, "Mechanism of the phase transition in quartz.," *Rep 2569*, 1962.

[81] K. Abe, K. Aboshi, K. Kawasaki, and T. Shigenari, "Lineshape of brillouin spectra in the incommensurate phase of quartz (sio_2): Analysis by fano's formula," *Ferroelectrics*, vol. 203, no. 1, pp. 153–165, 1997.

[82] M. Mączka, P. Kadłubański, P. T. C. Freire, B. Macalik, W. Paraguassu, K. Hermanowicz, and J. Hanuza, "Temperature- and pressure-induced phase transitions in the metal formate framework of [nd4][zn(dcoo)3] and [nh4][zn(hcoo)3]," *Inorganic Chemistry*, vol. 53, pp. 9615–9624, Sep 2014.

[83] A. Hushur, S. Gvasaliya, B. Roessli, S. Lushnikov, and S. Kojima, "Ferroelectric phase transition of stoichiometric lithium tantalate studied by raman, brillouin, and neutron scattering," *Phys. Rev. B*, vol. 76, p. 064104, Aug 2007.

[84] H. Mori, “Collective motion of particles at finite temperatures,” *Progress of Theoretical Physics*, vol. 28, no. 5, pp. 763–783, 1962.

[85] C. Carabatos-Nédelec and P. Becker, “Order–disorder and structural phase transitions in solid-state materials by Raman scattering analysis,” *Journal of Raman Spectroscopy*, vol. 28, no. 9, pp. 663–671, 1997.

[86] H. Yurtseven and M. Desticioglu, “Critical behaviour of the heat capacity near the alpha-beta phase transition in quartz,” *High Temperature Materials and Processes*, pp. 189–194, 2013.

[87] H. Yurtseven and S. Ateş, “Pippard relations and the analysis of the specific heat for the alpha-beta transition in quartz,” *"Int. J. Chem"*, vol. 2, p. 48.

[88] H. E. Stanley, *Introduction to Phase Transitions and Critical Phenomena*. Oxford University Press, 1971.

[89] J. J. Binney, N. J. Dowrick, A. J. Fisher, and M. E. J. Newman, *The theory of critical phenomena: An introduction to the renormalization group*. Oxford University Press Inc., 1992.

[90] J. Bethke and G. Eckold, “The influence of an external electric field on the incommensurate phase of quartz,” *Physica B: Condensed Matter*, vol. 180-181, pp. 323 – 325, 1992.

[91] O. Tari and H. Yurtseven, “Temperature dependence of magnetic and thermal properties of chiral HyFe and HyMn close to phase transitions by using the Landau mean field model,” *Materials Chemistry and Physics*, vol. 228, pp. 118 – 123, 2019.

[92] D. Durand, F. Denoyer, M. Lambert, L. Bernard, and R. Currat, “Etude par rayons X et par neutrons de la phase incommensurable du nitrite de sodium,” *Journal de Physique*, vol. 43, no. 1, pp. 149–154, 1982.

[93] F. Denoyer, A. H. Moudden, R. Currat, C. Vettier, A. Bellamy, and M. Lambert, “Effect of hydrostatic pressure on modulated structures in thiourea,” *Phys. Rev. B*, vol. 25, pp. 1697–1702, Feb 1982.

[94] C. K. Sarıkaya and H. Yurtseven, "Temperature dependence of the spontaneous polarization near the ferroelectric-paraelectric transition in $NaNO_2$," *High Temperature Materials and Processes*, vol. 32, no. 1, pp. 77 – 81, 22 Feb. 2013.

[95] H. Yurtseven and C. K. Sarikaya, "Investigation of the ferroelectric paraelectric phase transition in bulk and confined sodium nitrite," *Ferroelectrics*, vol. 467, no. 1, pp. 42–49, 2014.

[96] W. Press, B. Renker, H. Schulz, and H. Böhm, "Neutron scattering study of the one-dimensional ionic conductor β-eucryptite," *Phys. Rev. B*, vol. 21, pp. 1250–1257, Feb 1980.